18

Pathologic Anatomy of Nasolabial Clefts: Spectrum of the Microform Deformity and the Neuromeric Basis of Cleft Surgery

Michael H. Carstens

Introduction

The locus of the cleft defect is in the floor of the nose, the upper lip, and the alveolus, rather than the free border of the lip.

—Bard Cosman* [1]

The Microform Deformity and Its Variants: The Rosetta Stone of Cleft Pathology

During Napoleon Bonaparte's Egyptian campaign in 1799, a French soldier discovered a black basalt slab inscribed with ancient writing near the town of Rosetta, about 56 km north of Alexandria. The irregularly shaped stone, which would become known as the Rosetta Stone because of where it was found, contained fragments of passages written in three different scripts: Greek, Egyptian hieroglyphics and Egyptian demotic. The ancient Greek on the Rosetta Stone told archaeologists that it was inscribed by priests honoring the king of Egypt, Ptolemy V, in the second century BC (Fig. 18.1).

Perhaps even more surprising, the Greek passage announced that the three scripts were all of identical meaning. The artifact thus held the key to solving the riddle of hieroglyphics, a written language that had been 'dead' for nearly 2000 years.

When Napoleon, an emperor known for his enlightened view on education, art and culture, invaded Egypt in 1798, he took along a group of scholars and told them to seize all important cultural artifacts for France. Pierre Bouchard, one of Napoleon's soldiers, was aware of this order when he found the basalt stone, which was almost 1.2 m long and 0.8 m wide, at a fort near Rosetta.

When the British defeated Napoleon in 1801, they took possession of the Rosetta Stone. Several scholars, including

Fig. 18.1 The Rosetta stone. The discovery of the stela, written in two forms of ancient Egyptian as well as Greek, enabled scholars to decipher the hieroglyphic system. It currently resides in the British Museum (see text). [Courtesy of Mr. Blake Linder, Journalist for Caxton West Branch. Reprinted from the Roodepoort Record: https://roodepoort-northsider.co.za/278371/today-in-history-french-soldier-discovers-the-rosetta-stone-web/]

Englishman Thomas Young, made progress with the initial hieroglyphics analysis of the Rosetta Stone. French Egyptologist, Jean-Francois Champollion, who had taught himself ancient languages, ultimately cracked the code and deciphered the hieroglyphics using his knowledge of Greek as a guide.

Hieroglyphics used pictures to represent objects, sounds and groups of sounds. Once the Rosetta Stone inscriptions were translated, the language and culture of ancient Egypt were suddenly opened to scientists as never before.

The Rosetta Stone has been housed at the British Museum in London since 1802, except for a brief period during World War I. At that time, museum officials moved it to a separate underground location, along with other irreplaceable items from the museum's collection, to protect it from the threat of bombs.

—Blake Linder, Roodepoort *Northsider*

M. H. Carstens (✉)
Wake Forest Institute of Regenerative Medicine, Wake Forest University, Winston-Salem, NC, USA
e-mail: mcarsten@wakehealth.edu

M. H. Carstens (ed.), *The Embryologic Basis of Craniofacial Structure*, https://doi.org/10.1007/978-3-031-15636-6_18

In the study of congenital deformity, whenever a condition exists as a spectrum of presentations, the anatomy of its form fruste will point an accusatory finger at the embryologic defect. In 1938, Victor Veau conceptualized the cleft process as an "uninterrupted chain" of presentations from the subtle to the overt. Thus, the microform variant, the so-called "cleft lip nose" with a normal-appearing lip, constitutes the Rosetta Stone of clefts. Disciplined study of its anatomic features will reveal the following: (1) the exact location of the defect and its neuromere(s) of origin; (2) the effects exerted by the defect on the osseous and soft tissue surround; and (3) the developmental mechanisms by which these pathologies are produced.

The microform cleft established for me once and for all the locus of the deficiency site, the lateral nasal floor and piriform fossa. At the time I had stumbled on the stapedial system, or the premaxillary field as the primary defect. Instead I was conceptualizing cleft pathophysiology as a sequence of four *processes*: *deficiency*, *division*, *displacement* and *distortion*; these were the consequences of some unidentified "event."

"Biologic events at the deficiency site transform the surrounding functional matrix creating asymmetry of force vectors which, acting over time, cause distortions of otherwise normal structures in developmental fields adjacent to the cleft site. The microform cleft deficiency site, an abnormal developmental field, represents the cleft 'lesion' in its purest form. As such it provides insights into all other forms of cleft spatial and temporal aspects of perioral and nasal development."

The objective of this chapter is to explore spectrum of incomplete cleft using the microform variant as focus. Although in the original paper there were many concepts I did not understand, it proved a crucial step forward [2, 3]. Analysis of the *form fruste* variant revealed for the first time the location of the cleft "lesion." Dentoalveolar abnormalities in the microform convinced me that a deficiency in bone stock in the nasal floor was universal in all clefts and that it was somehow related, not only to the nasal deformity, but the lip cleft as well. What's more the deficit was somehow quantitative: the worse the bone deficit, the more pronounced were the soft tissue finings. Using the Carnegie system and SEMs by Hinrichsen I was able to reconstruct the structural events of lip closure [4]. What we can now bring to this story is the model of neuroangiosomes based on the stapedial system, the BMP4/SHH model of epithelial fusion and the insights of Talmant regarding the nasalis muscle complex and its misinsertion in the cleft state.

In sum, we can now explain the entire spectrum of cleft deformity and apply the concepts of DFR surgery to achieve an embryologically accurate correction.

We shall address the following topics

- Pathologic anatomy of the microform cleft
- Developmental sequence of the microform cleft
  - Developmental fields
  - Nasolabial fusion sequence
  - Lateral nasal process as a dysfunctional matrix
  - Biochemical evidence: the carbon monoxide hypothesis
- Muscle in cleft lip and cleft palate: histology and histochemistry
  - Diffusible morphogen model
- Clinical studies of microform cleft
  - Classification: Boo-Chai and Mulliken
- Neurovascular anatomy of the prolabium and premaxilla
- Developmental field reassignment and the incomplete cleft
- The pathology of nasal-labial-maxillary cleft lip and palate

Anatomic Features of the Microform Cleft (Figs. 18.2, 18.3, 18.4, 18.5, 18.6, 18.7, 18.8 and 18.9)

Previous reviews have described the characteristics of the minimal deformity [5–7]. The emphasis was placed upon the nose and soft tissue abnormalities of the lip. Comments about them were based on neuromeric model.

Alveolar abnormalities are basic to the pathological lesion of the minimal cleft. The deficiency of bone stock begins in the frontal process of premaxilla (PMxF) and extends downward to the lateral incisor zone (PMxB), causing a caudal lowering of the floor of the piriform fossa (and its vestibular lining). If something is wrong with the neural crest dental lamina, the teeth on the cleft will will erupt later. An occult cleft of the primary palate is sometimes present. As one move from the microform to the incomplete form, the alveolus may be frankly cleft. Frank deformation of the lateral piriform margin is universal in microform cleft; this represents the defect in PMxF.

Dental disturbances include the following: (1) missing or supernumerary teeth, (2) alterations in tooth size or shape, and (3) abnormal eruption pattern, including overcompensation by the mandibular dentition [8, 9]. The first two conditions arise from the *dental germ line* in situ. The third and fourth conditions reflect the *osseous environment* within which they form. Because the bone arises within a soft-tissue matrix, any deficiency or deformation of that matrix will alter the form and spatial positioning of the bone stock. The physical forces exerted on the alveolar bone (and ultimately on the dentition) are likewise affected.

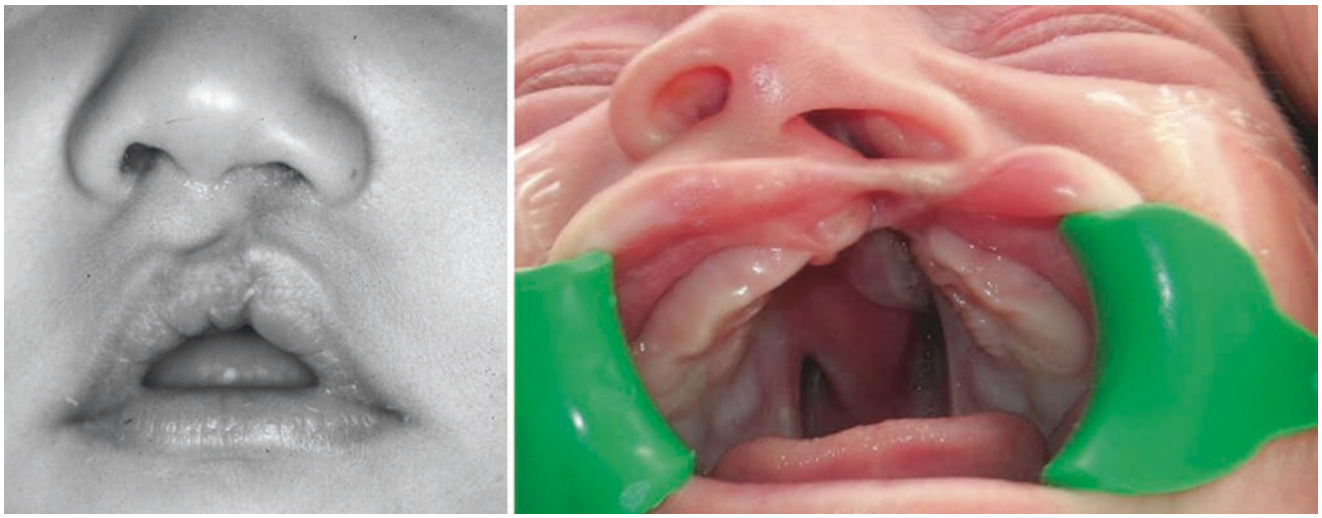

Fig. 18.2 Microform cleft. (Left): Note epithelial "scar does not approximate the left alar footplate. It tracks into the nasal floor. Note how reassignment of non-philtral prolabium "drapes" itself into the nasal floor. Nostril sill is "in-turned" and not readily seen. (Right): **Simonart's band** conducts mesenchyme from lateral-to-medial. It can also create an adhesion between maxillary alveolus and premaxillary alveolus. In this case, there does not seem to be bone between the two alveolar processes, making this an incomplete cleft lip with near complete primary palate cleft and a complete secondary palate cleft. Left: [Reprinted from Kim EK, Khang SK, Lee TL, Kim TG. Clinical features of the microform cleft lip and the ultrastructural characteristics of the orbicularis oris muscle. Cleft Palate–Craniofac J 2010; 47(3):297–302. With permission from SAGE Publishing]. Right: [Reprinted from Biljic F, Sozer OA. Diagnosis and presurgical orthopedics in infants with cleft lip and palate. Eur J General Dentistry 2015; 4(2): 41–47. With permission from Wolters Kluwer Health, Inc.]

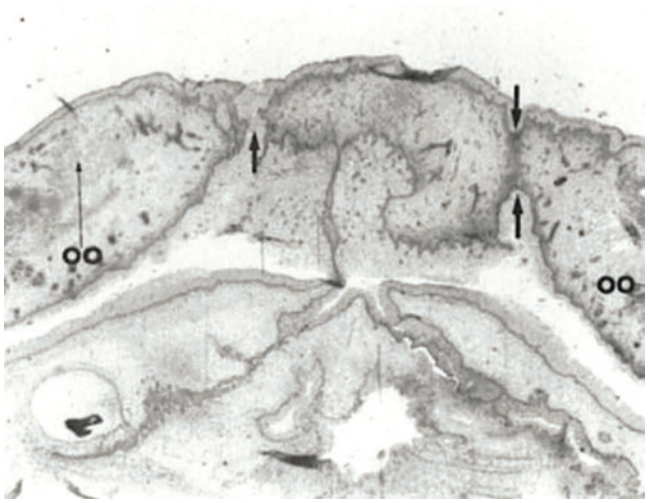

Fig. 18.3 Subepithelial cleft. A 18-week specimen with interruption of orbicularis oris (**00**) bilaterally. Note the complete connective tissue interruption on the left **(arrow)** but only partial interruption on the right (double arrow). The striking feature is the *fibrotic tissue* on the incomplete side: muscle cannot form. [Reprinted from Martin RA, Jones KL, Benirschke K. Extension of the cleft lip phenotype: The subepithelial cleft. Am J of Med Genet 1993; 47:744–747. With permission from John Wiley & Sons]

Nasal deformity is the *sine qua non* of the microform cleft

- Deficiency of the functional matrix (i.e., loss of PMxF and deficiency of PMxB) within the floor of the nose pulls the entire vestibular lining into the site. This sets up traction forces that deviate the nasal tip and the cephalic portion of the columella toward the cleft. The base of the columella is affected as well. Asymmetric muscle insertion of oblique fibers of Delaire (SOO) traction is to the non-cleft side.
- On the cleft side, the nostril floor is pulled downward into the bone deficit exerting *traction on the medial footplate*, drawing it downward and backward. The insertion of the paranasal muscles into the alar base is asymmetrical, causing it to drift laterally away from the midline. The *lateral alar crease* becomes indistinct, blending into the cheek.
- *Nasalis* fails to insert correctly over the canine and lateral incisor fossae. Instead it inserts falsely into the nasal floor, causing downward traction of the lateral crus.
  - Pars transversus inserts over the canine.
    In microform it inserts into the piriform fossa.
  - Pars alaris inserts over the lateral incisor.
    In microform it inserts into skin of the nostril sill.
- The *lower lateral cartilage* develops at 4 months' gestation within a deformed soft-tissue envelope. Thus, it is not surprising that it occupies a lateralized position. Boo-Chai and Tange reported that the alar cartilage separated from its Opposite member by fibrofatty tissue [10]. This is reminiscent of similar findings by Trott in bilateral cases [11]. Although there is no intrinsic change in the size of the alar cartilage, its distortion blunts the tip's definition and flattens out the alar rim.

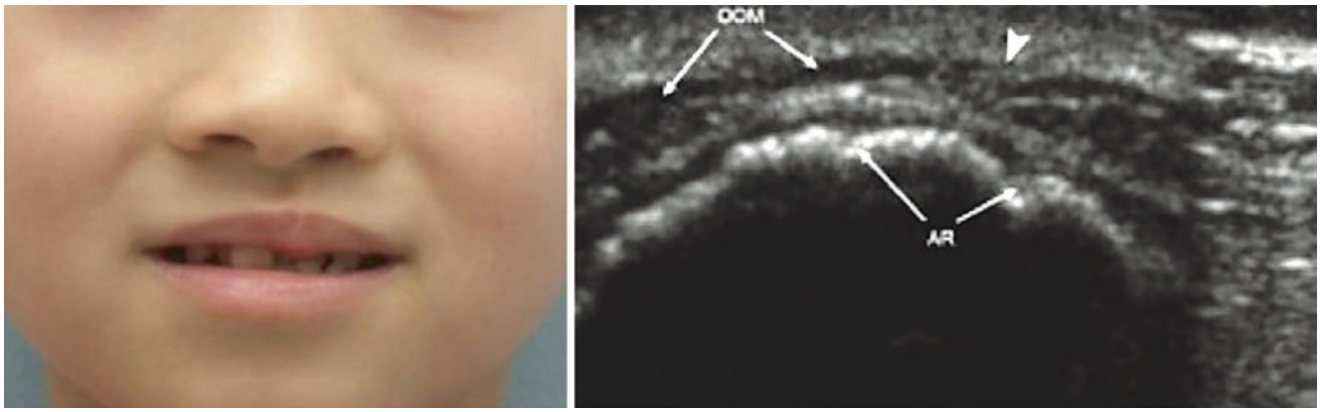

Fig. 18.4 Subepithelial and microform defects. Ultrasound images of the Proband S91C, which has an orbicularis oris muscle defect. Ultrasound images are taken in the transverse plane; the top of the image corresponds to the anterior structures; *OOM* orbicularis oris muscle, *AR* alveolar ridge. The arrowhead in (A) points to the discontinuity in the OOM of the proband. The subject's left is on the right. [Reprinted from Marzita ML. Subclinical features in non-syndromic cleft lip with or without cleft palate (CL/P): review of the evidence that subepithelial orbicularis oris muscle defects are part of an expanded phenotype for CL/P. Orthod Craniofacial Res 2007;10: 82–87. With permission from John Wiley & Sons]

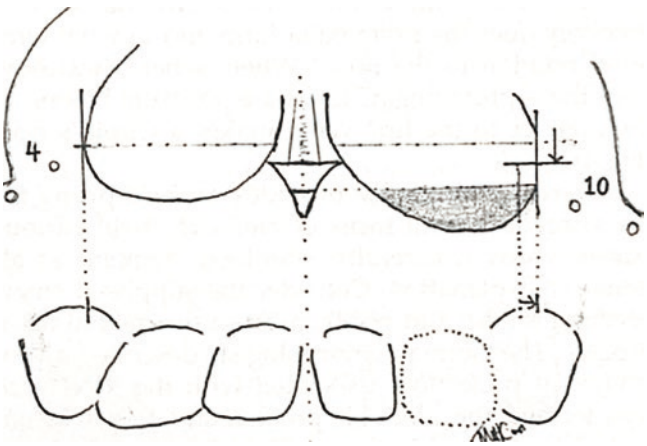

Fig. 18.5 Piriform fossa deficiency is universally present in microform cleft. Although the alveolus remains intact, the alveolus always has: (1) a "scooping out" of the lateral wall due to deficiency or absence of frontal process zone of premaxilla, PMxF; and (2) a depression in the nasal floor due to deficiency in lateral incisor zone of premaxilla, PMxB. Note that PMxF is a vertical outgrowth of PMxb. It marks the terminal perfusion of the medial nasopalatine axis. PMxF abuts against its counterpart, frontal process of maxilla, MxF, which is supplied by a small branch from the medial division of anterior superior alveolar artery before its exit from the sinus cavity. MxF provides housing for the third incisor. Volume deficit clearly seen. The cleft airway is compromised by tightening of the vestibule, abnormal nasalis and posterior septal reflection. Septum is forced over by increased hydraulic pressure in the normal airway during fetal breathing of amniotic fluid. [Courtesy of Michael Carstens, MD]

- The nostril sill is "hidden," being retracted backward into the deficiency site of the lateral vestibular wall.

Orbicularis oris has two layers which behave differently in the microform cleft

- The deep (sphincteric) layer of orbicularis (DOO) is unaffected [12, 13].
- The superficial (dilator) layer of orbicularis (SOO) does not "fill" the philtral columns. Even though the peripheral fibers of the deep layer fill out the vermilion, the superficial deficiency may draw up the mucocutaneous border into a notch.
- The oblique fibers of Delaire may not be inserted, causing a flattening of the upper lip just inferolateral to the columella.

Subepithelial manifestations in microform range from stria to fibrosis with a dimple on animation corresponding to SOO misinsertion. These subtleties are characterized by histologic changes consistent with fibrosis [14]. Ultrasound now demonstrates this fibrosis as a hypoechoic interruption in an otherwise hyporechoic (black) band corresponding to orbicularis [15, 16].

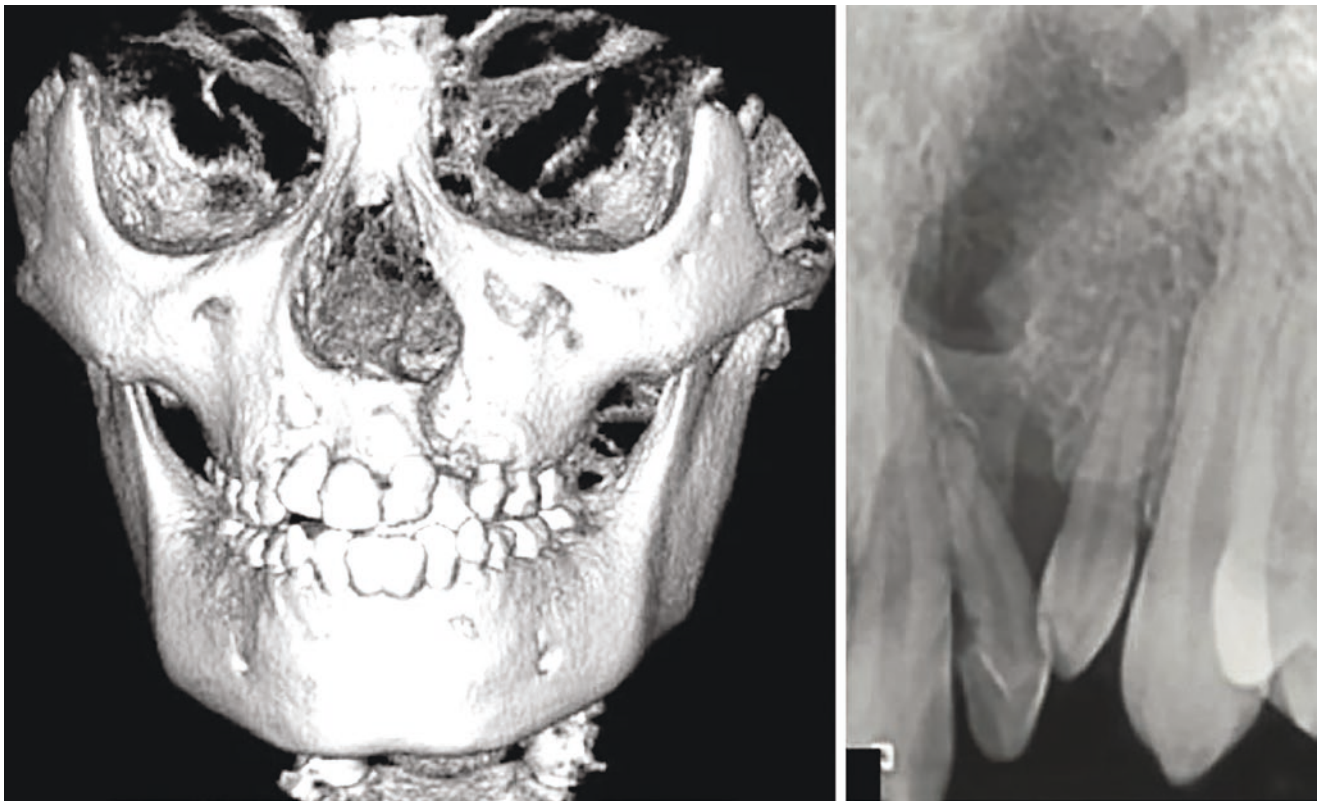

Fig. 18.6 Cone beam CT (CBCT) of primary palate cleft demonstrates typical piriform depression. Panorex of the same patient showing depression of lateral piriform wall and thinning of alveolar bone around the unerupted canine. Note reduction if bone volume in PMxA (central incisor) on the cleft side. [Reprinted from Machado G. CBCT imaging—A boon to orthodontics. Saudi Dental Journal 2015; 27(1): 12–21. With permission from Elsevier]

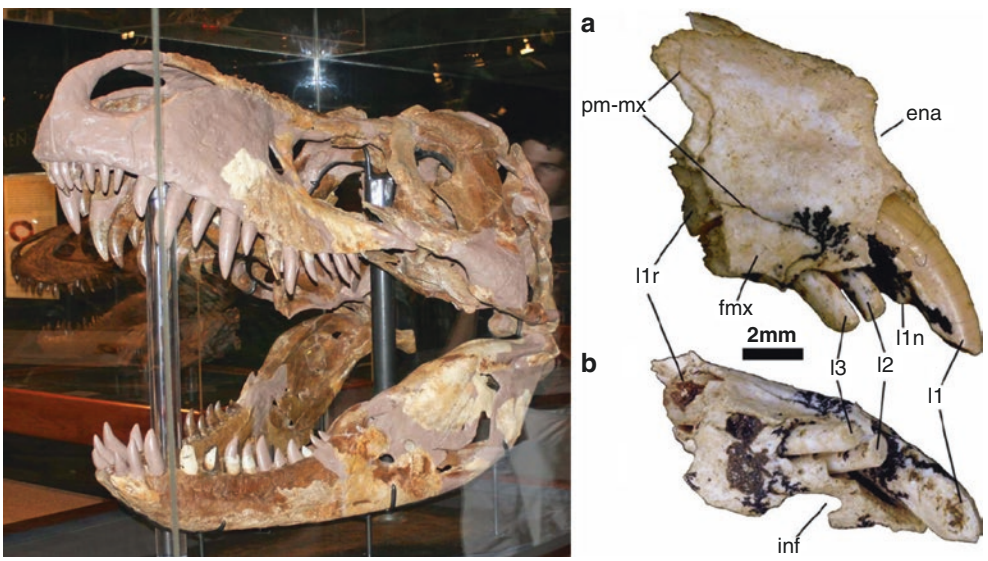

Fig. 18.7 Dental content of the premaxilla changes with evolution. (Left): *Tyrannosaurus rex* premaxilla had four teeth per side but these were not differentiated into incisors. The basal formula for placental mammals has three incisors in the premaxilla. (Right): (**a**, **b**) Prehistoric marsupial *Yalkaperidon,* shows basal dental formula with three incisors in its premaxilla, *Ena* external nasal aperture, *fmx* facial process of maxilla, *L1n* notch on distal surface of first premaxillary upper incisor for contact with first mandibular incisor, *I1r* open root of first upper incisor, *inf* incisive foramen, *pm-mx* premaxillary-maxillary suture. Left: [Reprinted from Wikimedia. Retrieved from: https://commons.wikimedia.org/wiki/File:T._rex_MOR_008.jpg. With permission from Creative Commons License4.0: https://creativecommons.org/licenses/by-sa/4.0/deed.en.] Right: [Reprinted from Beck RMD, Travouillon KJ, Aplin KPA, Godthelp H, Archer M. The osteology and systematics of the enigmatic Australian Oligo-Miocende metatherian, *Yalkaperidon* (Yalkaparidontidae; Yalkaparidontia? Australidelphia; Marsupialia). J Mammalian Evolution 2014; 21:127–172. doi:10.1007/s10914-013-9236-3. With permission from Springer Nature]

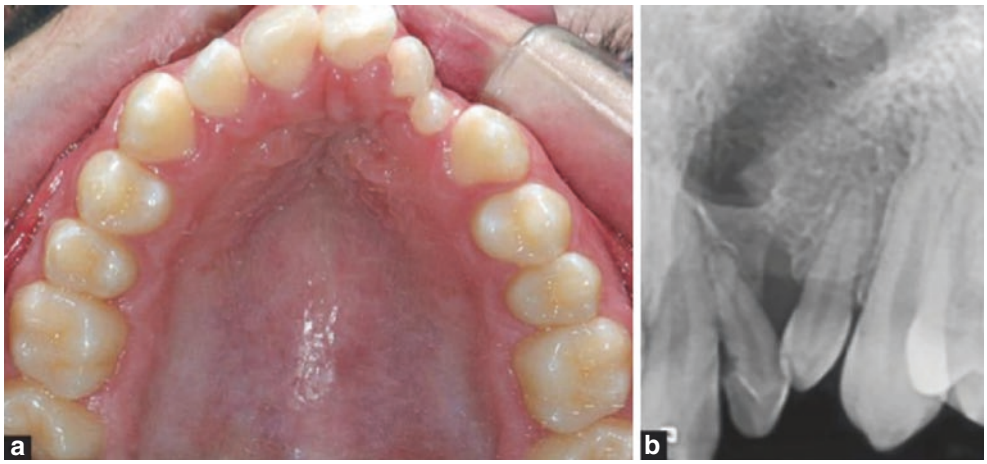

Fig. 18.8 Incisors are located on *either* side of alveolar cleft. (**a**) Oral view palate shows three incisors are present in the case of form fruste alveolar cleft. Permanent central incisor is forced to erupt over the mesial incisor. (**b**) Distal incisor in Mx1 is seen on the other side of the cleft. [Courtesy of Michael Carstens, MD]

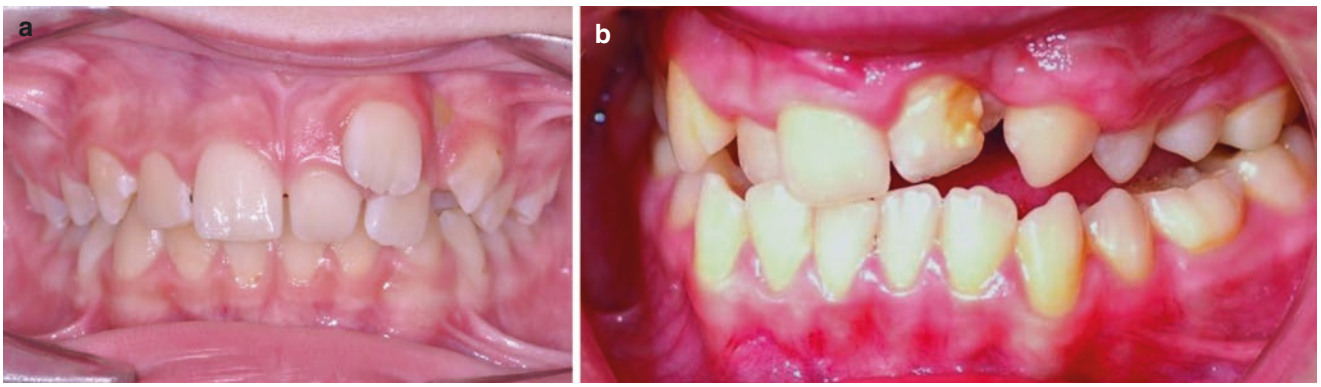

Fig. 18.9 Abnormal eruption. (**a**) Three incisors are present in the case of form fruste alveolar cleft. Permanent central incisor is forced to erupt over the mesial incisor. Distal incisor in Mx1 is seen on the other side of the cleft. Cleft-associated enamel hypoplasia. (**b**) Lateral incisor mesial to cleft shows severe enamel defect; the canine is affected to a lesser degree. (**a**) [Reproduced from Orthodontic Update (ISSN 1756-6401), by permission of George Warman Publications (UK) Ltd]. (**b**) [Reprinted from Pegelow M, Algardi N, Karsten AL-A. The prevalence of various dental characteristics in the primary and mixed dentition in patients born with non-syndromic unilateral cleft lip with or without cleft palate. Eur J Orthod 2012; 34(5):561–570. With permission from Oxford University Press]

Consequences of Muscle Imbalance in the Cleft State

Origin and Migration of Facial Muscles

The muscles surrounding and animating the nose and lip originate when the paraxial mesoderm of the sixth somitomere melds with neural crest from r4–r5 to produce the second pharyngeal arch which appears at Carnegie stage 10. Within the arch, myoblasts are segregated into three functional layers, each defined by its own fascia. *Buccopharyngeal fascia* contains pharyngeal constrictor buccinator and a partial contribution to superior constrictor. *Deep investing fascia* is dedicated to muscles of mastication: anterior digastric, stylohyoideus and evolutionary transformation in mammals, stapedius. *Superficial investing fascia* (SMAS) carries within it the muscles of facial expression and spreads below the subcutaneous fascia to envelop the entire face and head, and the anterior neck.

- It is of evolutionary interest that deep orbicularis, although programmed, just like buccinator, by the oral mucosa, does not share buccopharyngeal fascia with buccinator. The BPF stops at the modiolus.

By stage 12, the second arch has melded into the first arch to produce the maxillary process, MxP. This term, encrusted forever in our anatomic lexicon, is a misnomer because MxP subdivides along its axis. The upper zone containing r2/r4 neural crest becomes the maxilla and its supporting bone field. The lower zone with r3/r5 neural crestbecomes the mandible. The "fault line" between the zones extends from the oral commissures back to the external auditory canal. The embryonic separation can be observed in lateral facial clefts.

As we shall see, during stages 13 and 14, the first arch invades the floor of the frontonasal process and by stage 15 MxP has arrived in position. From here facial myoblasts are

carried within the flow of neural crest fascia in two arcs surrounding the orbit. The *supraorbital migration* brings Sm6 muscles to the forehead and glabella. The *infraorbital migration* provides all the rest, with the individual muscles developing in deep-to-superficial and lateral-to-medial sequences [17]. **Note**: *the terminal muscle in each migration inserts last and is the* ***most vulnerable*** *to disturbances at its insertion site*.

- Procerus is the terminal muscle of the supraorbital migration.
- Nasalis is the terminal muscle of the infraorbital migration.

Insertions of Facial Muscles: Two Mechanisms

Proximal-distal They can migrate into position within a structure, such as a fascia, which constitutes the primary insertion. Subsequently they seek out a secondary insertion into bone or dermis, when the latter manifests a BMP4 signal which is detected by the fascial envelope which follows the muscle into contact, sometimes becoming a tendon. Here are two examples. *Frontalis* begins in the SMAS and has its secondary insertion upward into the aponeurotic fascia of epicranium. *Orbicularis* DOO begins with a fascial condensation of SMAS at modiolus and then extends mesially to insert into contralateral DOO.

Distal-proximal In this mechanism, the muscle migrates all the way to the distal site and binds to it. In so doing, it retains its fascial envelope which constitutes a sort of "trail of bread crumbs," which marks the migration route. Subsequently the muscle extends backward along the trail until it encounters the next available insertion site. *Biceps brachii* forms a single muscle mass with primary insertion on the humerus. Secondary insertions are backwards to scapula, the long head to the glenoid and the short head to coracoid process. Nasalis migrates over the nasal dorsum to gain primary insertion to the contralateral muscle. Secondary insertions of nasalis are into two distinct sites of premaxilla: canine fossa and lateral incisor fossa.

Muscle Anatomy in Labionasal Clefts: The Muscle Ring Theory of Delaire

Faulty signals from underlying bone fields affect soft tissue fusion. Naturally the superficial layer is affected first. For this reason, in microform cleft, SOO becomes dysplastic first. Disruption of DOO follows the mucosal defect. The effect of these changes in microform cleft is subtle, seen primarily in the columellar base. But as the deformity increases in severity, lateral drift of the alar base is seen. Based on the anatomy of the complete cleft, alar drift has traditionally been ascribed to lateral traction exerted by periorbital muscles, but this construct cannot occur in the microform cleft because muscle continuity across the midline is preserved. The best explanation for alar drift in the microform is the false insertion of nasalis into the nostril sill.

Delaire and Markus described a system of three rings of facial muscle all converging on the lip. In this model, the pathologic anatomy of complete cleft lip results from the breakup of these rings, generating abnormal force vectors which drag the soft tissues of the face into asymmetry. Proper surgical treatment would consist in re-establishing facial balance. The moulding effect of facial muscles on the underlying maxilla was of concern for Bardach. These studies were important signposts refuting the idea that maxillary "hypoplasia" is intrinsic to the cleft condition. Retrusion of isolated envelope as can be seen in bilateral clefts [18, 19] is the result of unequal force vectors to the midline, leaving the cleft-side maxilla disconnected (Figs. 18.10, 18.11, 18.12, 18.13, 18.14, 18.15 and 18.16).

Nasalis is the *Forme Fruste* Muscle Involved in Nasolabial Clefts

The region above the primate premaxilla gives rise to small muscles with secondary insertion into the fossae above the incisors. As previously discussed, humans have a central and a lateral incisor but a third incisor is frequently present [20]. This is entirely unremarkable. Recall that dental specialization appears with placental mammals due to the complexities

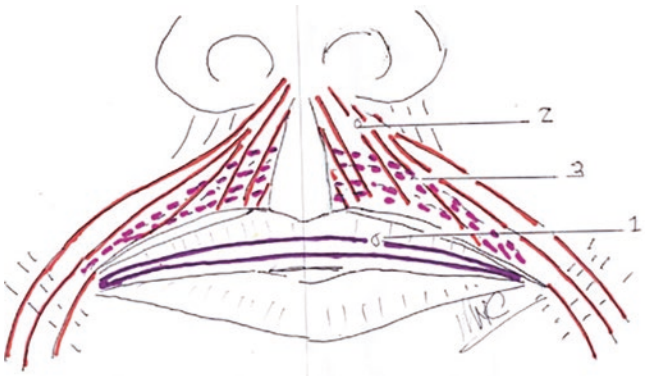

Fig. 18.10 Orbicularis oris fibers. Deep (sphincteric) layer of orbicularis oris (DOO) is almost completely hidden by superficial (dilator) layer of orbicularis oris (SOO) except at the vermilion were it presents as *pars marginalis*. Note that DOO is continuous caudal to Cupid's bow (philtral prolabium). SOO has two parts: *Pars transversalis* fibers (2) do not extend medial to the philtral column. They are blocked by r1 mesenchyme; *Pars obliquus* fibers (2) extend upward to blend with the columellar base. Delaire pointed out the importance of these fibers in establishing the "aesthetic drape" of the lip. Note the potential for confusion between these fibers and those of depressor septi nasi. Orbicularis is superficial to DSN and to the nasalis muscle bellies. DSN actually takes origin from the fossae above the central incisors. [Courtesy of Michael Carstens, MD]

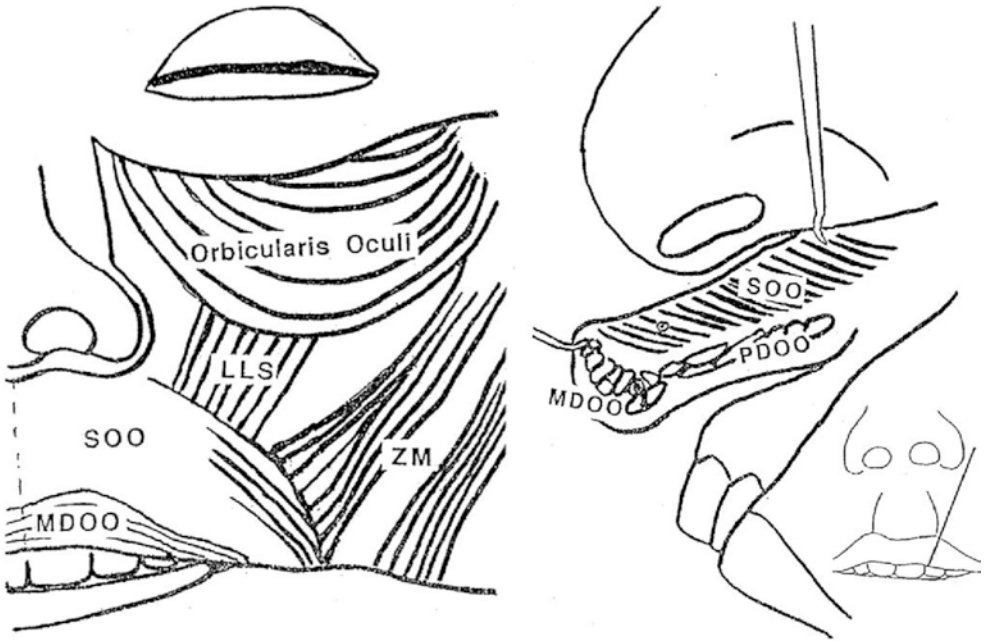

Fig. 18.11 Lateral lip element showing DOO and SOO. Note how the pars marginalis of DOO runs along the vermilion border and turns up to define the wet-dry mucosal line. Artery runs between the "J" of DOO and distal SOO. [Reprinted from Park CG, Ha B. The importance of accurate repair of the orbicularis oris muscle in the correction of unilateral cleft lip. Plast Reconstr Surg 1995;96(4):780–788. With permission from Wolters Kluwer Health, Inc.]

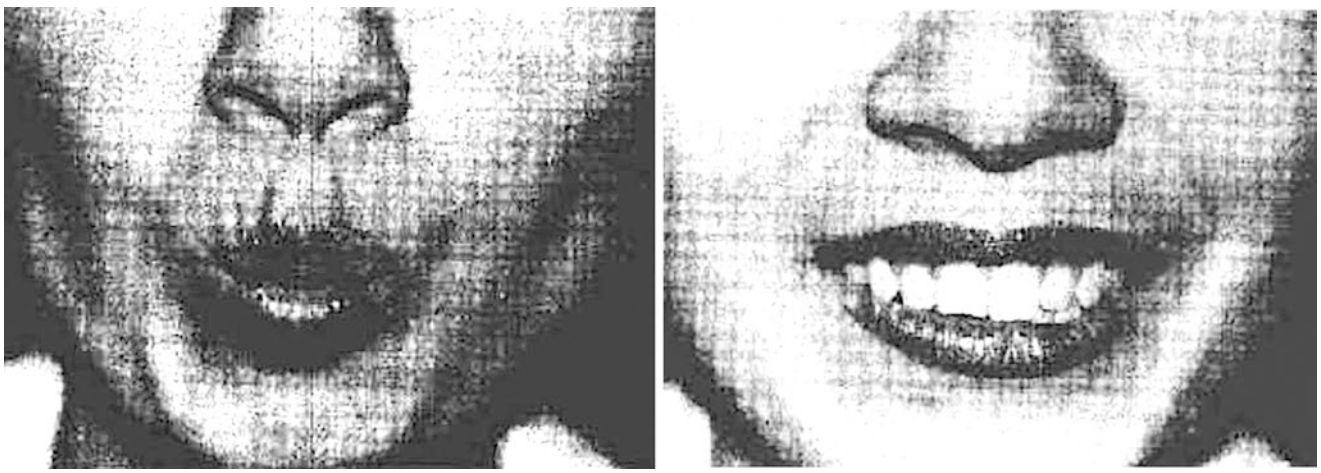

Fig. 18.12 Function of DOO versus SOO on the philtral columns. Note that DOO inserts into modiolus in the same plane as buccinator but does not have SMAS. [Reprinted from Park CG, Ha B. The importance of accurate repair of the orbicularis oris muscle in the correction of unilateral cleft lip. Plast Reconstr Surg 1995;96(4):780–788. With permission from Wolters Kluwer Health, Inc.]

of their chewing apparatus, the baseline formula being I3, C1, P4, M3. There is likely some type of suppression present in the normal state such that, in the presence of PMxB, the dental lamina of the third incisor that would correspond to PMxF does not develop. In development the bone above each of the 3 tooth roots, in response to morphogen BMP4, opens up (within a limited time frame), a secondary binding site for a muscle. These are:

- Central incisor: (PMxA) depressor septi nasi (DSN)
- Lateral incisor 1 (PMxB): medial head of nasalis
- Lateral incisor 2 (PMxF): lateral head of nasalis

Anatomic studies of these muscles have, by virtue of the overlying orbicularis and outdated terminology, resulted in confusion. The embryonic layering of the orbicularis complex is also not appreciated. A good example of this is the so-called caninus muscle, *levator anguli oris*. LAO lies deep to the 4 heads of *quadratus labii superioris* (also called levator labii oris). The primary insertion of LAO is at modiolus and its secondary insertion into the "canine fossa," located high up on the face of the maxilla, just below the infraorbital foramen. This fossa is a misnomer, having nothing to do with canine tooth. It is separated from incisor fossa by the *canine ridge*, an eminence properly due to the root of the canine.

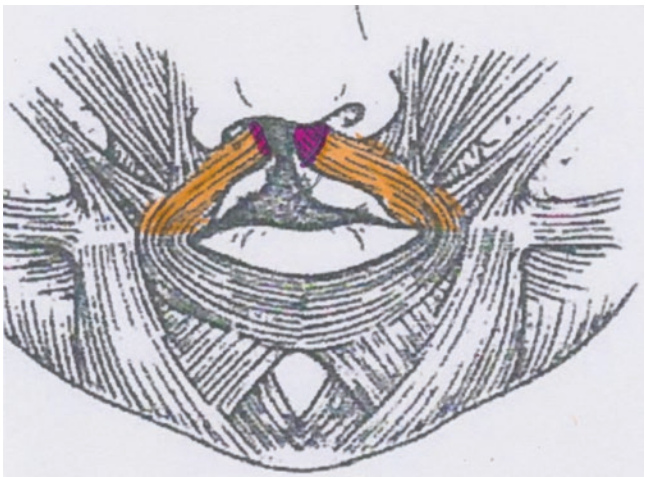

Fig. 18.13 Unilateral cleft lip showing interruption of muscles. Note the unbalanced muscle pull on the columella. [Reprinted from Slaughter WB, Henry JW, Berger JC. Changes in blood vessel patterns in bilateral cleft lip. Plast Reconstr Surg Transplant Bull. 1960 Aug;26:166–79. With permission from Wolters Kluwer Health, Inc.]

- LAO lies lateral to canine ridge
- Lateral head of nasalis inserts medial to canine ridge

Depressor septi nasi and nasalis have been confused with one another due to technical execution of the dissection. De Souza Pinto, began from under the lip, proceeding upward through orbicularis, described depressor septi nasi as having *three* heads, with the most medial being directed to the septum and the lateral two being inserted into the accessory cartilages of the nose. In reality, he actually described the two heads of nasalis, seen in situ on the premaxilla. Because he did not complete the dissection above the cartilages, he missed the functional relationship with the remainder of nasalis. His study correctly recognized DSN to be of significance for the aesthetic management of the nasal lip, but this was not related to the functional significance of the latter two heads (Figs. 18.17, 18.18, 18.19, 18.20, 18.21 and 18.22).

Rohrich provides a good review of DSN studies. Barbosa correctly showed DSN to relate strictly to septum. He noted

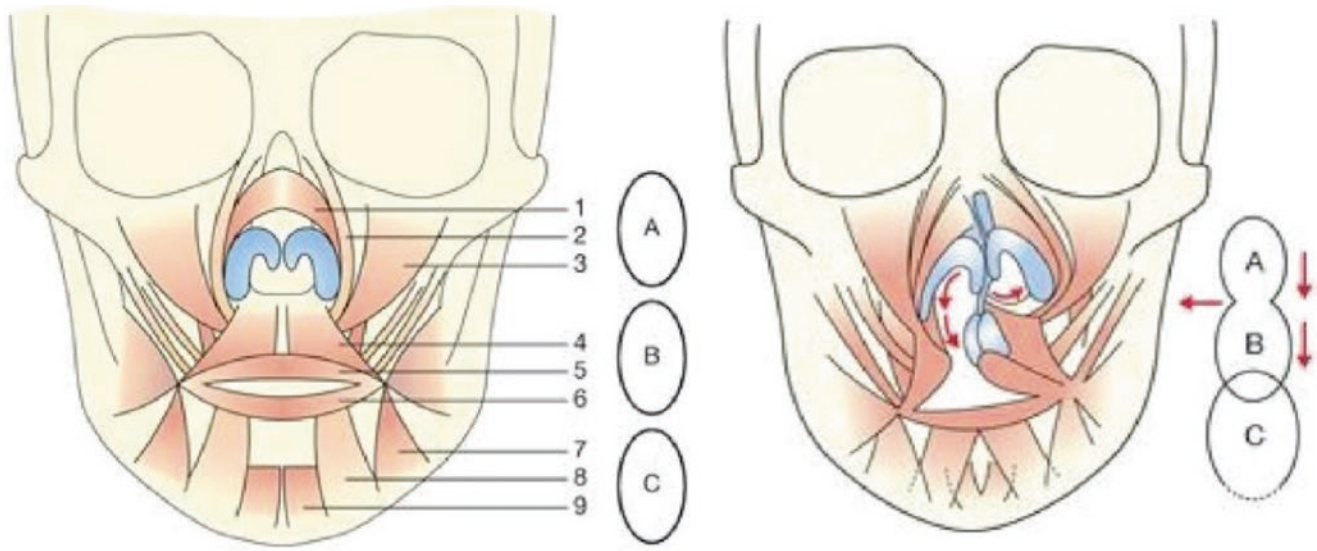

Fig. 18.14 Muscle ring theory of Delaire. A, nasolabial muscles (1–3), B, bilabial muscles (4–6), C, labiomental muscles (7–9). Nasalis pars transversalis (1), levator labii superioris et alaeque nasi (2), levator labii superioris (3), orbicularis obliquus (4), orbicularis transversus (5), orbicularis lower lip (7), depressor labii inferioris (8), mentalis (9). [Reprinted from Markus AF, Delaire J. Primary closure of cleft lip. Br J Oral Maxillofac Surg 1993; 31(5):261–291. With permission from Elsevier]

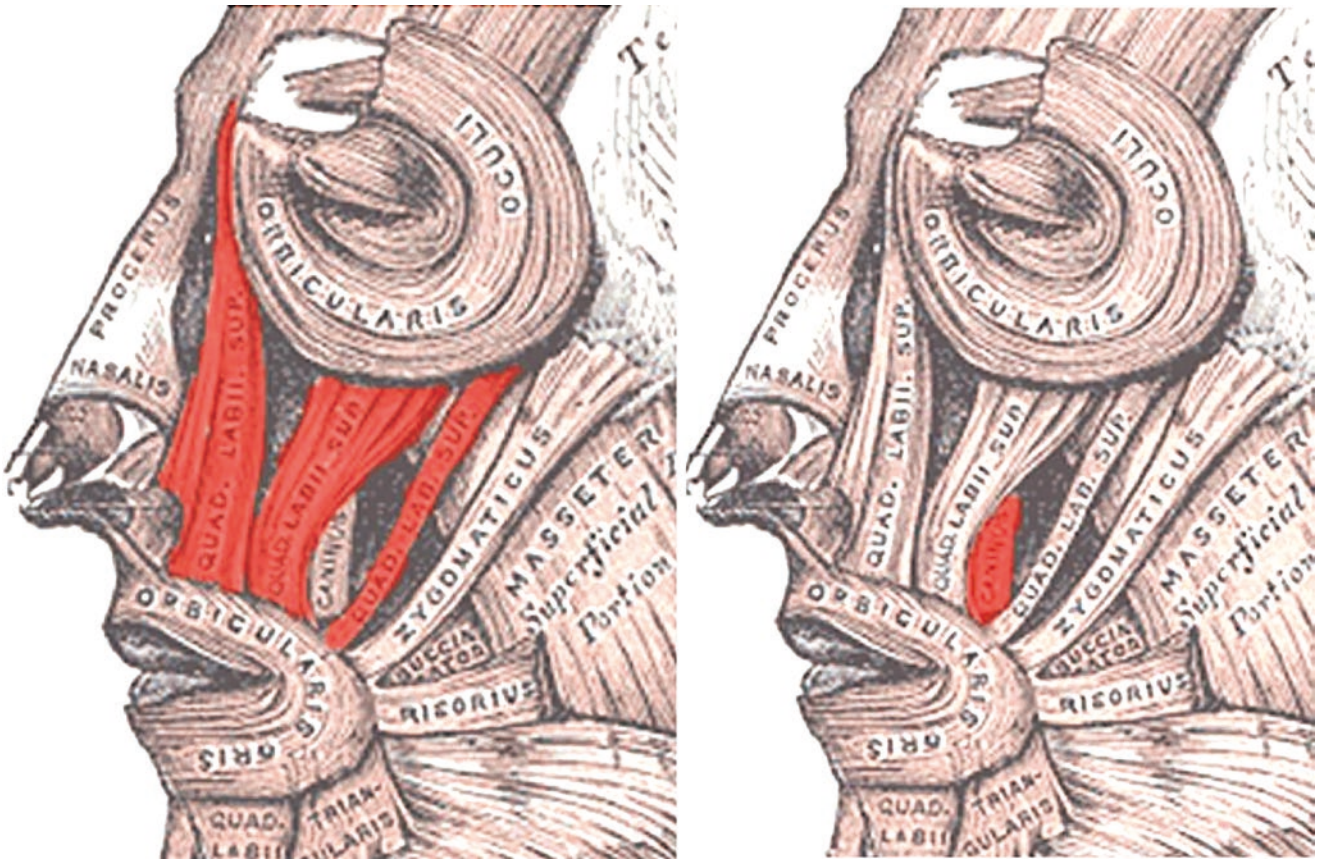

Fig. 18.15 Muscles inserting into upper lip and modiolus. *Superficial layer* Levator labii superioris (red), also known as quadratus, due to its 4 heads. The medial 3 have primary insertion into the SMAS of upper fibers of orbicularis. The lateral head has primary insertion into modiolus and is coplanar with zygomaticus major and risorius. *Deep layer* includes buccinator and caninus, also known as levator anguli oris. LAO has primary insertion at modiolus and secondary insertion into the misnamed canine fossa. Canine root. [Reprinted from Lewis, Warren H (ed). Gray's Anatomy of the Human Body, 20th American Edition. Philadelphia, PA: Lea & Febiger, 1918]

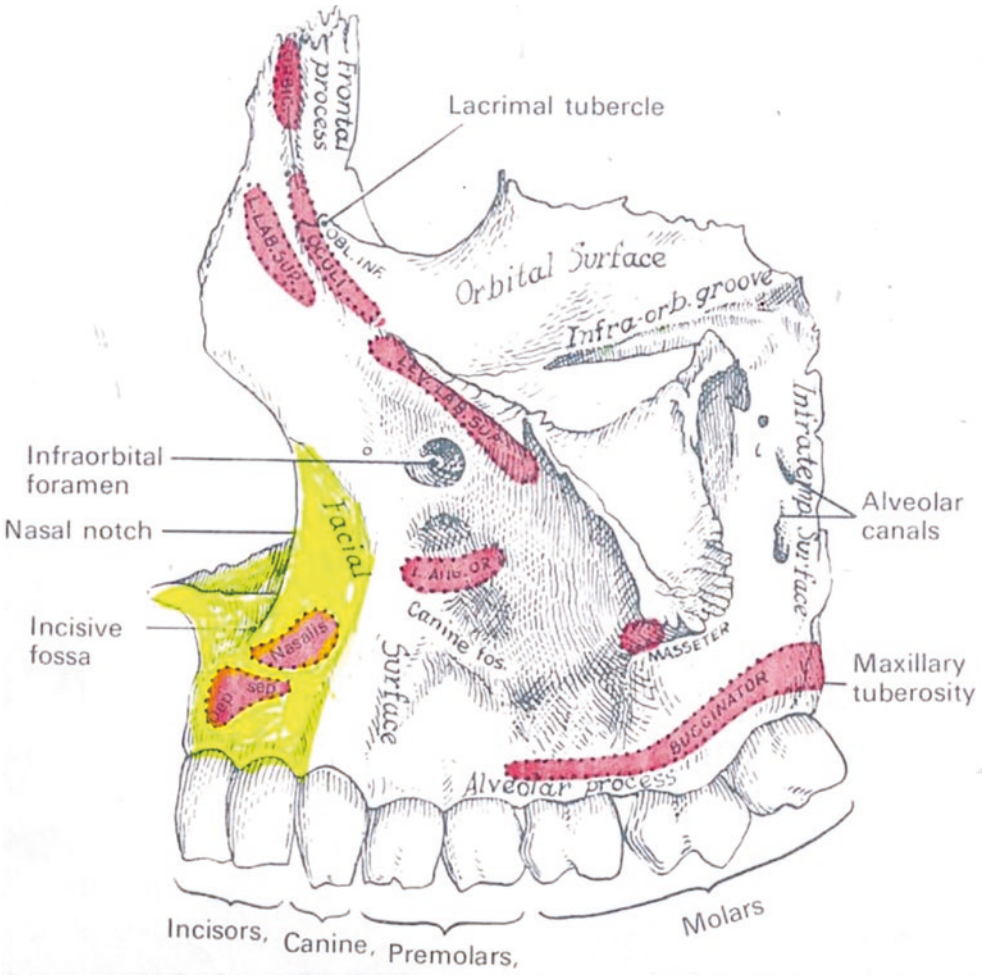

Fig. 18.16 Levator anguli oris and canine fossa. Note: (1) Triangular area over central incisor is insertion for depressor septi nasi. (2) Broad area over lateral incisor extending to canine ridge bears insertion of two heads of nasalis. (3) The canine ridge extends upward in curvilinear path as lateral piriform wall. Medially it shelters lateral head of nasalis. Laterally, it defines the canine fossa, so-labeled, beneath infraorbital foramen as the secondary insertion of caninus, i.e., levator anguli oris. Premaxilla (yellow) has frontal process, PMxF, ascending from lateral incisor process, PMxB, This zone is overlapped by frontal process of maxilla, MxF. This zone, between incisor 2 and canine is biologically capable of have a third incisor mesial to canine. [Reprinted from Lewis, Warren H (ed). Gray's Anatomy of the Human Body, 20th American Edition. Philadelphia, PA: Lea & Febiger, 1918]

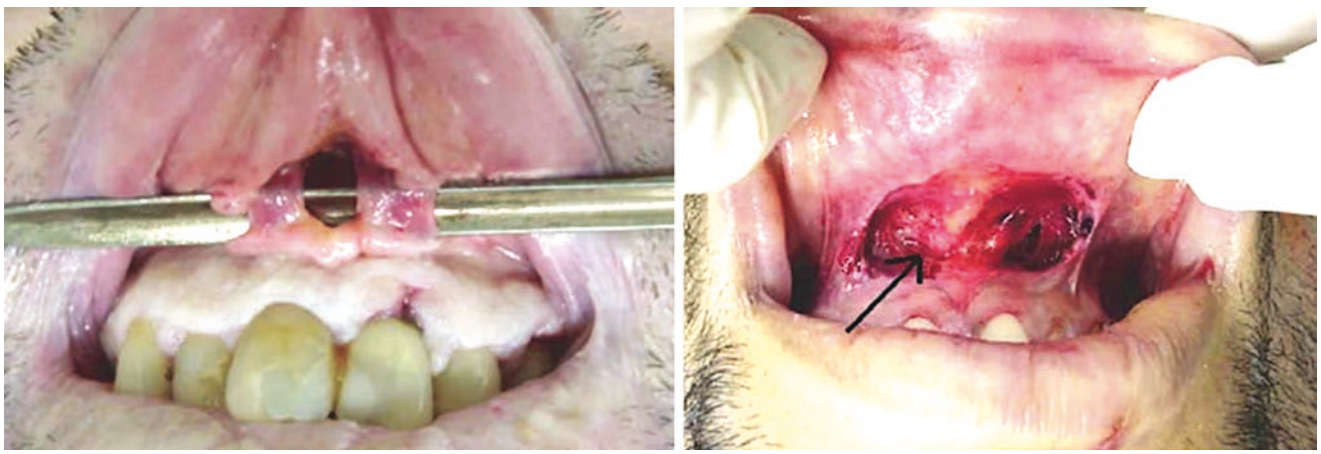

Fig. 18.17 Depressor septi nasi. Paired muscle bellies have primary insertion above the incisors. In UCLP, DSN on the cleft side fails to insert correctly over PMxA. It shift its insertion mesially to join with the DSN on the non-cleft side. Together, they exert traction on Pitanguy's ligament to traction the columellar base toward the non-cleft side. **Unilateral DSN**. [Reprinted from Barbosa MV, Nahas FX, Fereria LM. Anatomy of the depressor septi nasi. J Plast Surg Hand Surg. 2013 Apr;47(2):102–5. With permission from Taylor & Francis]

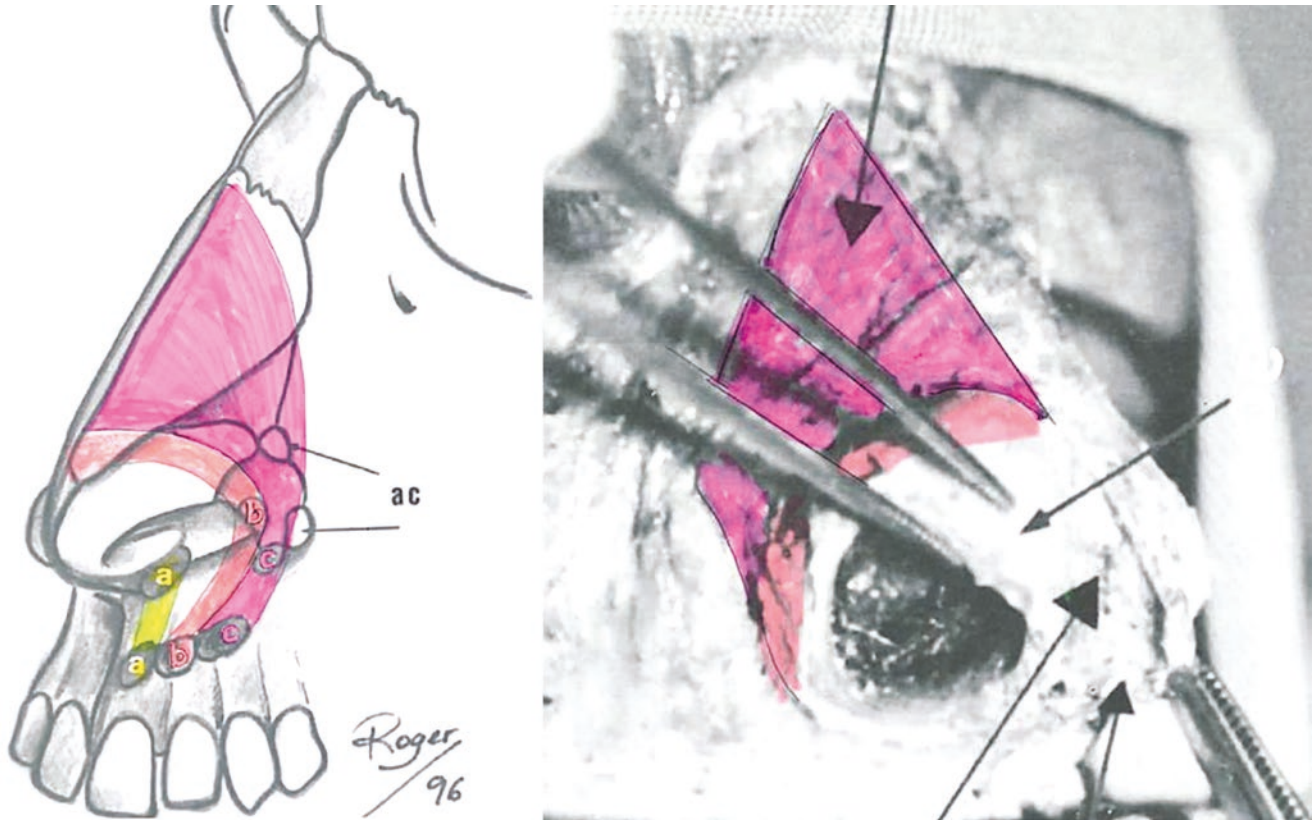

Fig. 18.18 DSN and nasalis. This is a very important concept. De Souza and others confuse lateral muscles as DSN with multiple heads. Nasalis, the rightful occupant of lateral incisor and canine insertion sites, was missed because of the direction of dissection was from below-upward

- DSN above the central incisor (yellow) acts on the mobile septum through the dermocartilagenous ligament (Pitanguy)
- Medial head of nasalis (tangerine) inserts above lateral incisor and extends over the alar cartilage as *pars alaris*
- Lateral head of nasalis (pink) inserts above canine and extends over the dorsum as *pars transversalis*

On the right we have a median section showing DSN (yellow) inserting into orbicularis (orange) and upward into the ligament of Pitanguy (P), i.e., the dermocartilagenous ligament (brown) sweeping in front of the septum (it is easily de identified) and over the midline of the dorsum. Traction on P pulls the nasal tip down with facial animation, especially smiling

[Modified from De Souza Pinto EB, Porto Da Rocha R, Queiroz Filho W, et al. Anatomy of the median part of the septum depressor muscle in aesthetic surgery. Aesth. Plast. Surg. 1998;22:111–115. With permission from Springer Nature]

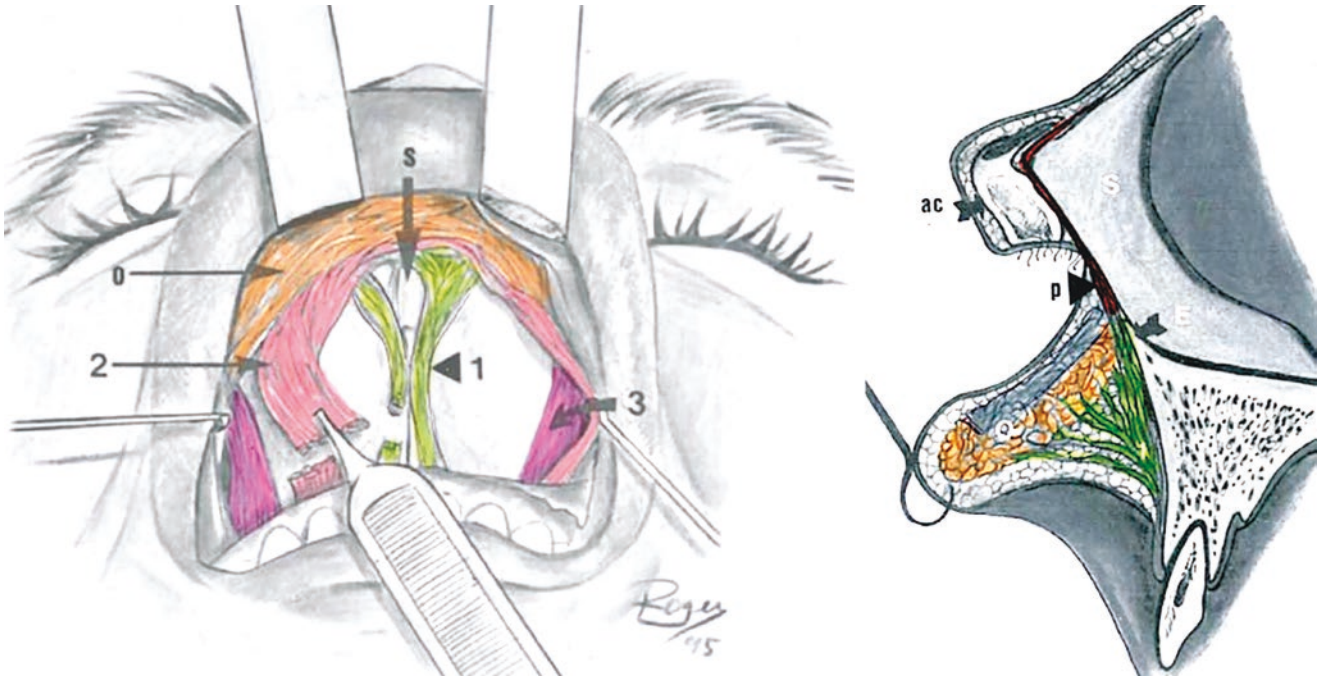

Fig. 18.19 DSN and nasalis. This is a very important concept. De Souza and others confuse lateral muscles as DSN with multiple heads. Nasalis, the rightful occupant of lateral incisor and canine insertion sites, was missed because of the direction of dissection was from below-upward. DSN above the central incisor (yellow) acts on the mobile septum through the dermocartilagenous ligament (Pitanguy). Medial head of nasalis (tangerine) inserts above lateral incisor and extends over the alar cartilage as pars alaris. Lateral head of nasalis (pink) inserts above canine and extends over the dorsum as pars transversalis. On the right we have a median section showing (1) DSN (yellow) inserting into orbicularis (orange) and upward into the ligament of Pitanguy (P), i.e., the dermocartilagenous ligament (brown) sweeping in front of the septum (it is easily de identified) and over the midline of the dorsum. Traction on P pulls the nasal tip down with facial animation, especially smiling. [Modified from De Souza Pinto EB, Porto Da Rocha R, Queiroz Filho W, et al. Anatomy of the median part of the septum depressor muscle in aesthetic surgery. Aesth. Plast. Surg. 1998;22:111–115. With permission from Springer Nature]

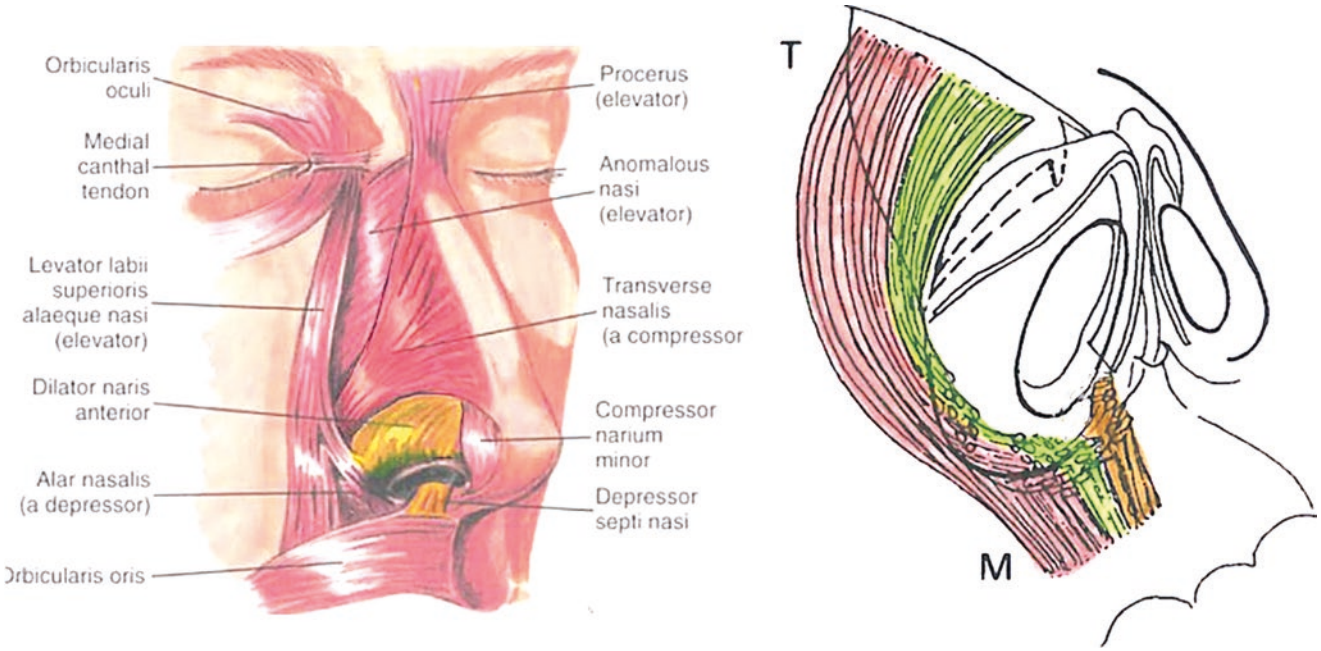

Fig. 18.20 Nasal muscles. Recall that the dental formula for placental mammals is I3, C1, P4, M3. Thus, the premaxilla has three potential binding sites. The site over canine is at the junction of premaxilla and maxilla. The most mesial zone of maxilla frequently houses a third incisor. *Pars transversus* (pink) inserts into the canine fossa. Pars alaris (lemon) inserts above lateral incisor. Depressor septi nasi inserts above the central incisor. The first two muscles act as dilators of the nasal airway. DSN has a midline insertion and tractions on the ligament of Pitanguy. Left: [Reprinted from Markus AF, Delaire J. Functional primary closure of cleft lip. Br J Oral Maxillofac Surg 1993; 31(5):281–291. With permission from Elsevier.] Right: [Courtesy of Michael Carstens, MD]

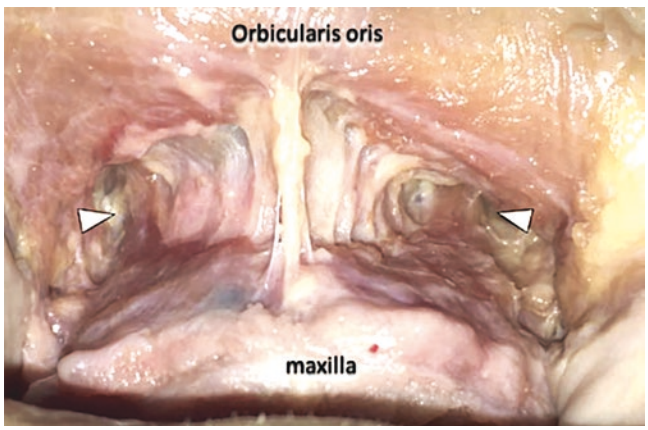

Fig. 18.21 Nasalis and depressor septi nasi in situ. DSN fibers are yellowish and ascend in the midline through orbicularis to seek out the ligament of Pitanguy, not seen because it is on the other side of the orbicularis. Nasalis fibers are a darker red color. The space between the muscles connect the floor of the piriform fossa. [Reprinted from Iwanga J, Watanabe K, Schmidt CK, Voin V, Alonso F, Oskouian J, Tubbs RS. Anatomical study and comprehensive review of the incisivus labii superioris (nasalis) muscle: application to lip and cosmetic surgery. Cureus 2017; 9(9): e1689. DOI 10.7759/cureus.1689. with permission from Creative Commons License 3.0: https://creativecommons.org/licenses/by/3.0/us/]

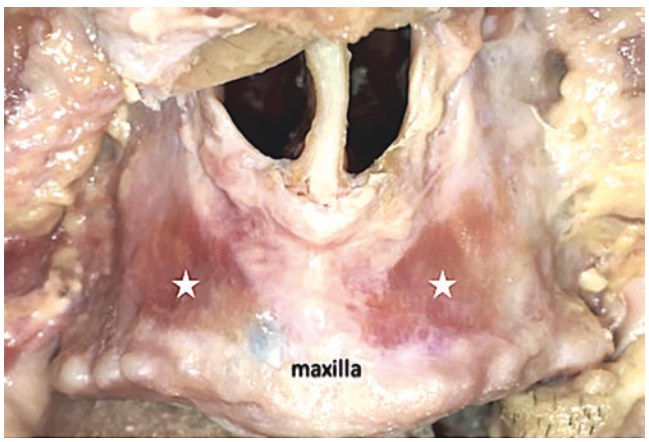

Fig. 18.22 Nasalis in situ over lateral incisor and canine. Fibers of depressor septi nasi (yellow color) over central incisor have been transected. They insert into the ligament of Pitanguy which lies directly in front of the septum. [Reprinted from Iwanga J, Watanabe K, Schmidt CK, Voin V, Alonso F, Oskouian J, Tubbs RS. Anatomical study and comprehensive review of the incisivus labii superioris (nasalis) muscle: application to lip and cosmetic surgery. Cureus 2017; 9(9): e1689. DOI 10.7759/cureus.1689. With permission from Creative Commons License 3.0: https://creativecommons.org/licenses/by/3.0/us/]

the absence of DSN in complete UCL. He also identified a case of rudimentary right-sided DSN, causing deflection of the columellar base to the left. This is of potential value in microform cleft, as it could contribute to deflection of the columellar base. The roles of DSN in clefts are as follows:

- DSN is a deep layer muscle. It forms prior to orbicularis. If a defect in the PMxA binding site exists, DSN from the cleft side could shift over to compete with and bind to the PMxA site on the non-cleft side
- Complete CL, only one DSN is present; complete BCL, it is absent
- The fate of DSN myoblasts in the lateral lip in cleft is unknown

Nasalis has suffered by virtue of terminology as well. Iwanaga and Tubbs provide a comprehensive study of nasalis, which they termed *incisivus labii superioris* (ILS). In their model, they considered ILS to have an inferior part which inserted into premaxilla (the sites are correctly identified) and then inserted into orbicularis. They then describe a superior part of ILS that continues from orbicularis upward to blend into nasalis. Of greatest importance is their demonstration of nasalis function with contraction causing opening of the nasal vestibule at the level of external valve (Figs. 18.23 and 18.24). The rotation-advancement operation misinserts the nasalis with a subsequent compromises in nasal function on the cleft side (Figs. 18.25 and 18.26).

Pathophysiology of Nasalis in the Cleft Condition

In the cleft state, nasalis is always correctly inserted into the nose, with lateral head, *pars transversalis*, draped over the dorsum and medial head, *pars alaris*, sweeping around the margin of lateral crus. The second step is where the error occurs. The binding sites at canine ridge and lateral incisor are not available. Lateral head inserts into the piriform fossa and lateral head into the nostril sill; nasalis now becomes a constrictor.

This condition is readily diagnosed. One observes the patient's breathing while seated with the head tilted backward, from the submental vertex position looking into the nostril and from the vertex submental position, standing behind the patient, looking downward over the dorsum. Observe degree of alar flare on forced breathing. Now, with the patient occluding the aperture of each airway with a fingertip placed gently at the introitus, not compressing the nostril, observe the nostrils and alar motion on forced respiration. Differences between the two sides are readily appreciated and can be photographed.

Standard cleft repairs from Millard's rotation-advancement to Delaire's functional muscle repair have emphasized the correct suture of the lateral lip muscles to the midline, thus creating the "aesthetic drape" of the lip. "Functional closure can now be started, commencing with the closure of the nasal floor from behind forwards… The periosteum, transverse nasalis and myrtiformis muscles are identified and sutured to the midline" [21]. This concept is widely employed by surgeons working in the subperiosteal plane. Those dissecting above the periosteum [22] still anchor the lateral lip element as a unit, often not separating DOO from SOO. In any case, the effect is the same: locking in nasalis as a constrictor, contrary to its function.

Using the outdated concept of nasalis as curving around the ala to blend with orbicularis, I illustrated this incorrectly as well in the 2004 iteration of functional matrix cleft repair before the discovery of the Padget and the angiosome map. The lateral nasal wall was released to free up the nostril sill flap and replace it with a turbinate flap (the latter tissue is still a valuable technique) (Figs. 18.27, 18.28 and 18.29). Despite this, the nasal airway did not improve. In retrospect, I was guilty of reassigning nasalis to the wrong place. Bagatain and Larrabee demonstrate the rescue of nasalis muscle through an incision below the nostril sill, only to anchor them medially. The consequences should be quite clear (Fig. 18.30).

Righting the Wrong

In the surgical technique section of this chapter, we will look at incision design as applied to the microform and incomplete variants and how nasalis can be accessed. The details of developmental field reassignment surgery are left, in large measure to Chap. 19. Suffice it to say that, in revision surgery, it is *always* possible to retrieve nasalis and anchor it correctly to the periosteum and buccal sulcus above the canine.

The decision whether nasalis reconstruction is worthwhile must be based on the perception of the patient of function and aesthetics. If elevating the dome and lateral crus with a cotton tip applicator opens the airway, the diagnosis is made. On occlusion of the non-cleft side the patient should experience a perceptible improvement in breathing. The test is equally valid for bilateral cases, except there is no control… just the sense of better airflow. In cases where the alar cartilage deformity is significant, nasalis reconstruction will also improve the long-term outcome. In most cases, the objective sense of relief experienced by the patient to the first test far outweighs aesthetic concerns.

In Sum

- Microforms not requiring takedown of the lip: access via nostril sill incision and intraoral dissection.
- Microforms and incomplete forms requiring lip takedown: access nasalis in the standard manner via the lateral lip incision and intraoral subperiosteal exposure.

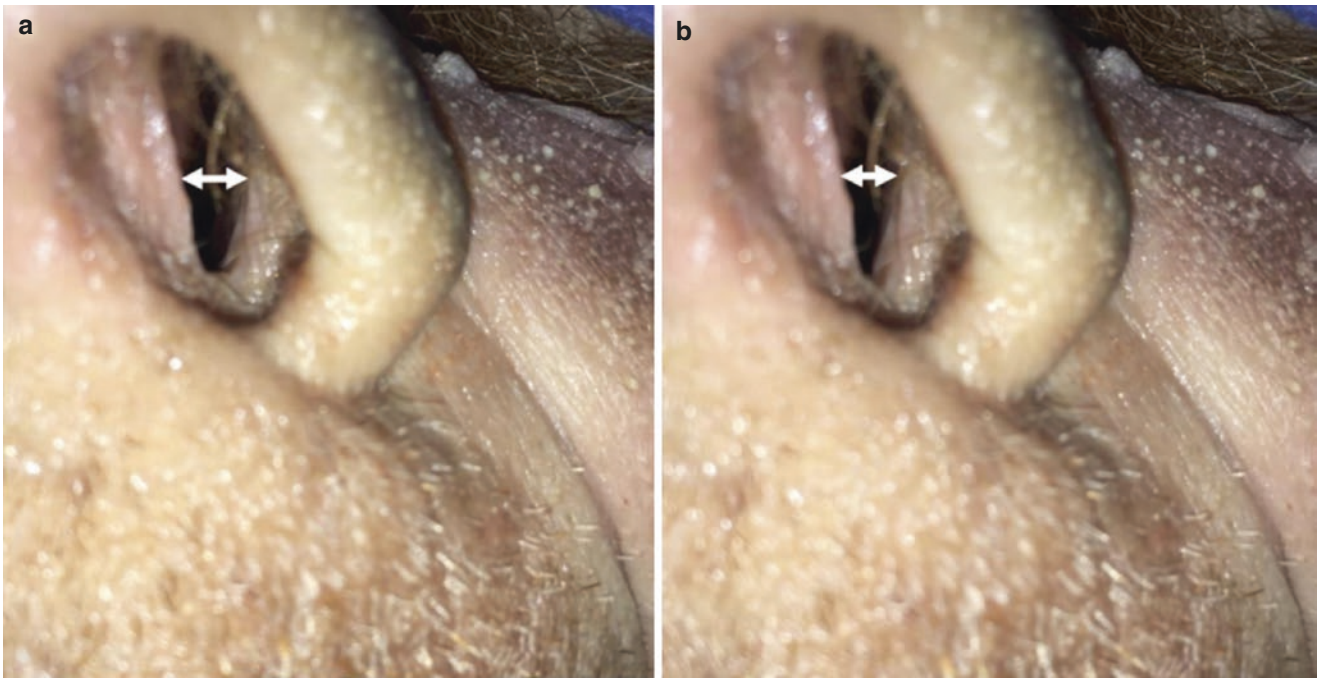

Fig. 18.23 External nasal valve and the function of nasalis. Nasal valve opens with muscle retraction (**a**) and closes in the relaxed state (**b**). [Reprinted from Iwanga J, Watanabe K, Schmidt CK, Voin V, Alonso F, Oskouian J, Tubbs RS. Anatomical study and comprehensive review of the incisivus labbii superioris (nasalis) muscle: application to lip and cosmetic surgery. Cureus 2017; 9(9): e1689. DOI 10.7759/cureus.1689. With permission from Creative Commons License 3.0: https://creativecommons.org/licenses/by/3.0/us/]

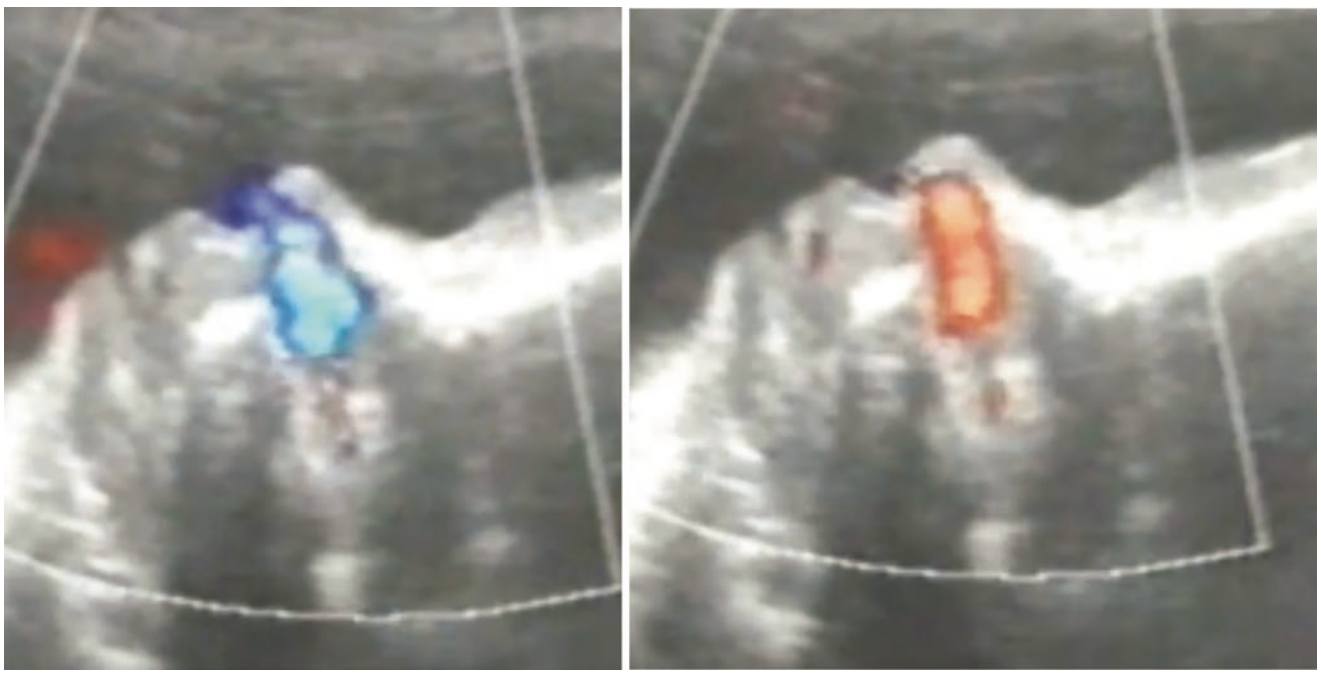

Fig. 18.24 Fetal breathing. Fetal breathing was first reported by Boddy and Dawes in 1975 and reviews by Fox in 1976. It begins between 40 and 60 days. Amniotic fluid exerts a hydraulic pressure effect within the nasal chambers that shape the septum. For a video of this process go to the link below. Knowledge of this process profoundly affected Talmant's concept of airway reconstruction. The link below demonstrates nasal breathing https://doi.org/10.1093/oxfordjournals.bmb.a071237 (nasal only). This link shows both nasal and oral breathing. You can actually see the **nasal chambers expand and contract**. The **heart** can be seen as well. https://www.youtube.com/watch?v=g2voFRimLXw (my favorite). [Courtesy of Jean-Claude Talmant]

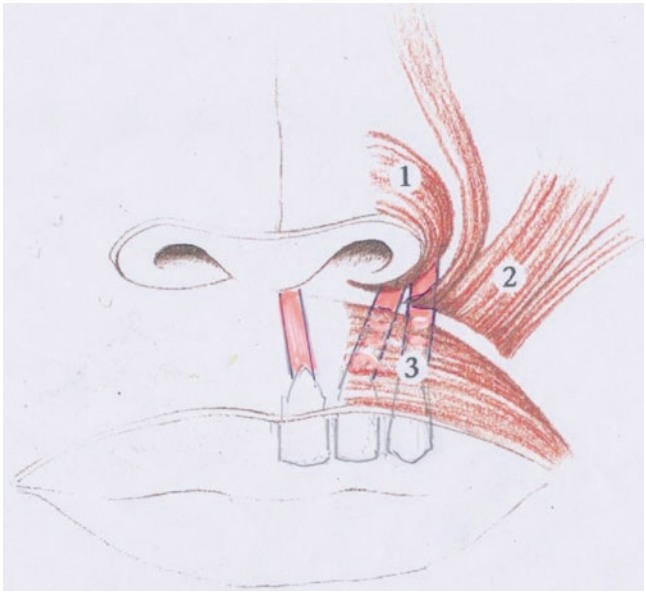

Fig. 18.25 Nasalis misconception. This is a standard model of nasalis, with it curling around the ala and terminating in the sill. The alternative shows depressor septi nasi muscle over the central incisor and the two heads of nasalis over lateral incisor and canine. Note theses are higher that DOO the upper border of which terminates in the sulcus. Key: (1) nasalis; (2) levator labii superioris and zygomaticus major; (3) orbicularis. [Courtesy of Michael Carstens, MD]

Neurovascular Map of the Prolabium: The Philtral Prolabium Versus the Non-philtral Prolabium

In this section, we consider the angiosomes that supply the facial midline, specifically the distribution of r1 mesenchyme originating from the midbrain neural crest in association with the frontonasal process versus r2 mesenchyme originating from the hindbrain in association with the first pharyngeal arch and with the muscles of the second arch. We shall see that the map of these tissues are perfused by the StV1 anterior ethmoid axis and the StV2 medial nasopalatine axis.

Injection Studies

Early arteriography of the entire carotid system by Miroslav Fará demonstrates relevant findings (Figs. 18.31, 18.32, 18.33 and 18.34).

Experimental data are provided here from fetal injection studies reported in 2002. These first disclosed the existence of distinct embryonic components in the columella and prolabium, thereby showing (1) rotation-advancement to be incompatible with developmental fields, and (2) the exis-

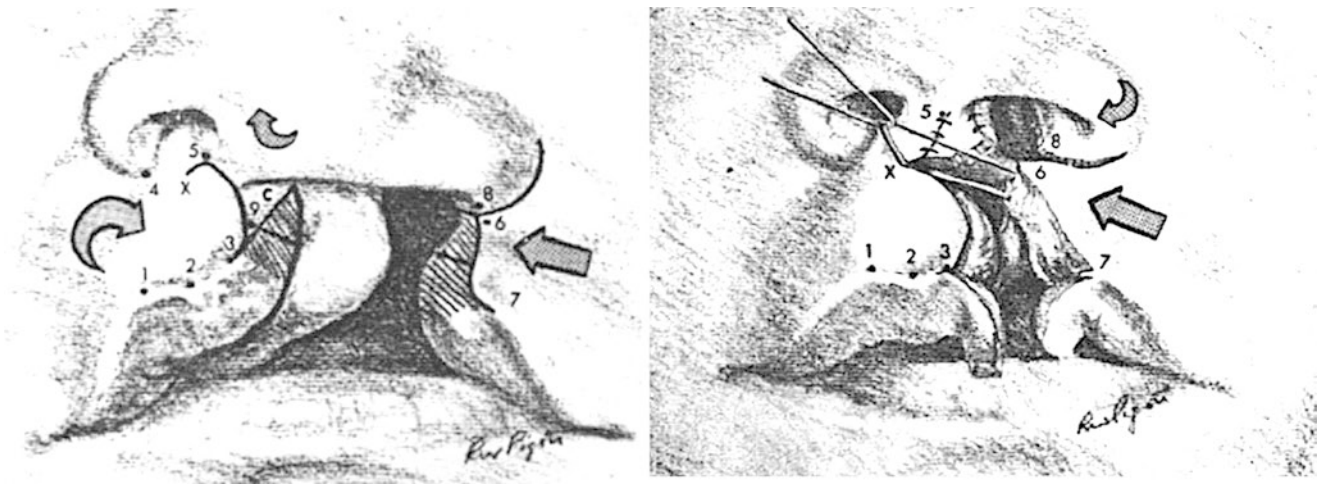

Fig. 18.26 Millard rotation-advancement. Rotation incision (3–5-x) cuts across the arterial supply to philtrum, making its blood suppy dependent on the lateral lip element on the non-cleft side. Perialar incision breaks the aesthetic drape of the nose and lip. The rotation nothing more than a ***trompe l'oil***; it is necessary only if one defines the prolabium as being a single embryonic unit… which it is not. Lateral lip on the cleft side is opened (7–8) and the muscle sutured en-bloc to the base of the columella. ***Note*** DFR measures the philtral width equal to the columella with the cleft side peak very close to Millard point 2. [Reprinted from Fisher DM, Sommerlad BC. Cleft lip, cleft palate, and velopharyngeal insufficiency. Plast Reconstr Surg 2011; 128 (4): 342e–360e. With permission from Wolters Kluwer Health, Inc.]

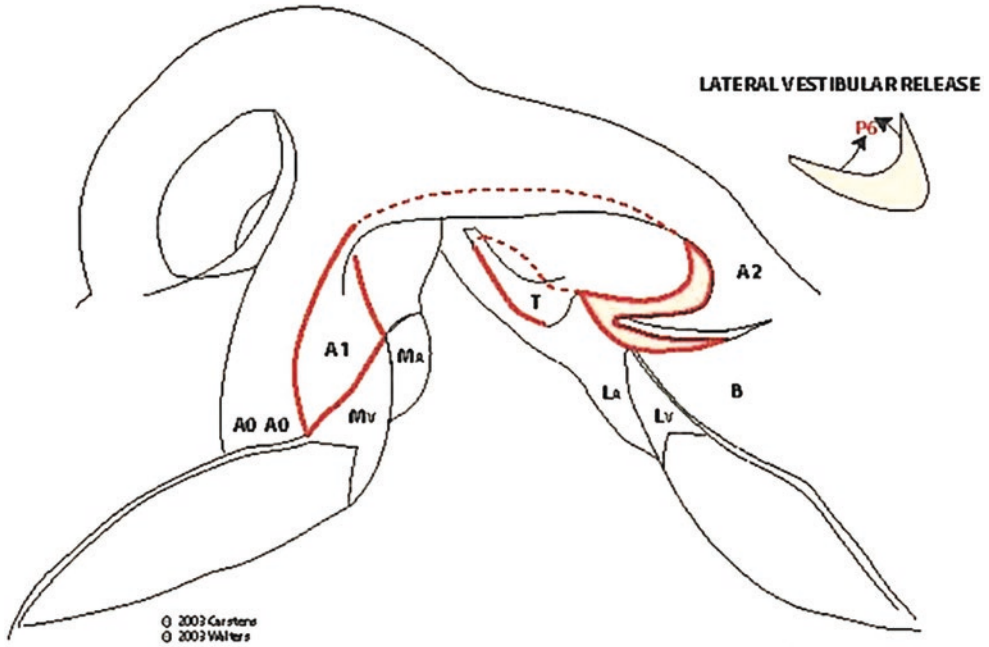

Fig. 18.27 Original design for functional matrix repair recognized the width of the true philtrum as being that of the width of the columella. Remaining non-philtral prolabium (based on medial nasopalatine) was kept in continuity with medial crus based on anterior ethmoid. The combination flap advanced the medial crus and provided tissue based on the columella for the nasal floor. The flap is designated **NPP-LCC**: the non-philtral prolabium lateral columellar chondrocutaneous flap. Releasing incision behind the nostril sill received a turbinate flap… still usefuls (Fisher 2005) but the true advancement of the vestibular lining would not be achieved in DFR until I learned of the Talmant maneuver which would separate it bluntly from the level of piriform fossa all the way up to the undersurface of the nasal bones (see Chap. 19 for details). [Courtesy of Michael Carstens, MD]

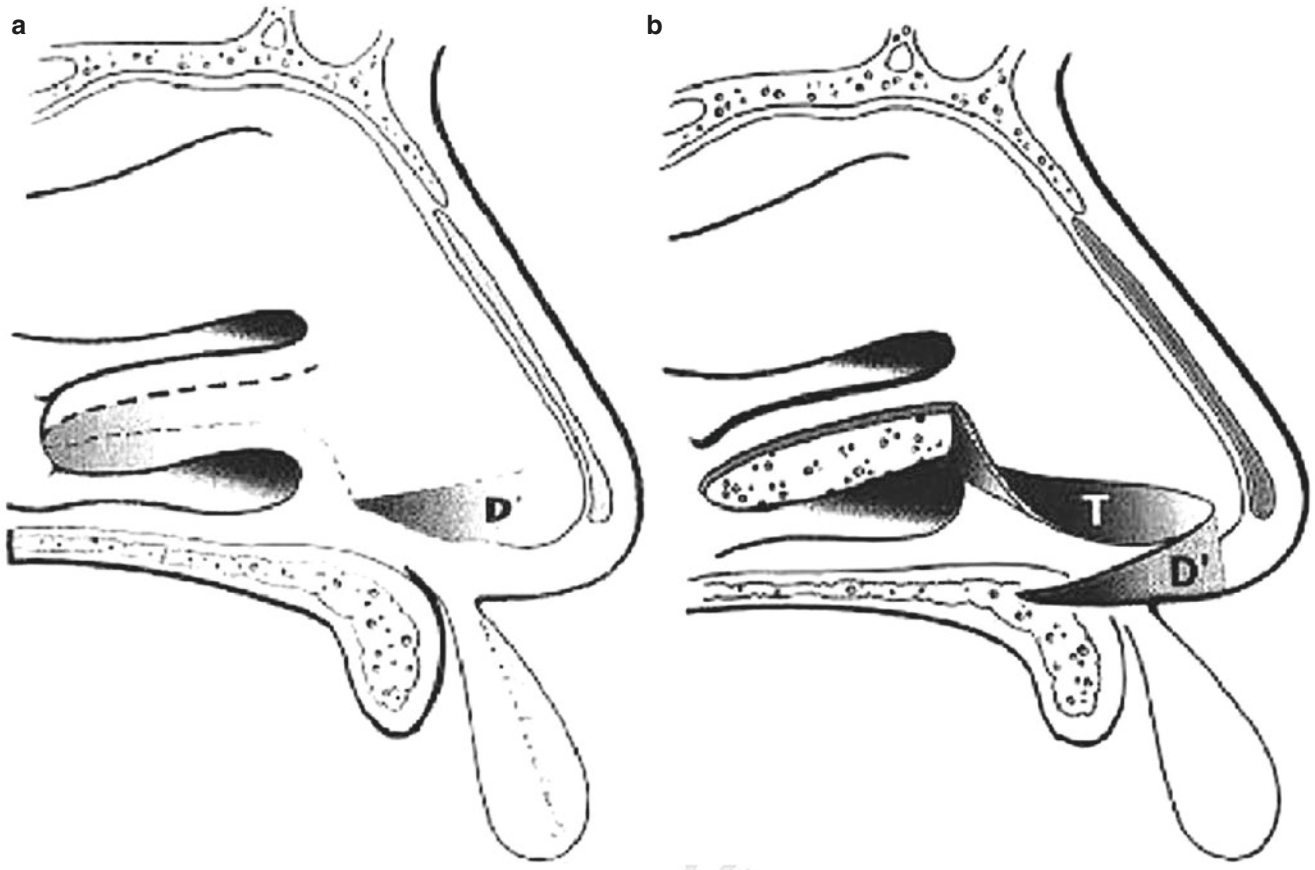

Fig. 18.28 Turbinate flap. (**a**) I started using this flap to replace the deficit left behind when the nostril sill flap D was rotated outward from the lateral nasal wall. The turbinate flap is simple to harvest. The donor side can be cauterized and mucosalizes over in 2–3 weeks. Parallel incisions create a "bucket-handle" flap with an anterior base. (**b**) The NPP-LCC reaches only the medial half of the nasal floor. Suturing it all the way over into the D′ defect will create a contraction band along the nasal floor and compromise the width of the airway. This flap remains quite useful. [Courtesy of Michael Carstens, MD]

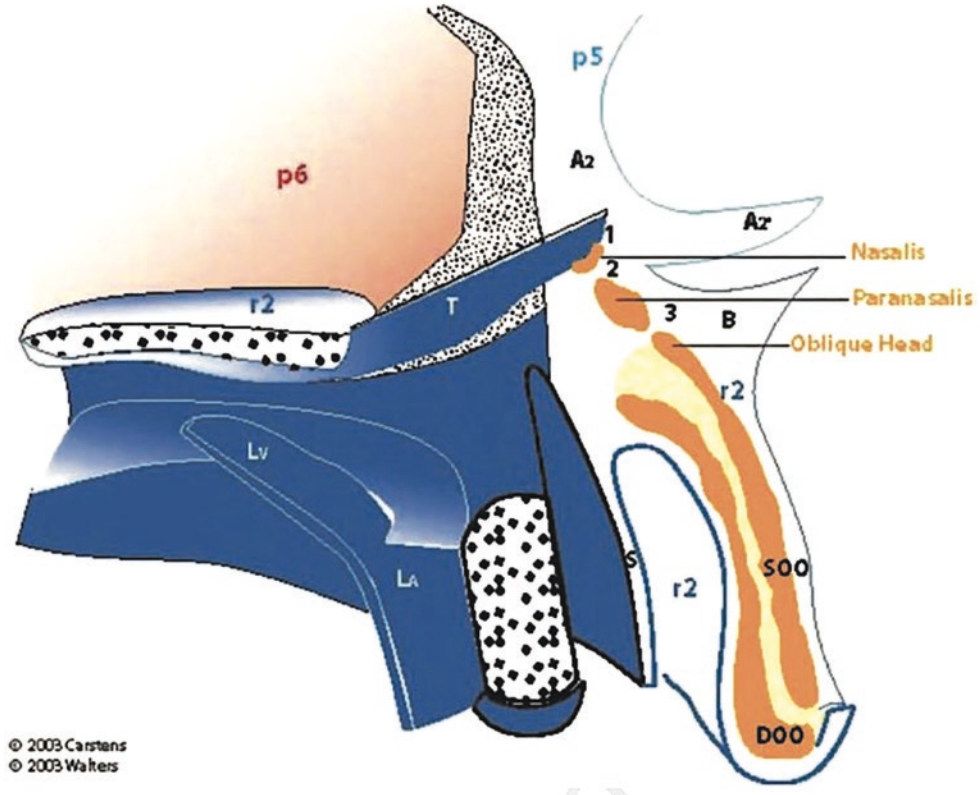

Fig. 18.29 Lateral wall dissection. The design of this dissection shows three mistakes I made along the way to DFR repair

- First, I thought "tightness" of the vestibular lining (p6) was due to a local defect in the lateral piriform fossa; and that this could be released and patched with a turbinate flap (T) or composite graft. This move, combined with alar cartilage repositioning, would result in an improved airway. This was flat-out wrong. Release of p6 takes place using wide mobilization between the layers (Talman maneuver)
- Second, the release of the sliding sulcus flap (S) by a gingival incision and the reflection of mucoperiosteal flap (L_A) from the alveolar cleft margin were used to create a primary gingivoperiosteoplasty (GPP). This is not necessary. The best algorithm is closure of the nasal floor at lip repair followed by AEP closure of all remaining walls except the anterior. These steps eliminate fistula. Grafting at age 4 is completed using an S flap
- Third, nasalis is not small, Its lateral head. Its lateral head (1) must be retrieved from the piriform fossa and the medial head (2) from the nostril sill. The following concept, in my own words (2004) remains in use in most UCL repairs and is embryologically *wrong*
- "Nasalis complex sutured to the ipsilateral membranous septum achieves vertical and anteroposterior alar base positions."

This drawing does correctly show DOO and SOO. It also recognizes the oblique fibers of Delaire at the apex of SOO. Suture of these to base of columella achieves final aesthetic "drape" of the lip
[Courtesy of Michael Carstens, MD]

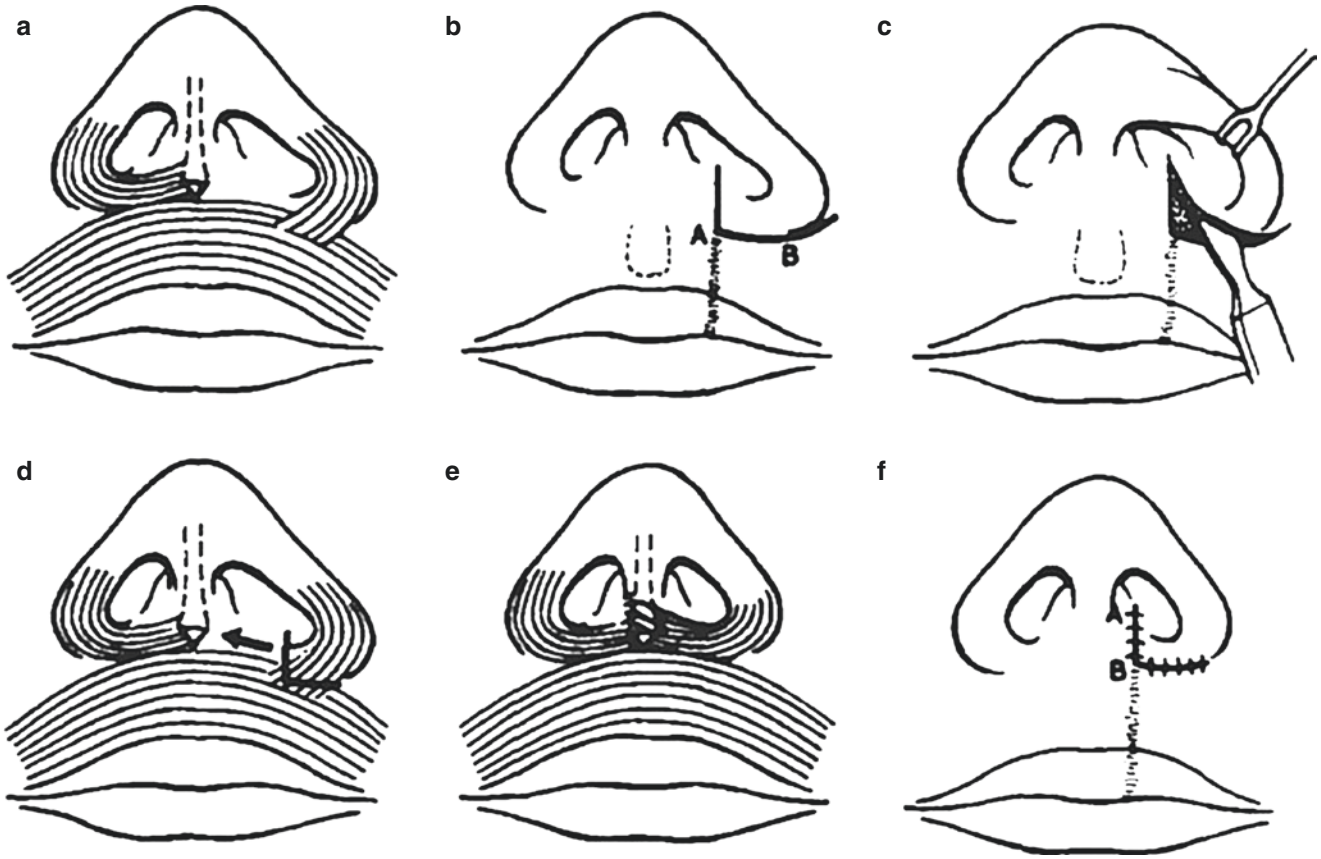

Fig. 18.30 Secondary repair of the nasalis leads to nasal obstruction. (**a**) Nasalis remains mal-positioned after virtually **all** cleft repairs. (**b**, **c**) Nasalis dissection does indeed involve "fishing the muscle out" with an anterior peri-alar incision. The latter should *not* extend laterally around the side of the alar base. (**d**) The three primary mistakes with nasalis dissection are:

- failure to separate it from orbicularis
- failure to free it from the piriform fossa
- suture fixation of the muscle to the midline

(**e**) Using the same incision design, correct repositioning of nasalis to the mucoperiosteum and sulcus at the canine can be achieved

[Reprinted from Bagatain M, Khosh M, Nishoka G, Larrabbe WF Jr. Isolated nasalis reconstruction in secondary unilateral cleft lip nasal reconstruction. Laryngoscope 1999; 109 (2 Pt 1):320–323. With permission from John Wiley & Sons]

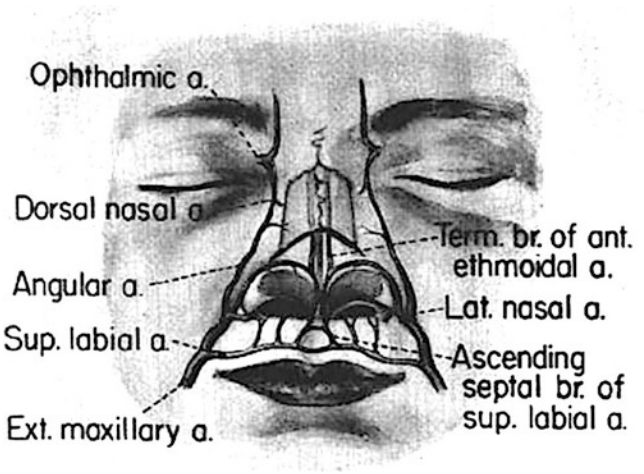

Fig. 18.31 Arterial supply to normal upper lip in normal. Millard popularized Slaughter's drawings. The paired StV1 anterior ethmoids are shown emerging from beneath the nasal bones and travelling in a midline depression just above the septum. StV1 dorsal nasals connect with ECA angular at the level of the alae. ECA and ethmoids anastomose over the alar cartilages, along the nasal floor and descend into the philtrum. Slaughter could have readily guessed about the separate circulations if selective dye injections had been used. Connection between greater palatine and the medial nasopalatine axis occurs via the incisive canal. [Reprinted from Slaughter WB, Henry JW, Berger JC. Changes in blood vessel patterns in bilateral cleft lip. Plast Reconstr Surg 1960; 26(2):161–179. With permission from Wolters Kluwer Health, Inc.]

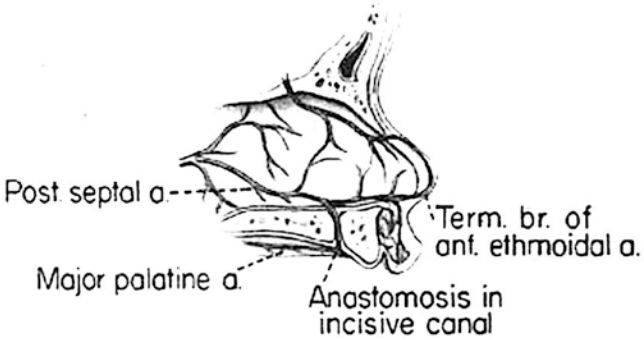

Fig. 18.32 Original drawing by Slaughter showing that the **terminal branch of anterior ethmoid** supplied the midline of the philtru. He but did not recognize the separate circulations of StV1 and StV2. [Reprinted from Slaughter WB, Henry JW, Berger JC. Changes in blood vessel patterns in bilateral cleft lip. Plast Reconstr Surg 1960; 26(2):161–179. With permission from Wolters Kluwer Health, Inc.]

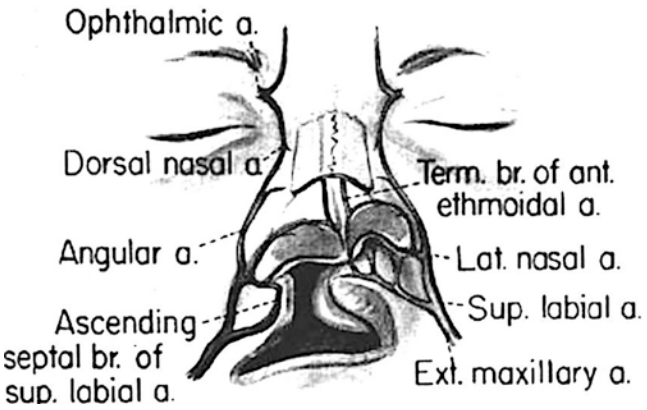

Fig. 18.33 Incomplete right-sided cleft with soft tissue "bridge" between alar base (LNP) and columella/prolabium (MNP). Note the presence of arterial supply in the bridge. [Reprinted from Slaughter WB, Henry JW, Berger JC. Changes in blood vessel patterns in bilateral cleft lip. Plast Reconstr Surg 1960; 26(2):161–179. With permission from Wolters Kluwer Health, Inc.]

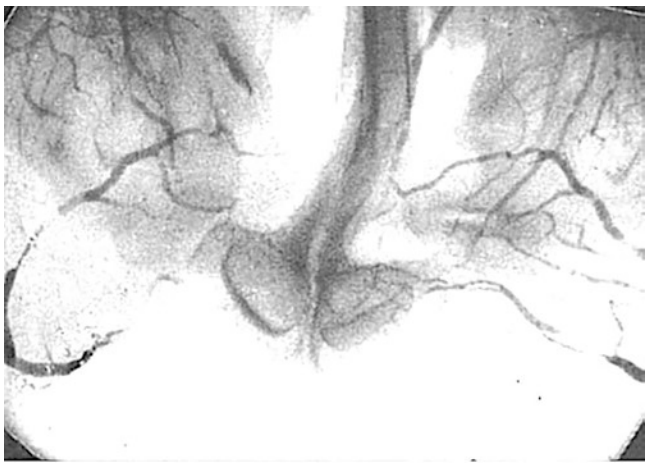

Fig. 18.34 Prolabial blood supply in bilateral cleft lip. Arteriography by Fará but this finding went unrecognized. Here paired anterior ethmoid vessels are seen descending. "The underdevelopment of the muscles and the poorer blood supply in *the half of the philtrum facing the cleft* (**non-philtral prolabium**) suggests that the ability of the orbicularis to grow across the midline is limited. It is as if the muscles of one half of the lip are incapable of supplying with muscle the part that actually belongs to the other side." "in the prolabium there was always a rich vascular network starting in the septal (aa. nasales posteriores septi) and the columellar (aa. ethmoidalis anterior)." [Reprinted from Fará M. Anatomy and arteriography of cleft lips in stillborn children. Plast Reconstr Surg 1968; 42(1):29–36. With permission from Wolters Kluwer Health, Inc.]

tence of an embryonic separation plane using a modified straight-line incision based on mapping the prolabium according to its neurovascular fields, discarding the "obvious" point 3 as assumed for the previous 50 years. The series included several cases of holoprosencephaly, cebocephaly, etc. which I previously described, so we shall concentrate on normal specimens and a fetal specimen with right-sided complete unilateral cleft lip.

Methodology

Fetuses under the age of 22 weeks were presented for necropsy at the Neonatal Pathology Section, Department of Pathology, Kaiser Hospital Oakland, under the direction of Dr. Geoffrey Machin. The common carotid arteries were cannulated with a #25 catheter. Ligation of the external carotid, subclavian and vertebral arteries was performed. Blue dye was injected; 6–10 cc of dye were sufficient per case. Photographs were taken using a copy stand with a Nikon 105 mm lens at f22 and f32 and Kodak ASA 100 Ektachrome film.

After examination of the face, cerebrectomy was performed and the skull base examined. In selected cases all midline structures were resected en-bloc. Each of these specimens consisted of the following: cribriform plate, crista galli and ethmoid sinuses, the lateral wall of the nose, the entire palate, nose including nasal bones, columella, philtrum, septum, vomer and the perpendicular plate of the ethmoid. The specimen was separated posteriorly from the skull base at the spheno-ethmoid junction. Step-wise dissection of the lateral wall of the nose and the palate was carried out to determine the extent of dye perfusion. The final specimen consisted of all midline nasal structures and ethmoid structures, the premaxilla and the lateral wall of the nose to the level of the inferior turbinate (Figs. 18.35, 18.36, 18.37, 18.38, 18.39, 18.40, 18.41, 18.42 and 18.43).

Case 1 Normal Fetus (Fig. 18.35)

Injection of the right common carotid resulted in a blush seen first at the right upper eyelid but then spreading to the supratrochlear skin. As more injectate was administered, pinpoint stains appeared on the scalp (emissary veins), indicating full perfusion of the brain. Similar findings (but to a lesser degree) appeared on the left side indicating midline crossover of the dye. The next finding was a faint blush in the midline of the upper lip at the vermilion of the tubercle followed by lateral spread along the lip. No dye was noted in the skin of the nasal dorsum, cheek or upper lip (see plates).

The nasal skin was split down the midline, revealing paired anterior ethmoid arteries at the upper border of the upper lateral cartilages. These vessels ran in parallel along the upper border of the septum, then turning caudally to pass through the philtrum and thence to the vermilion border. Collateral flow into the external carotid lateral nasal and upper labial branches was noted.

Fig. 18.35 Specimen 1 injection of ICA with ligation of the ECA. Any branches of ECA seen can only come via backflow through anastomoses. Skin is intact. Note the blush of injectate in the nasal tip from anterior ethmoids with backfill along the rim of left nostril and into the right labial artery beneath the wet-dry mucosal junction. [Courtesy of Michael Carstens, MD]

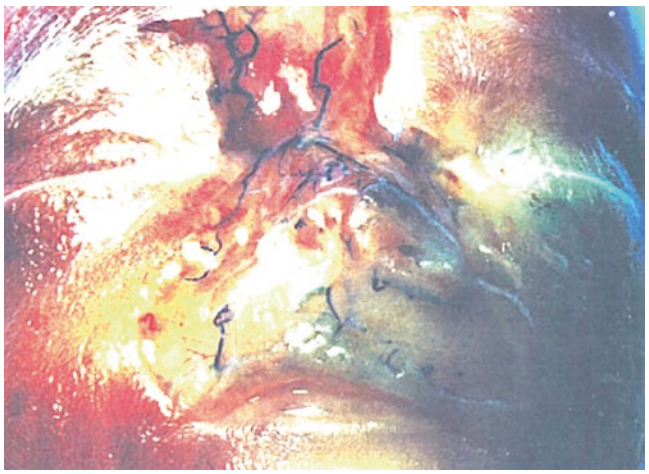

Fig. 18.36 Specimen 2 having the same injection protocol. StV1 arteries are seen after removal of nasal skin. Anterior ethmoids and lateral nasals from infratrochlear artery. Philtral artery is seen in intact skin. Backflow into ECA is seen below the left nostril sill and vertical ascending branch from the labial. [Courtesy of Michael Carstens, MD]

Reflection of the anterior scalp flap revealed an expected perfusion of the supraorbital and supratrochlear vessels. Although the staining pattern was bilateral, the intensity of staining was greater on the right side. At cerebrectomy two normal olfactory nerves were noted. Dye was seen in isolated vessels running in parallel with the supraorbital artery along the interior surface of the frontal bone. Intense staining of the cribriform plate terminated abruptly at the frontoethmoid margins.

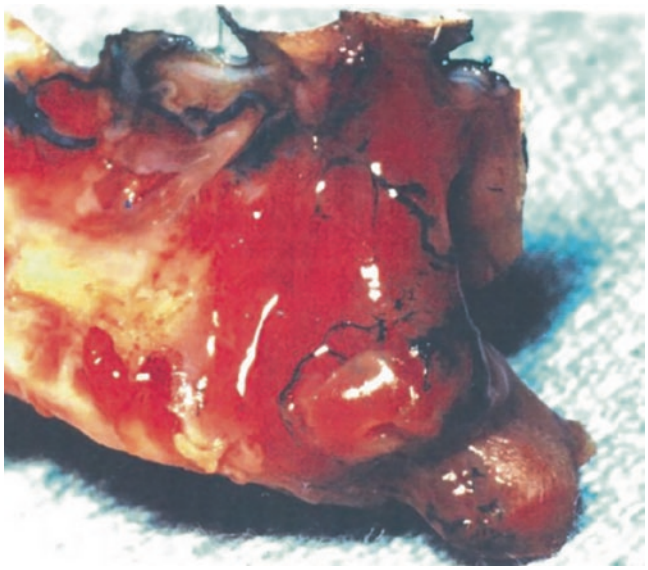

Fig. 18.37 Specimen 3 oblique. Oblique view of en-bloc dissection shows ethmoids coursing forward and then emerging beneath right nasal bone. [Courtesy of Michael Carstens, MD]

Fig. 18.38 Specimen 3 oblique diagram. [Courtesy of Michael Carstens, MD]

En-bloc resection of the midline resulted in a rectangular box of tissue with the cribriform plate and crista galli constituted its superior margin. The inferior (oral) margin of the specimen disclosed dye running to the anterior nasal spine. The entire hard palate and alveolar ridges (excluding the premaxilla) disclosed no evidence whatsoever of perfusion. When the palate was dissected away from the premaxilla and vomer, no dye was noted at the cut edges of the specimen. Midline section of the lip leaving the nose intact revealed continuity of dye between the philtrum and columella, between the philtrum and premaxilla and between the premaxilla and the base of the nose.

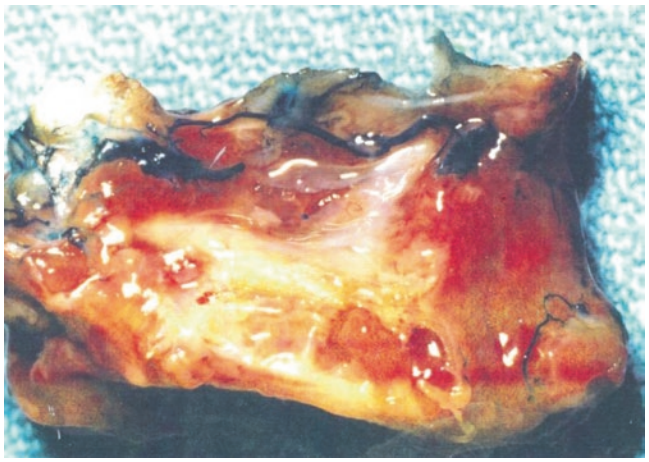

Fig. 18.39 Specimen 3 lateral. [Courtesy of Michael Carstens, MD]

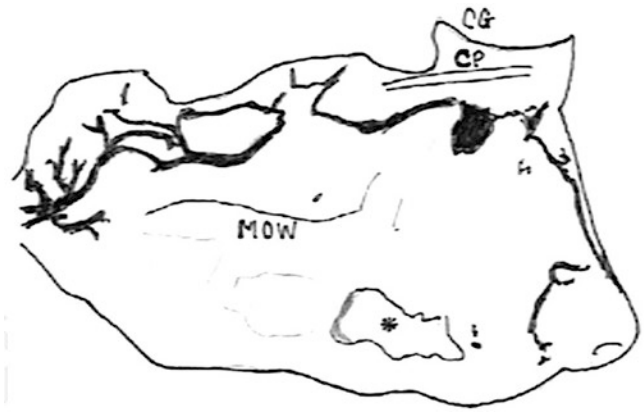

Fig. 18.40 Specimen 3 lateral diagram. [Courtesy of Michael Carstens, MD]

- StV1 in the philtrum has anastomosis with StV2 to premaxilla and anterior nasal spine

Staining of the lateral wall of the nose was limited to its *upper half*, terminating at the level of the orbital floor. The lower half of the lateral margin (consisting of the medial wall of the maxilla) and the palate was resected. No staining was noted along the superior border of the specimen, i.e., inferior turbinate. Thus, the border of StV1 anterior and posterior ethmoids was to the level of middle turbinate.

Along the lateral wall of the nose, dye was noted in the posterior and anterior ethmoid arteries. The latter was seen penetrating into the anterior ethmoid air cells, subsequently to re-emerge from under the nasal bones, running its course astride the septum to penetrate the columella and philtrum as previously described. The lateral wall dissection permitted examination of the perpendicular plate and septum.

Dye was seen in continuity with the nasal side of the cribriform plate, running down the upper border of the septum. It did not perfuse the vomer.

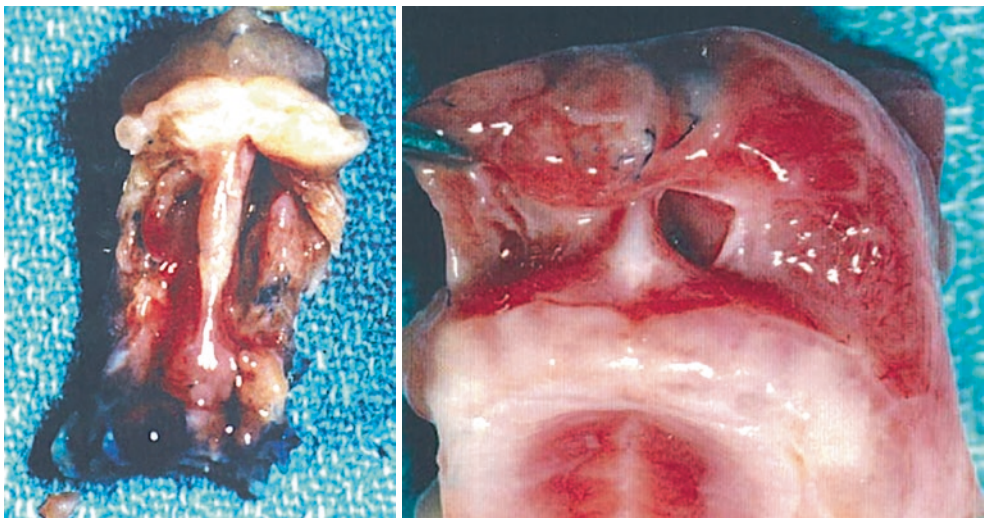

Fig. 18.41 Specimens 1 and 2, palatal view. (Left) Specimen X has a midline cleft palate. The nasal cavity has been dissected free en-bloc with StV1 fields of ethmoid and septum and the lateral nasal walls to the level of inferior turbinate. Hard palate has been removed. (Right) Specimen Y has an intact palate. Mucoperiosteal cover over the premaxilla has been elevated to show the [Courtesy of Michael Carstens, MD]

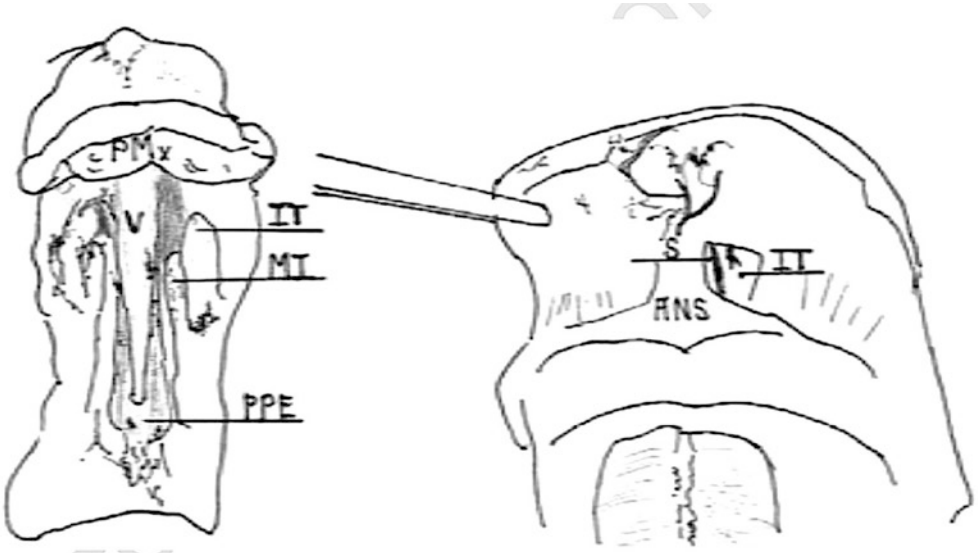

Fig. 18.42 Diagram of 1.1 and 2.1. [Courtesy of Michael Carstens, MD]

Fig. 18.43 Specimen 4 unilateral cleft lip and alveolus. Secondary palate is intact here. [Courtesy of Michael Carstens, MD]

Case #2 Normal Fetus (Fig. 18.36)

Ten cc of dye divided between both common carotids produced the same sequence of blush production but in equal intensity on both sides. Dye was seen transcutaneously (perhaps due to the greater volume of injectate or symmetry of its application) along the nasal dorsum. *Two vessels were seen running vertically through the columella*. A blush appeared in the center of the vermilion, spreading laterally on both sides to the commissures. This represented backflow from the philtral arteries into the labial arteries. Although the paired vessels were not seen transcutaneously in the philtrum, removal of the skin from the tip of the nose, columella, philtrum and lip demonstrated the paired vessels running from the columella to the vermilion border. Backflow of dye from the medial canthus into the angular artery and from the nasal dorsum into the alae via anastomoses with the external carotid system was consistent with standard anatomic description. Vertically oriented arteries filled from the labial arcade were seen in the late injection phase (as expected).

En-bloc resection of the StV1 fields was performed. Once again, both the lower lateral nasal walls and palate were not perfused. Upon resection of these structures dye was noted in the turbinates and along the upper course of vomer. A diffuse blush involved the septum; along its caudal border the *antero-posterior course of the medial sphenopalatine* artery was noted transmucosally. This occurred from back diffusion.

Case #3 Right Unilateral Cleft Lip and Primary Palate (Secondary Palate Intact) (Figs. 18.37, 18.38, 18.39 and 18.40)

Having the two StV1 fields intact, in this specimen two vessels ran from the columella into the vermilion of the lip on the non-cleft lip side. The vessels defined a perfusion zone as the true philtrum or **philtral prolabium (PP)**. The vessels were 2–4 mm apart. The remainder of the prolabium was *lateral* to these vessels. It could be defined as the **non-philtral prolabium (NPP)**. Continuity of dye between the septum and the premaxilla (via backflow) was present. The brain was normal with a well-defined and perfused cribriform plate; two olfactory bulbs of equal size were present.

Clinical Applications of Blood Supply: Dissection of the Prolabium

Where Does the Non-philtral Prolabium Come From?

As a consequence of the above studies I asked myself the question: If we don't see the non-philtral prolabium in the normal state, why does it appear on the cleft side of the philtrum in the unilateral and on both sides of the philtrum in the bilateral? Where does this tissue really belong? The immediate answer to this question was the realization that in complete clefts, if the alveolar housing of the lateral incisor were gone, so too would been soft tissue overlying that zone, a patch of tissue that resided in the nasal floor. Although the alveolar defect represented a defect of intraosseous perfusion from medial nasopalatine, perhaps the blood supply to that soft tissue remained.

Conclusions

- The blood supply to the non-philtral prolabium is medial nasopalatine artery.
- The base of the NPP flap is located directly below the footplate of the medial crus. This constitutes a field boundary between the StV1 axis of the columella and membranous septum and the StV2 axis of the vomer.
- NPP can be dissection away from the philtrum and transposed into the floor of the nose… where it was supposed to be.

How to Define the Philtral Prolabium (Fig. 18.44)

Although our focus here is the microform cleft, this is a good time to reiterate the measurements that define the philtral and non-philtral zones of the prolabium. In all but the most subtle of microforms, an NPP zone can always be found. It coincides with the skin "scar" but as the microform worsens, NPP gets wider and encompasses more tissue.

For right now, let's take the simple case of a complete UCL. The perfusion territory of the anterior ethmoids runs downward from the columella as philtral prolabium. Its width is equal to the distance *x* between the footplates of the columella. When marking the prolabium, completely ignore what you always considered point 1 of the Millard system, the so-called "center" of the prolabium. This is based on a geometric *trompe de l'oil*. Do not be fooled by cheap imitations! Instead, mark the philtral column on the non-cleft side… point 2 of the Millard system. Now mark distance *x*

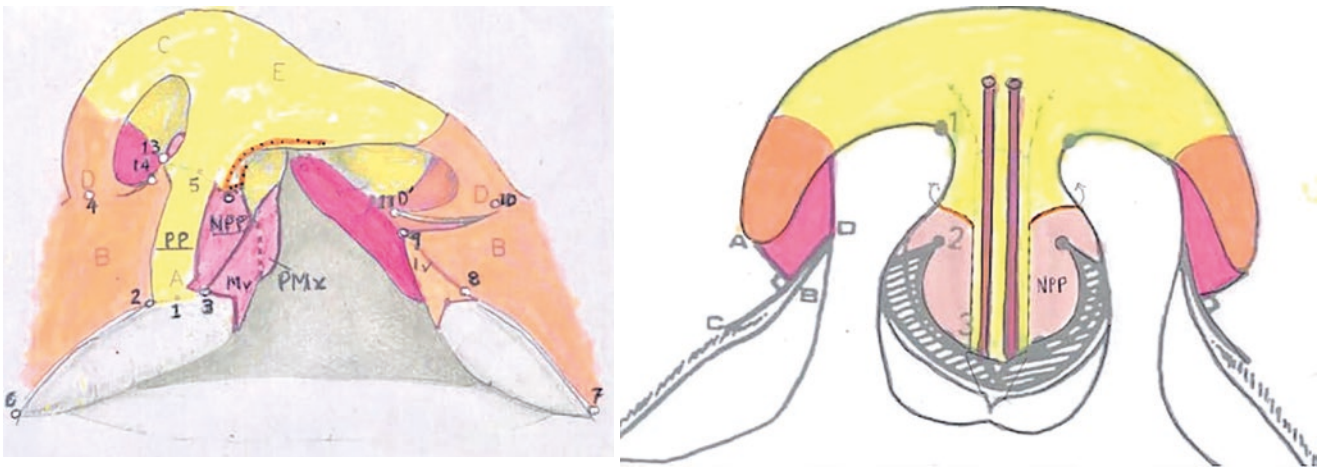

Fig. 18.44 Mesenchymal map of the prolabium. Philtral prolabium (yellow) and non-philtral prolabium (pink) can be elevated en-bloc and then separated. Entire NPP goes in nasal floor:

- Frontonasal process (yellow): r1 neural crest, StV1 neurovascular supply, anterior ethmoids
- Lateral nasal process invaded by PMx (orange): r2 + r4 neural crest, StV2 infraorbital and ECA facial
- Medial nasal process invaded by first arch (pink): r2 neural crest, StV2 medial nasopalatine

Medial crus is elevated as a lateral columellar chondrocutaneous flap to match the normal side and NPP is translated into nasal floor. Technical details are given in Chap. 19

Left: [Courtesy of Michael Carstens, MD]

Right: [Modified from Song R, Lin C, Zhao Yu. A new method for unilateral complete cleft lip repair. Plast Reconstr Surg 1998; 102(6):1848–1852. With permission from Wolters Kluwer Health, Inc.]

from point 2. This is point 3 the true height of the philtral column on the cleft side. You will find that it is often remarkably close to the original point 1! Voila! The true philtral prolabium, is visually about 1–2 mm wider than the columella. This permits a small back-cut right above the white roll for height adjustment with a single z-plasty flap from the lateral side. Everything else is pared away.

NPP is separated from PP with a full thickness straight-line incision extending up the footplate of medial crus. Here the incision *made only through skin* curves straight backward beneath crus. You can slip a scissors into the incision and, hugging the inner surface of medial crus, get right into the nasal tip. On the other side, the NPP flap can be freed up by gentle spreading staying above it at all times. It will rotate without tension into the nasal floor behind the nostril sill or into a releasing incision for the medial crus as the situation warrants.

- In microforms, NPP flap can be just skin and subcutaneous tissue but it can still be rotated. This was originally described by Vissiaronov as a "scar flap."

Arteriography by Fará was carried out in 15 fetuses with various forms of cleft and 1 normal specimen (Figs. 18.31, 18.32, 18.33 and 18.34). The common carotids were injected, thus perfusing arteries of all three systems supplying the face: StV1 from ophthalmic/ICA, StV2 from internal maxillary/ECA and facial from the ECA. In the bilateral cleft, he correctly identified paired anterior ethmoid vessels are seen descending into prolabium: "…in the prolabium there was always a rich vascular network starting in the septal (aa. nasales posteriores septi) and the columellar (aa. ethmoidalis anterior)." He thus described a dual contribution from StV1 into the superficial layer of prolabium and StV2 into its deep layer which, under normal circumstances, is occupied by the DOO.

"The underdevelopment of the muscles and the poorer blood supply in *the half of the philtrum facing the cleft* (***non****-philtral prolabium*) suggests that the ability of the orbicularis to grow across the midline is limited. It is as if the muscles of one half of the lip were incapable of supplying with muscle the part that actually belongs to the other side." What he observed was that the DOO of non-philtral prolabium is not normal, as we shall see shortly in our discussion of cleft margin histochemistry.

Developmental Sequence of Microform Cleft

The Outdated (But Useful) Concept of Facial "Processes"

The level of discussion of facial development available in standard texts is inadequate to explain the variations of cleft. Clinicians treating clefts are generally familiar with two schools of thought: the nineteenth century theory of *aberrant ectodermal process fusion* and Stark's twentieth century concept of *defective mesodermal migration* [23]. Although either one can be applied to the emergence of the lateral nasal process and the advancement of the maxilla, they are

vague when it comes to the formation of midline structures. How precisely does the premaxilla form and in what temporal relation to the nose? When, where and how does the septum begin? Does the philtrum belong to the nose or to the lip? What makes a Cupid's bow?

Nature continually provides *materia prima* for the surgeon in the form of clefts in their various guises which, if carefully examined, demand an alternative explanation. Consider the supposed emergence of the lip and philtrum from the medial nasal process. The German embryologists described a ventromedial projection associated with the MNP as the ***globular process***; this structure was observed to descend in the midline to form the central lip [24, 25]. However, the blood supply to the columella and philtrum is derived from the ICA, whereas that of the MNP comes from the facial artery [26, 27]. These two structures can be separated surgically [28]. Patients with arrhinia have no nostrils; yet they have a fully developed Cupid's bow [29–32]. Holoprosencephaly presents us with varying degrees of frontonasal dysplasia or aplasia.

It should be noted that controversy exists as to the propriety of the term "**process**." Firmly embedded in the literature from the nineteenth century onward, the term implies an unwarranted degree of separateness. Although externally these embryonic entities appear distinct, they share a common mesenchyme more internally. The term "**prominence**" is much more suited to the situation. It recognizes that the surfaces of embryonic subunits are thrown into relief by underlying concentrations of mesenchyme. The biochemical interactions between the epithelium and the mesenchyme determine the clinical behavior of that process in the developmental process. What's more, prominences are not homogeneous blocks of tissue: they are accumulations of developmental fields defined by neuroangiosomes.

I found the concepts of processes and prominences vague and unhelpful. Moreover, they did not seem to square with neurovascular anatomy. As it turns out, a developmental field refers to tissues supplied by a single neuroangiosome or collection of neuroangiosomes, which behaves in an autonomous manner when separated from partner fields. Fields have identifiable sources of neurovascular support; in the face corresponding to branches of the trigeminal and stapedial systems, supplemented by the external carotid circulation.

As you can see below, the 2000 field concept still vague but it was about to become much more anatomic. In December, 1999 at John Rubenstein's neuroembryology lab I became aware of the prosomeric system. By 2002 this morphed into a neuromeric model for the Tessier cleft classification. Injection studies had separated out the blood supply to the midline between internal carotid and external carotid systems. But the precise definition of neuromeric fields based on specific branches of the stapedial system would elude me until much later upon the discover of Dorcas Padget's work.

"Observations such as these are most compatible with a model of separate pairs of embryonic tissue blocs termed "fields" that interact with each other to produce the nose and mouth. Fields do not display discrete epithelial separations; they are mesodermal prominences with a separate blood supply. They are not static but possess mass, directionality and timing. Partner fields are those required to interact to form a structure. For example, contact between the lateral lip element (B field) draws down the ipsilateral philtral column (A field). Clefts prevent such normal interactions from taking place. Fields are consequently forced to occupy stereotypical aberrant locations; the resulting arrangement defines the appearance of the cleft lip-nasal complex. This is known as **field mismatch**. A fundamental goal of cleft repair is the surgical reassignment of fields into their proper relationships."

Embryonic Contents of Facial Processes After Placode Invagination

Note: Reference the cranial placode map (Fig. 18.45).

MxP: Maxillary process

- first arch (r2): skin/mucosa, muscles of mastication (Sm4), DIF zygomaticomaxillary complex, internal maxillary, V2 sensory
- second arch (r4): no skin/no mucosa, muscles of facial expression (Sm6), SIF/SMAS (r4 neural crest), ECA facial artery, VII motor only

MNP: Medial nasal process

- Skin cover, FNO; mesenchyme (r1), StV1 anterior ethmoid artery, terminal nerve

LNP: Lateral nasal process

- Skin cover, FNO + r2; mesenchyme (r1 + r2), neuroepithelium (hp2), mesenchyme (r1 and r2), StV1 lateral nasal and facial

FNP: Frontonasal process

- Skin cover, FNO; mesenchyme r1, muscles of facial expression (Sm6), SIF/SMAS

Globular process (r1) This r1 mass "extends" from MNP, forms prolabium

Premaxillary process (r2) extends beneath prolabium

DOO: Deep layer of orbicularis oris

- Sub-mucosal *pars peripheralis*
- Sub-vermilion *pars peripheralis*

SOO: Superficial layer of orbicularis oris

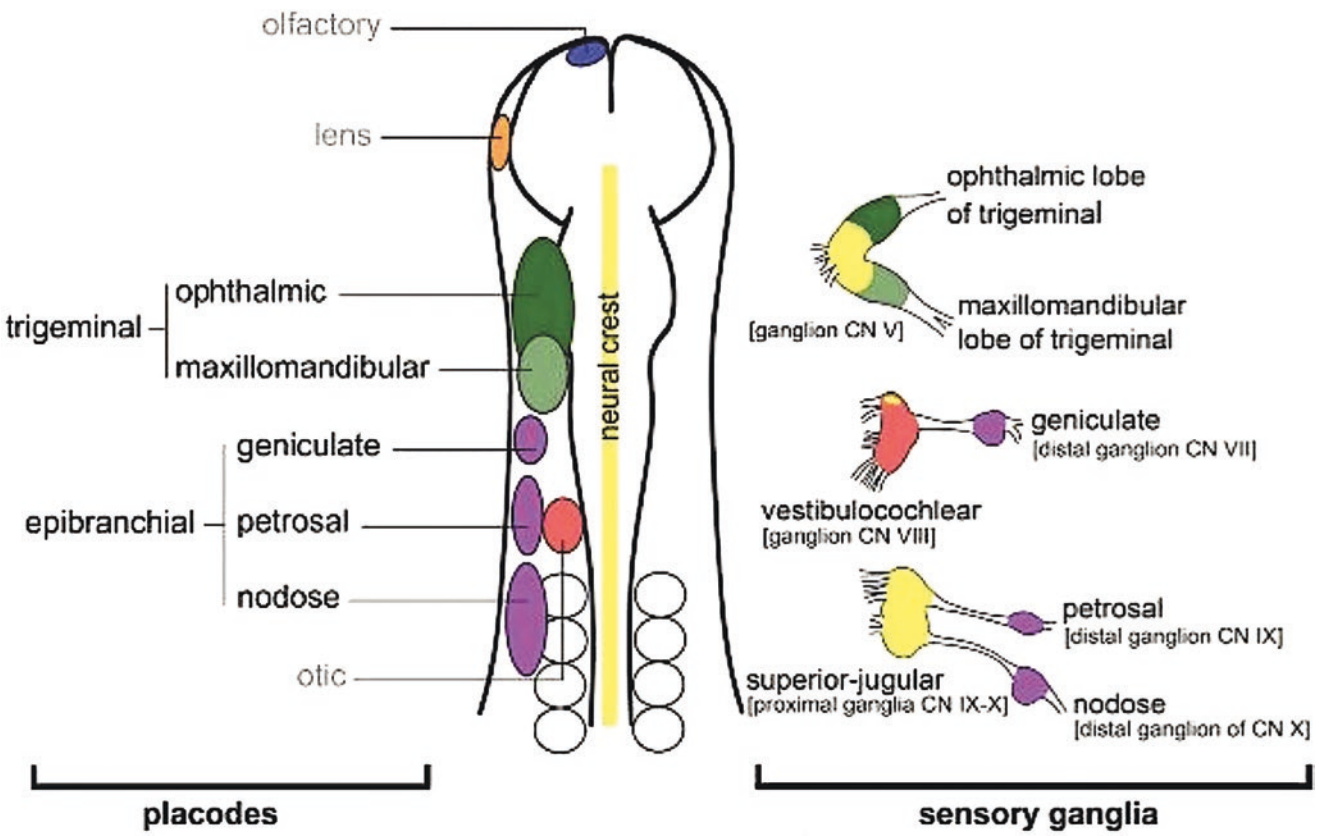

Fig. 18.45 Placodes in chick embryo (The anatomy is analogous in mammals). Nasal placode is the basis for the medial and lateral nasal processes. Trigeminal and epibranchial placodes contribution to sensory neurons. Sensory ganglia and the placodes from which they arise are color-coded. The position of the trigeminal and epibranchial placodes is shown on the left side. Trigeminal at rhombomeres r1–r3. Corresponding sensory ganglia to which they contribute are depicted on the right. The neural crest (yellow) contributes neurons to the proximal aspect of the trigeminal ganglion complex of cranial nerve V, and the distal aspect of cranial nerves VII, IX, and X. Optic appears first at Carnegie stage 11. Forebrain matures later with optic placode forming first then nasal placode. [Reprinted from Baker CV, Bronner-Fraser M. (2001). Vertebrate cranial placodes I: Embryonic induction. Dev Biol 2001; 232: 1–61. With permission from Elsevier]

Frontonasal Process, Prolabium and Premaxilla

This section references Chap. 4 on the formation of the face but goes into greater detail. It is essential material to understand the formation of the lip.

The original concept of FNP was proposed in 1948 by Streeter, O'Rahilly in which paired premaxillary processes were thought to fuse with a frontal field to create a single frontonasal process [33, 34]. This was combined with the notion of a midline septal cartilage originating from the chondrocranium from which the architecture of the oronasal cavity is somehow derived [35–38]. This construct lumps together tissues from different neuromeric sources and blood supplies.

- Tissues originating from the frontonasal process (FNP) remain as the forehead, superior-medial orbit, ethmoid complex, nasal chambers, nasal envelope, septum, columella and philtrum. Its mesenchyme is r1 and its neuroangiosomes arise as StV1 branches from the ophthalmic stem.

Neuromeric Model of Fronto-Naso-Orbital Development

Carnegie Stages to the Time of Lip Formation

- *Stage 8* Recall that FNP projects forward from r0 notochord and Rathke's pouch like a proboscis. FNP results from the rolling-up of the neural tube corresponding to forebrain. The skin cover of FNP is hp2 epithelium and p1–p3 neural crest dermis. Encased within the proboscis is the developing prosencephalon. The space between the skin and brain is occupied by angioblasts, probably derived from the prechordal mesoderm. The make endothelial component of the primitive head plexus. Each side of the FNP has 3 placodes: adenohypophyseal, olfactory and optic
- *Stage 9* first arch forms and neural crest migration begins. RNC from r1–r3 admixes with the head plexus, forms meninges and lays down r1 mesenchyme for the sphenethmoid complex
- *Stage 10* second arch forms

  - Invasion of ventral FNP by first arch
- *Stage 11* third arch forms; first and second arches meld together to form B fields
  - Invasion of LNP by first arch
- *Stage 12* fourth arch forms, B fields now in physical contact with FNP which allows r2 mesenchyme to migrate into position under the surface of FNP in the future mouth
  - Invasion of LNP by second arch
- *Stage 13* fifth arch forms
  - The primärer nasenböden (primary nasal floor) falls apart
  - Behind MNP is medial r2 mesenchyme
  - Behind LNP is lateral r2 mesenchyme
  - Continuity of r2 mesenchyme is posterior (the future sphenopalatine notch)
- *Stage 14* lip formation sequence begins

Recall that the nasal placodes sink into the r1 mesenchyme of FNP to set up two nasal chambers. These are widely separated by a central block of r1 which subsequently undergoes apoptosis. There is no mouth; the entire FNP is r1 in front of the brain.

Embryonic folding begins at stage 9. By stage 10 MxP becomes confluent with FNP, first at its posterolateral corner and then fusing progressively further forward. Confluence of MxP with FNP and later with LNP allows for the sharing of mesenchyme. Let's walk through this three-step process.

Recall that nasal placodes are physically connected with the underlying forebrain. As the surrounding FNP mesenchyme expands forward, the placodes stay stable; they therefore appear to be mechanically "retracted" backwards into the r1 mesenchyme of FNP. This creates a nasal chamber lined by specialized hp2 placodal epithelium. The lateral wall contains neurons of the olfactory system (OS) and the medial wall contain neurons of the accessory olfactory system and the terminal nerve (cranial nerve 0). At this time the back wall of the chamber is closed. The nasal cavity is a blind sac exclusively within the FNP. Later on, when the primary nasal floor of the sac (*primärer nasenböden*) breaks down, the two nasal cavities are now in continuity with the developing oral cavity.

The **first interaction** between MxP and FNP occurs at stage 10 and takes place (logically) at site of origin of first arch at the posterior border of the frontonasal process. Recall that the placodes are widely displaced. They come together in the midline as the result of apoptosis within the central block of r1 sphenethmoid mesenchyme. Recall further that the hp2 epithelial "skin" of the FNP comes from the neural folds of the forebrain. As the two side of the FNP approximate each other ventrally, above what will be the mouth, first arch ectoderm and mesenchyme "chase" the retreating hp2 skin until reaching the undersurface of what is the medial wall of the nasal chamber.

Neuroangiosomes invade from StV2. They bifurcate within the floor of the primary nasal sacs. The nasal walls are now two-tiered.

- Medial wall has the StV1 fields of the ethmoid and septum above, and StV2 fields of vomer/premaxilla.
- Lateral wall has StV1 upper and middle turbinates above and StV2 inferior turbinate + palatine bone complex (P1–P3) below.

When the bottom of the primary nasal floor opens, the two branches of the nasopalatine axis are physical separated as medial nasopalatine to vomer and premaxilla and lateral nasopalatine to lateral nasal wall but they remain connected posteriorly at the back wall of the nose.

The **second interaction** between MxP and FNP takes place anteriorly along the surface of the developing face. It involves the invasion of the lateral nasal process first by first arch skin and mesenchyme and later by second arch mesenchyme. Here's what happens.

- Simultaneous with the "invagination" of the placodes, the r1 mesenchyme that was surrounding them expands, throwing the surface of the FNP on either side of the nasal chamber into two prominences, the media nasal process (MNP) and the lateral nasal process (LNP),
- Blood supply of MNP remains StV1 but the LNP is quickly invaded by MxP such that the mesenchymal composition of caudal half switches from r1 MNC to r2 and r4 RNC from the first arch/second arch complex.

In the roof of the future mouth (originally covered by PNC skin) first arch mesenchyme "chases" the retreating FNP to become the floor of the primitive nose. When the primary nasal floors break down, we now have paired nasal chambers and a mouth.

- Laterally, r2 mesenchyme makes up the lower lateral wall of the nose: the **inferior turbinate** and **palatine bone complex.**
- Medially, r2 mesenchyme makes up the lower medial wall of the nose as the **vomer** fields.
- MNC r1 neural crest mesenchyme lying adjacent to MNPs expands, supplied by the anterior ethmoid angiosome running down columella, to form the **philtral prolabial processes**.
- RNC r2 neural crest deep to MNP proliferates, supplied by the medial nasopalatine angiosome. These become the **premaxillary processes**.
- RNC r2 neural crest produces terminal soft tissue buds from the vomer-premaxillary junction. These become the **non-philtral prolabial processes**.

Developmental Fields of the Vomer and Premaxilla

The following sequence is demonstrated in the SEMs of Hinrichsen and the staged drawings by Krause

- *33 days*, r2 mesenchyme in the roof of the future oral cavity presents itself as V-shaped swellings just beneath the medial wall of the nasal chamber. As development proceeds, the V narrows and fuses in a posteroanterior manner. This represents the fusion of the vomer fields. Above the compaction of the medial nasal walls forms a sandwich within which perpendicular ethmoid plate and septum will develop.
- *41 days*, two anterior swellings appear.
  - Premaxilla is a continuation of the vomer field.
  - Prolabium buds from the medioventral corner of MNP.
- *48–50 days*, vomer field fusion has reached the posterior border of the premaxillae (the incisive foramen). At this point, palatal shelf elevation can be observed.
- 56 days, fusion of the premaxillae is complete.
- **In sum**: At 56 days, completed facial midline consists of paired field complexes of stacked-like boxes.
  - Upper boxes (r1): ethmoid complex, nasal envelope, columella and philtral prolabium.
  - Lower boxes (r2): vomer, premaxilla and non-philtral.

Lip–Nose Fusion Sequence

The actual events surrounding the closure of the lip are not well documented in the literature. Nevertheless, SEM work by Hinrichsen and drawings of staged embryos by Krause provided a wonderful opportunity to depict this process in diagrammatic form. What follows, referenced to Figs. 18.46, 18.47, 18.48 and 18.49, is my best guess as to the sequence of individual events and their timing by Carnegie stage. Note carefully the events inside the oral cavity.

Development of the upper lip takes place between Carnegie stages 14 and 18. Let's look at the following visual model. For the sake of brevity, let A = FNP; B = MxP (combining first and second arch tissues); C = MNP; and D = LMP. Invasion of the FNP floor and of the ventral half of LNP by first arch mesenchyme has already taken place. The *primärer nasenböden* has broken down and r2 tissue can be seen inside the nasal cavity. Note: yellow = r1 and pink = r2.

Step 1 D fuses to C. This takes place by means of "Simonart's band." The gap separating the ventral edges of LNP and MNP is bridged by an epithelial strand of r2 tissue produced by D field. This is an energy-dependent process that is oxygen dependent in the mouse. Simonart's band is the form fruste of the nasal sill. It provides a conduit for mesenchymal flow from B medially. It lies internal to the eventual fusion point of D with C [39]. Simonart's band will not form under two conditions:

- A complete cleft of the primary palate positions the LNP too far laterally from the midline: the critical contact distance is exceeded.
- Metabolic failure due to environmental agents blocks synthesis of the band.

Failure: **complete cleft lip**. No further B field tissue migration

Step 2 B fuses to D/C complex. This is a sequential step with MxP fusing first to LNP and then translating to MNP.

Failure: **complete cleft lip + Simonart's band**

Step 3 B fuses to A. Carnegie stage 17. The expansion of the medial and caudal aspect of MNP, previously called "the globular process," creates the philtral prolabium (PP). In the meantime, tucked inside, r2 non-philtral prolabium (NPP) adds to the medial nasal floor. In the presence of a cleft between A (philtral prolabium) and B (lateral lip element), the NPP becomes visible and fuses with PP to create the prolabium we are accustomed to see in bilateral cleft lip.

- When B joins A, the PPP descends.
- The filling up of the lip is deep-to-superficial and dorsal-to-ventral
- Premaxilla differentiates later

Failure: **incomplete cleft lip**

Step 4 Development and insertion of oronasal musculature: The deep layer of the orbicularis is unified well before the superficial layer. The oblique head of the orbicularis levator labii et alaeque nasi and pars alaris of nasalis insert last.

Failure: **minimal cleft lip**

Scientific Importance of the Minimal Cleft Sequence

To the reader: *Often in the process of investigation, we become misled by a misunderstanding of a particular term. At the time of the original paper, I had not yet stumbled upon the neuromeric system. Therefore, I kept referring to a cleft "event" of unknown nature and was seeking to understand the pathology of cleft as a series of "processes" unleashed by the event. As it turned out, processes are useful but I got*

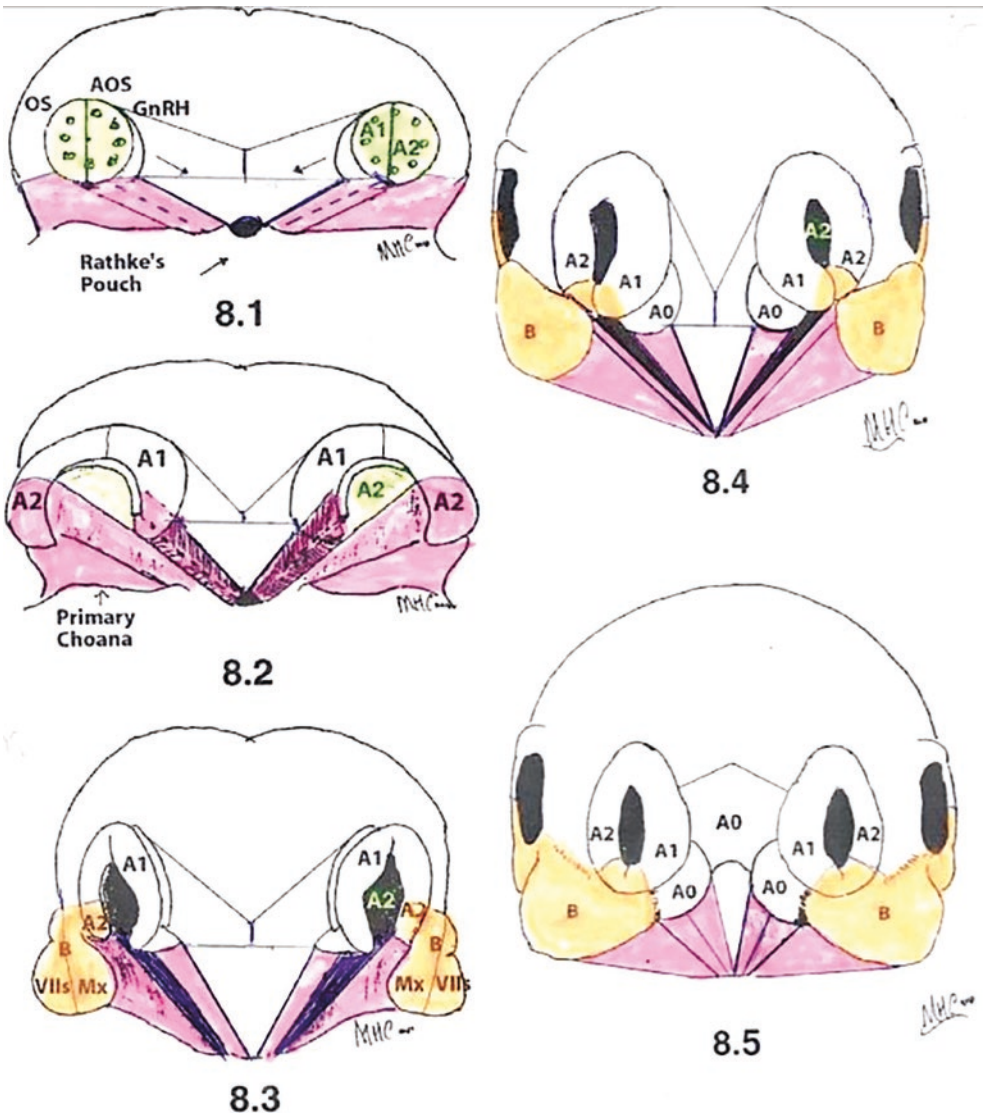

Fig. 18.46 Midline facial development. The developmental pattern nasal cavity is seen here in 3-dimensional representation, begins with two columns of r1 neural crest running forward in divergent fashion from Rathke's pouch to the nasal placodes. This tissue provides the scaffolding by which olfactory neurons from the lateral placode and GnRh neurons from the medial placode will find their way to the brain. Fusion of the StV1 ethmoid fields and the StV2 vomer-premaxillary fields occurs in posteroanterior fashion. Apoptosis of r1 sphenethmoid mesenchyme is requisite for proper medial positioning of the orbits. The following are mouse versus Carnegie (human) stages. Key: r1 mesenchyme, white; r2 mesenchyme from first arch, pink; r2 + r4 mesenchyme from PMx (the amalgams of first and second arches)

8.1 = Stage 13 (28 days), floor of frontal nasal process, composes of r1 mesenchyme is invaded by r2

8.2 = Stage 14 (32 days): primary nasal floor is riven, r2 from first arch mesenchyme and StV2 to LNP, first and second arches fused into PMx

8.3 = Stage 15, early (33 days): PMx fuses to side of LNP. Not color change to orange

8.4 = Stage 15, late (35 days): LNP fuses to MNP. Simonart's band was the intitiating step. MxP advances forward reach caudal tip of LNP. Globular process (A0) emerges caudal tip of MNP

8.5 = Stage 16, early (36 days): MxP has moved to caudal tip of MNP and is fused with globular processes (A0) which are much larger. Columns of r2 mesenchyme for vomer and premaxilla are prominent

[Courtesy of Michael Carstens, MD]

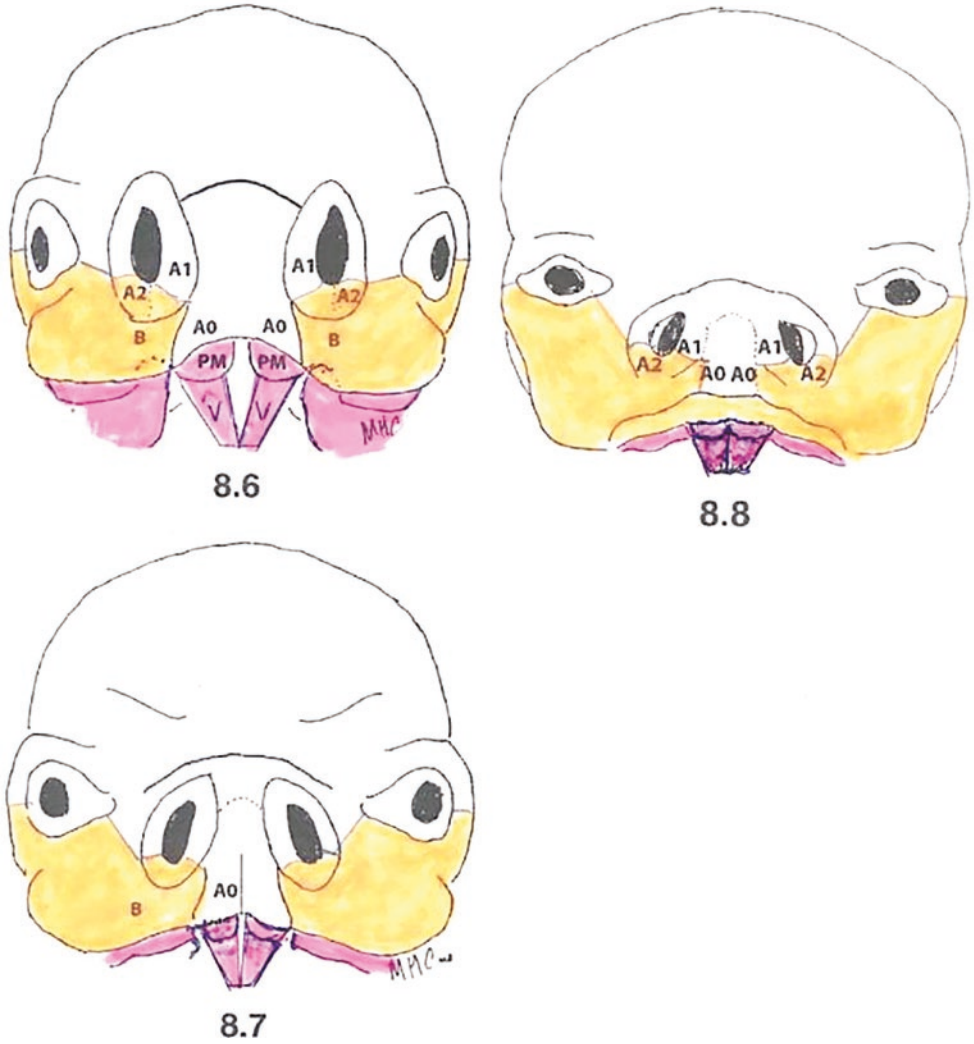

Fig. 18.47 Midline facial development. The developmental pattern nasal cavity is seen here in 3-dimensional representation, begins with two columns of r1 neural crest running forward in divergent fashion from Rathke's pouch to the nasal placodes. This tissue provides the scaffolding by which olfactory neurons from the lateral placode and GnRh neurons from the medial placode will find their way to the brain. Fusion of the StV1 ethmoid fields and the StV2 vomer-premaxillary fields occurs in posteroanterior fashion. Apoptosis of r1 sphenethmoid mesenchyme is requisite for proper medial positioning of the orbits. The following are mouse versus Carnegie (human) stages. Key: r1 mesenchyme, white; r2 mesenchyme from first arch, pink; r2 + r4 mesenchyme from PMx (the amalgams of first and second arches)
8.6 = Stage 16, late (37 days): premaxillae and alveolar processes prominent. Palatal shelves vertical
8.7 = Stage 17 (41 days), vomer-premaxillary columns approximating
8.8 = Stage 18 (44–46 days): eyes frontalized, nasal tip definition
[Courtesy of Michael Carstens, MD]

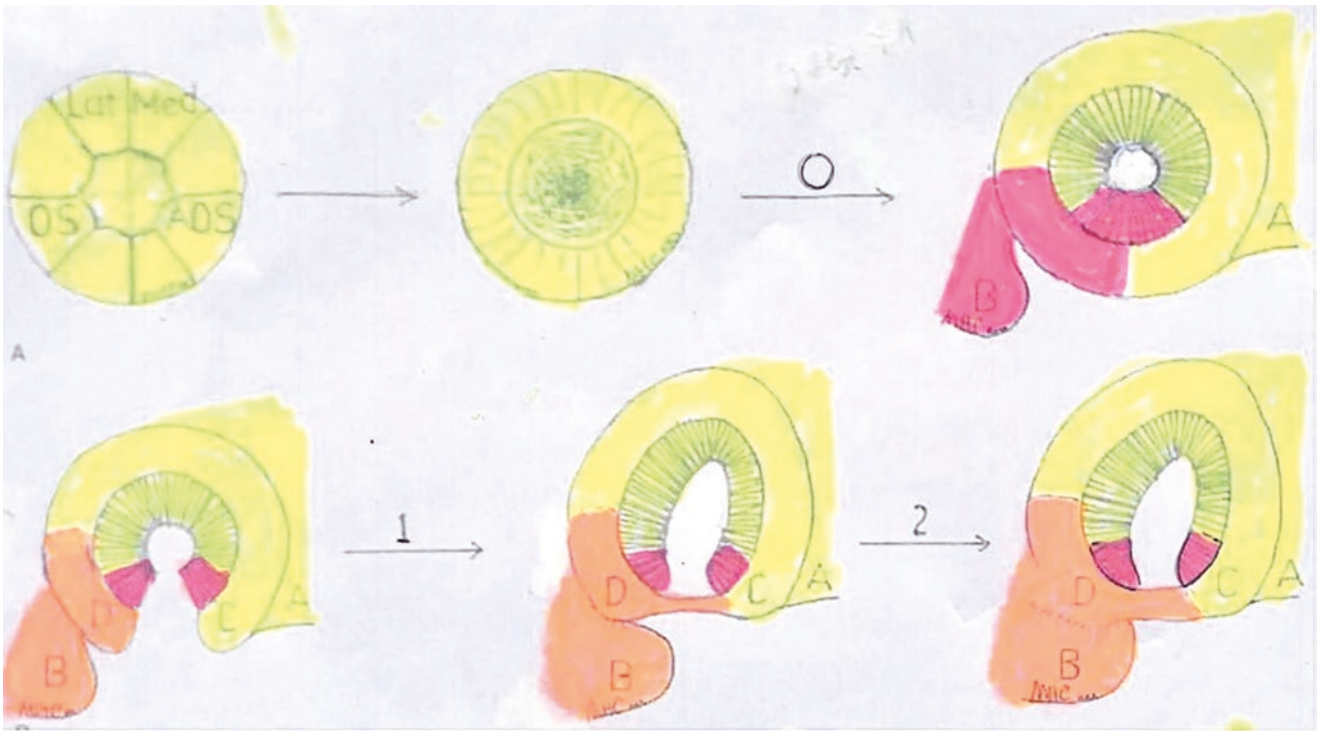

Fig. 18.48 Nasolabial closure sequence 1–2. *Key*: A = prolabium. B = lateral lip element (MxP) containing first and second arch neural crest mesenchyme and facial muscle, C = medial nasal process (MNP), D = lateral nasal process (LNP)
Step 0: preparation. Stages 11–13: Nasal floor, lateral nasal wall, and caudal LNP invaded by first arch (red). Stage 14: dissolution of nasal floor and approximation of MxP. Stage 15 MxP fuses to LNP
Step 1: Simonart's band. LNP, now transformed and activated by blood supply from StV2 and ECA
- Arrest at this point = **complete cleft lip**

Step 2: Migration of lateral lip element PMx to reach MNP
Nota bene: normal lip development can proceed both sides but non-syndromic apoptotic failure will lead to midline widening
[Courtesy of Michael Carstens, MD]

them initially in the wrong order (division, deficiency, displacement and distortion) when in point of fact it was the deficiency in the r1 premaxillary field that led via *a critical lack of BMP4 synthesis to the epithelial fusion failure…and therefore to division. So, to repeat for the umpteenth time, the term "cleft" is itself a misnomer, an intellectual trap. It is simply a failure of normal tissue behavior due to abnormal biochemical signals arising from a site of mesenchymal deficiency. To illustrate this point, I include here the original language. To be sure, microform cleft is important but I kept missing the bigger picture*.

"The sequential nature of the clefting process is best seen in the minimal deformity. The clef ting 'event' happens in the lateral margin of what will be the floor of the nose in step 1. If the event is severe, a full-blown complete cleft lip will result. Lesser degrees of abnormality imply progressively milder forms of expression in the lip. *This is wrong. The problem is not in the lip by in the nasal floor*. The minimal deformity defines the outer border of this envelope, which is the definition of the philtrum at step 4. Median clefts do not show a piriform deformity because the pathologic event occurs in the midline A fields (the r1 neural crest mesenchyme of the FNP)."

It is precisely at this paragraph that I had a change of concept. Except that a fine deficiency of neural crest mesenchyme is the static outcome of angiosome failure, not an "event" in itself. "The fundamental event of cleft formation is the creation of a deficiency state in the floor of the nose. All the remaining processes of cleft (division, displacement and distortion) follow from this single event. When the anatomy of the nasal floor in clefts is compared with normal development, the location of this deficiency site is defined. The known embryonic events that create this site can be analyzed to further define how the deficiency state is created. *This led subsequently to differential dye injections and the discovery of the neurovascular fields in the facial midline*.

- The lessons of the microform cleft were the first step toward the development of the neuromeric model.

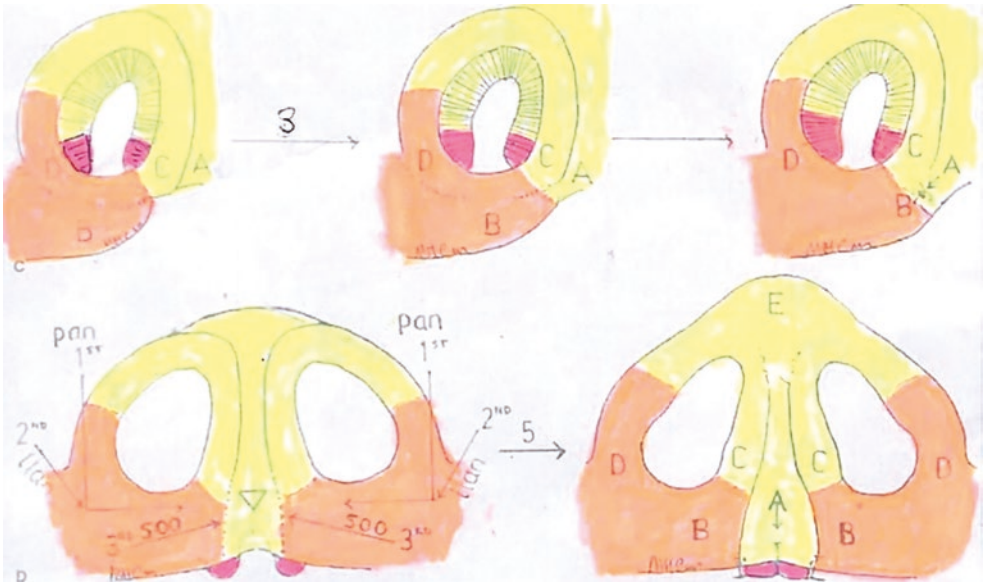

Fig. 18.49 Nasolabial closure sequence 1–2. *Key*: A = prolabium. B = lateral lip element (MxP) containing first and second arch neural crest mesenchyme and facial muscle, C = medial nasal process (MNP), D = lateral nasal process (LNP)
Step 3: Mesenchymal transfer from lateral lip element to prolabium. Transfer begins when B–A reaches 1/3 lip height. Probably reflect the *timing* such that myoblasts are present at the margin of lateral lip element
- Arrest at this point = **incomplete cleft lip**

Step 4: Development of alveolar processes of both maxilla and premaxillae
Step 5: Fusion of alveolar processes, midline fusion and development of the nasal tip
Nota bene: normal lip development can proceed both sides but non-syndromic apoptotic failure will lead to midline widening
[Courtesy of Michael Carstens, MD]

Functional Matrix: Dysfunction in the Lateral Nasal Process

Membranous bone is a Johnny-come-lately in the formation of the face. The evidence that facial bone formation responds to its soft-tissue template has been exhaustively reviewed by Enlow [40]. Distortions in that template are faithfully mirrored by skeletal architecture. *Thus, the morphology of the piriform aperture in the floor of the cleft-lip nose is an "impression" of a dysfunctional matrix.*

- The functional matrix concept of ML Moss describes composite blocks of tissue having independent developmental, origin, vascularity and function [41, 42].
- A narrow zone of deficiency thus exists at the anterolateral border of the piriform; this extends interiorly to the beginning of the inferior turbinate. When the alar complex is sufficiently freed from the piriform so as to assume a normal configuration, this zone will require coverage with mucosa. *This is the first description of the defect in the frontal process of the premaxilla* (Fig. 18.7).

Deformities of the nasal capsule have been documented in studies comparing cleft patients with normal controls [43]. The piriform aperture appears "expanded" and the nasal floor is displaced caudally. These changes occur because the bone has formed within a distorted matrix. Despite this, the cross-sectional area of the airway in adult cleft patients was found by Hairfield and Warren to be reduced 59% [44]. This is caused by alterations in the size and shape of the septum and vomer, enlarged turbinates and vomerine spurs. Kimes demonstrated altered growth rates for these structures in cleft patients.

- *These airway findings anticipate the work of Talmant in the dysfunctional airway but the unrecognized problem he addressed is the pathologic misinsertion of the nasalis muscle.*

The quantitative absence of soft tissue at this juncture is the cleft site accompanied by a proportional deficit of bone. All further manifestations of the cleft follow from this. The periosteal attachment to this deficient and distorted site perpetuates the deformity. As growth proceeds, asymmetries of force vectors continue to open up the cleft site. Surgical reversal of this ongoing process in infancy, while facial growth is explosive, is a fundamental principle of DFR cleft repair.

This requires a surgical redefinition of the cleft condition followed by reconstruction of all tissue elements to their pre-cleft state. Restitution of the original functional matrix is the only manner by which subsequent biologic growth can be normalized.

Release of the dysfunctional matrix from the piriform fossa requires addition of tissue to replace the mucosal deficit. Vermilion paring flaps can be combined with an anteriorly based turbinate flap to accomplish this task 52–53. By virtue of their geometry being at right angles to one other, these flaps achieve a three-dimensional release of the vestibule.

- *Once again, I was dead wrong. Talmant's work disclosed that the problem of the "entrapped" vestibular lining was not that it was small, but rather abnormally stretched by nasalis so that is became mismatched to the overlying soft tissues. Nasalis reassignment and blunt subperiosteal and subperichondrial release eliminate this faux vestibular defect. As a side benefit, the mysterious vestibular "web" disappears*.

Anatomical Evidence (Figs. 18.50, 18.51, 18.52, 18.53, 18.54, 18.55, 18.56, 18.57 and 18.58)

Several lines of experimental data provide evidence that: (1) a specific region in the floor of the nose exists where fusion occurs; (2) growth of the lateral nasal process plays a crucial role in the fusion process; (3) changes in cell proliferation in the LNP (D field) are stage-specific; (4) the actual fusion event is of very short duration; and (5) the final configuration of the lip/nose complex involves a stagespecific mesenchymal translation to the midline. This evidence will be discussed below in sequence.

Where is the Fusion Site?

Scanning electron microscopy demonstrates dramatic changes in the configurations of the LNP, MNP and MxP between Carnegie stages 14 and 18 [45, 46]. As the fields move toward one another and prepare to fuse, a series of morphological and biochemical changes occur; these are most pronounced in the fusion zone—the caudal aspect of the LNP and the MNP. In mouse embryos, epithelial "preparation" at the base of the nasal pit includes loss of microvilli, phenotypic differences and intracellular inclusions indicative of –degeneration in otherwise normal appearing cells [47–55]. Concanavalin A binds selectively at the fusion points of both the LNP and MNP [56].

As the nasal epithelia and mesenchyme differentiate toward fusion (cell death), DNA synthesis decreases. When Wilson and coworkers studied the nasal region of rhesus embryos of advancing developmental age, DNA synthesis decreased successively from the placode stage to the nasal groove to the primary nasal cavity [57]. These findings can be localized to the caudal aspect of the LNP and MNP. DNA synthesis studies of mice [58] and rats [58] show epithelial activity at the fusion site of the nasal groove to be reduced compared with the nonfusion area superior to it. Cell kinetics in the murine fusion region are likewise diminished when labeled with tritiated thymidine [56].

Gui et al. studied the proliferative characteristics of these tissues in mouse embryos using pulse labeling with 5-bromodeoxyuridine to determine epithelial cell proliferation and mesenchymal cell density at differing levels of the

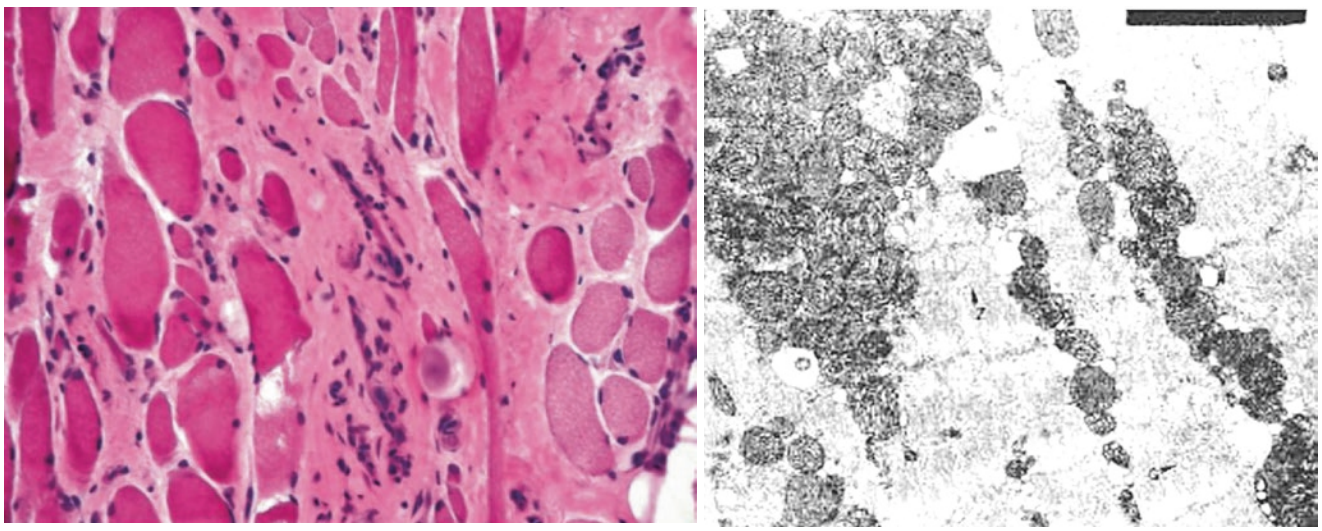

Fig. 18.50 Cleft muscle histology and ultrastructure. *Left*: Muscle at the cleft margin in both cleft lip and cleft palate displays variability of fibers type and size from normal and patterns of disorganization, and fibrosis at the microscopic level both: *Right*: Ultrastructural changes are seen as well, characterized by abnormal clumps of mitochondria with lateration in the cristae. Left: [Reprinted from Lazzeri D. Dystrophic-like alteration characterize orbicularis oris and palatopharyngeus muscles in patients affected by cleft lip and palate. Cleft Palate Craniofac J 2008; 45(6):587–591. With permission from SAGE Publishing.] Right: [Reprinted from Schendel SA, Pearl RM, De'Armond SJ. Pathophysiology of cleft lip muscle. Plast Reconstr Surg 1989; 83(5):777–784. With permission from Wolters Kluwer Health, Inc.]

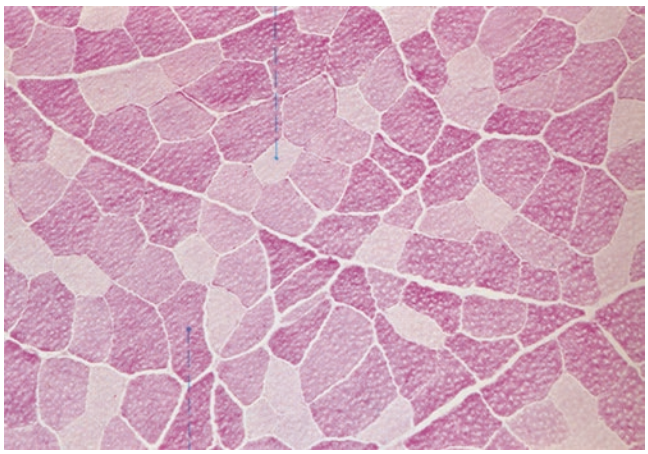

Fig. 18.51 Muscle fiber type. Type 1: Preferentially formed during embryonic phase of myogenesis. The fibers are small, red in color (very vascular), use aerobic respiration to make ATP red color, have lots of mitochondria, and are characterized by slow fatigability for endurance. Type 2A: Preferentially formed during fetal phase of myogenesis. The fibers are larger, white in color (less well perfused), use both aerobic and anaerobic metabolism, have fewer mitochondria, and show easy fatigability for explosive force. Type 2B: same a 2A but uses strictly gycolytic anaerobic metabolism. [Reprinted from Frithjof Hammersen Sobotta's Atlas of Microscopic Anatomy Urban and Scharzenberg, 1985]

nasal groove [59]. These findings were correlated with developmental age, using tail somite number as an indicator. This experimental design permitted three-dimensional variations among four specific regions of the nasal fields. LNP-MNP fusion occurred only at the most caudal (D) level. At tail somite 3, the D-level epithelial labeling index was significantly lower than levels A–C. As the embryo approached TS11, DNA synthesis rapid declined to near zero. The labeling index of the MNP did not reach zero until later at TS13.

Mesenchymal Mass

The mass of the nasal prominences is not equal. In human embryos Warbrick found more rapid mesenchymal expansion on the medial side; these observations were not site-specific [60]. Differences in the LNP versus the MNP were also noted in the mesenchyme. At all tail somite stages (TS3–TS11) of the LNP, labeling was lower at the fusion site (level D). In the MNP, a statistically significant change in labeling between the non-fusion levels and the fusion site did not occur until TS7. Fusion occurred between TS5 and TS7. Gui concluded that *differences in mesenchymal mass* between the—fusion and non-fusion regions of the LNP versus the

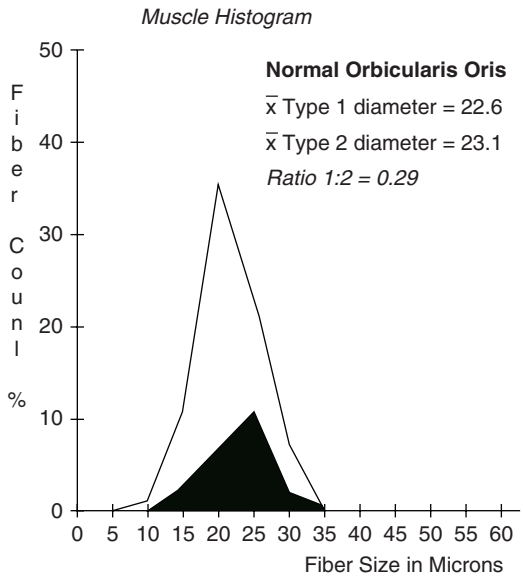

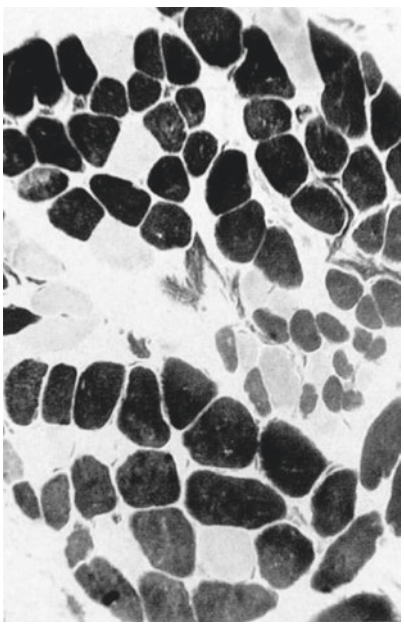

Fig. 18.52 Normal orbicularis muscle from biopsy site unrelated to the cleft margin. Note fiber type with type 1 < type 2, similar fiber diameters, and histology (light staining fibers are type 1 and dark staining fibers are type 2). [Reprinted from de Chalain T, Zuker R, Acklery C. Histologic, histochemical and ultrastructural analysis of soft tissues from cleft and normal lips. Plast Reconstr Surg 2001; 108(3):605–611. With permission from Wolters Kluwer Health, Inc.]

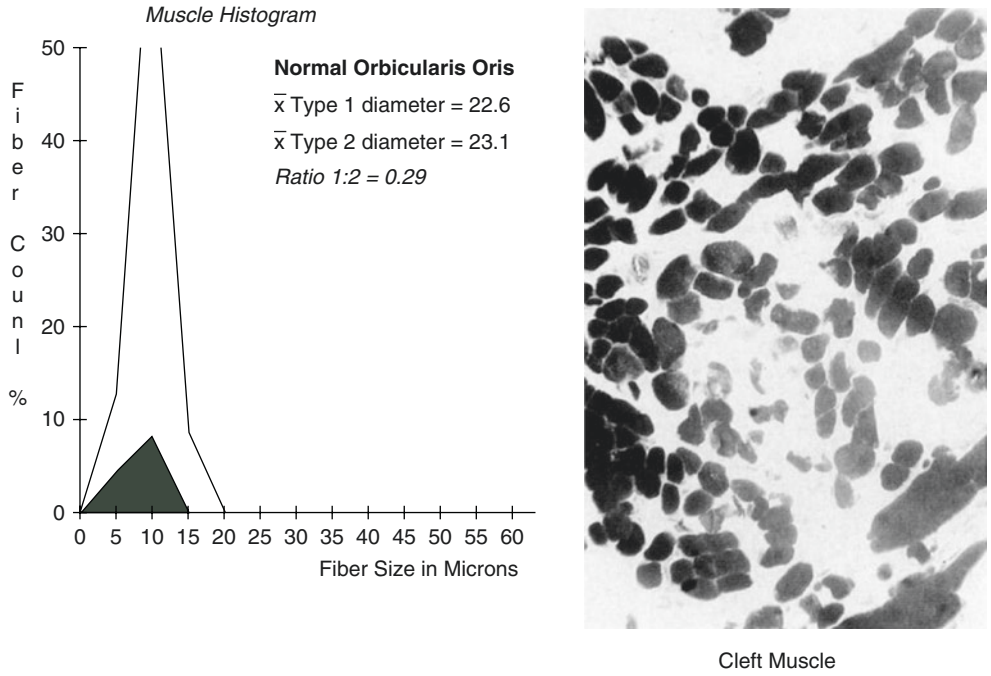

Fig. 18.53 Cleft orbicularis muscle. Type 1 fibers are reduced compared to type 2. Fiber size of type 2 is 50% of normal. Note hypoplasia of the muscle fibers. [Reprinted from de Chalain T, Zuker R, Acklery C. Histologic, histochemical and ultrastructural analysis of soft tissues from cleft and normal lips. Plast Reconstr Surg 2001; 108(3):605–611. With permission from Wolters Kluwer Health, Inc.]

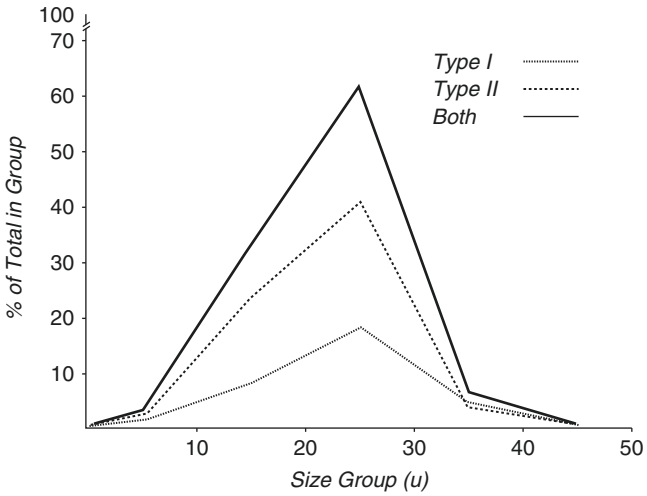

Fig. 18.54 Normal orbicularis muscle histogram Schendel. Type 1 30.3%, Type 2 69.7%. Average type 1 fiber diameter 23.5 μm, Average type 2 fiber diameter 22.4 μm. Note fiber diameters in normal facial muscle are about 50% smaller than for limb muscle. [Reprinted from Schendel SA, Pearl M, De Armond SJ. Pathophysiology of cleft lip muscle. Plast Reconstr Surg 1989;83(3):777–923. With permission from Wolters Kluwer Health, Inc.]

MNP have significance in terms of their relative roles in the fusion process:

"It is believed that the bulk of the MNP in the non-fusing areas expands more rapidly than that of the LNP.... Concerning the presumptive fusion area, we hypothesize conversely that the bulk of the LNP mesenchyme at the side of the nasal groove expands more rapidly than that in the MNP at the other side.... The LNP at the fusion area remarkably protrudes to contact with the MNP. Since DNA synthesis of the LNP epithelium in the fusing area decreases sooner than that of the MNP, it is suggested that *the LNP mesenchyme plays a more important role* in the initial contact between both prominences a t the fusion area, being associated with the epithelial differentiation in the LNP."

Defective genetic programming could alter the coordination of the timetable for field closure. Two genetic loci that cause deficiencies in size of the facial prominences are now associated with cleft lip-producing strains of mice [61]. Alterations in coding or regulation of a growth factor or receptor could impair successful outgrowth or fusion of the LNP and MNP. Once translation of the MxP across the LNP/MNP "bridge" is under way, deficiencies in mesenchymal "flow" may occur. Serial sections of the nasal contact zone in normal and cleft-susceptible mice were measured by Wang and Diewert. In the cleft strains, both the enlargement of the epithelial seam and its "filling out" by a mesenchymal bridge were delayed by tail somite stage compared with normal. Forward growth of the maxillary process was also correlated by Wang with mesenchymal bridge development in both normal and cleft strains.

Fusion itself is of short duration. Surf ace changes in the epithelia are a marker, with disappearance of microvilli seen on scanning electron microscopy at TS6 about 12 h before contact [62]. As the nasal epithelium prepares for fusion between TSS and TS7, alterations in its cellular kinetics occur. The selective decrease in DNA synthesis noted about 6–8 h before fusion further defines the window

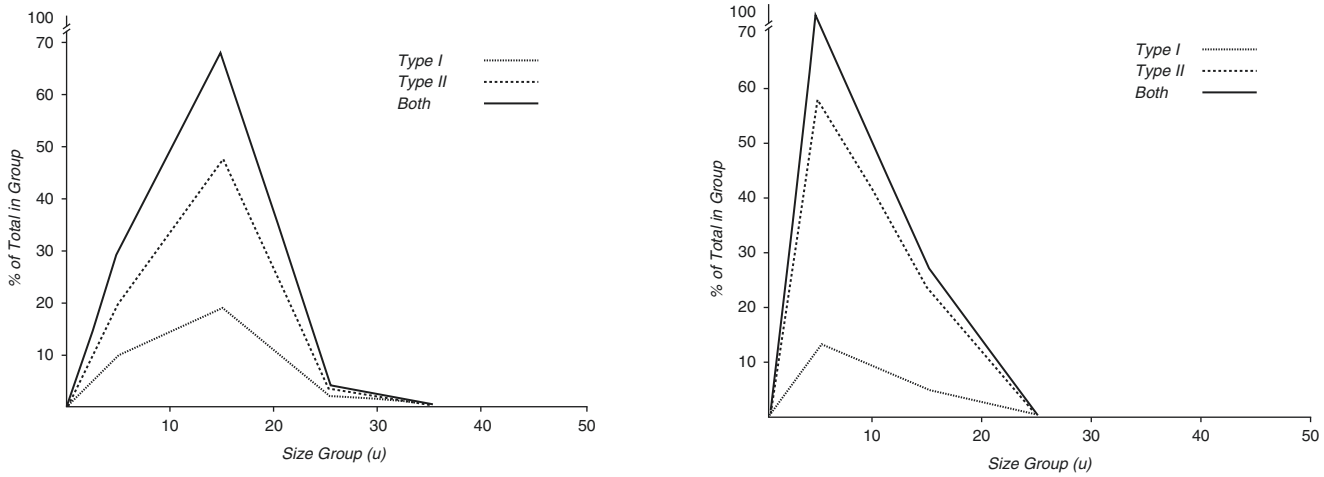

Fig. 18.55 Cleft orbicularis muscle histograms Schendel. Left: Non-cleft side. Type 1, 29.2%; type 2, 70.8%. Average type 1 diameter is 11.1 μm. Average type 2 diameter is 11.8 μm. Right: Cleft side Type 1, 17.4%; type 2, 82.6% Average type 1 diameter is 8.9 μm. Average type 2 diameter is 8.9 μm. [Reprinted from Schendel SA, Pearl M, De Armond SJ. Pathophysiology of cleft lip muscle. Plast Reconstr Surg 1989;83(3):777–923. With permission from Wolters Kluwer Health, Inc.]

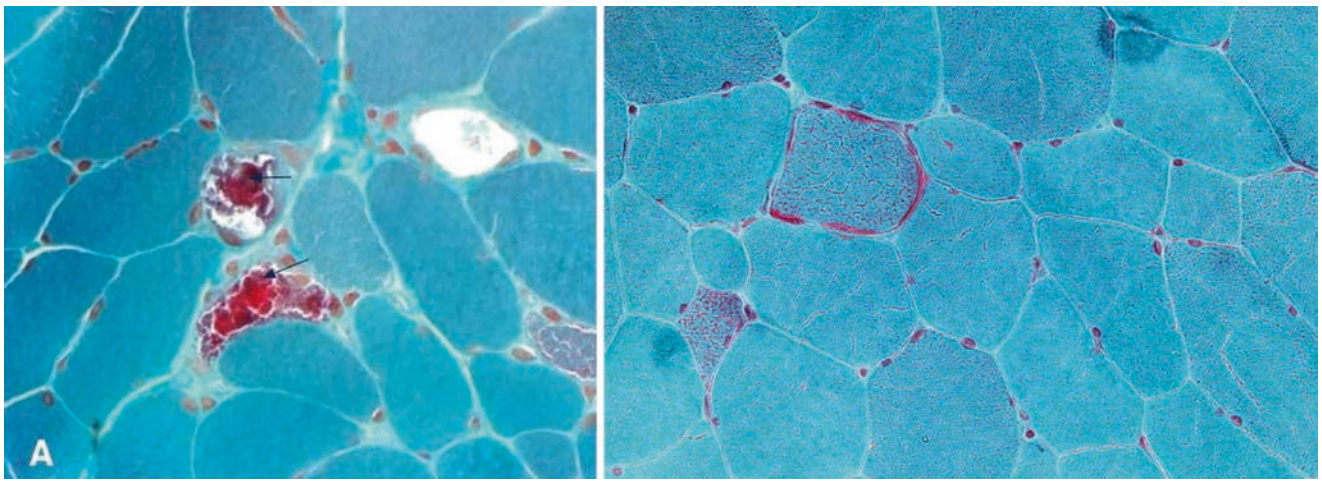

Fig. 18.56 Gomori stain. MERFF is characterized by myopathy with myoclonus, seizures, and cerebellar degeneration. Muscle biopsy in this disease shows ragged red fibers (therefore its name). Diseases of the mitochondria can be caused by defects in nuclear or mitochondrial DNA and result in decreased energy availability for cell processes. When muscle is stained with Gomori Trichrome, characteristic ragged-red fibers are visible under the microscope. This appearance is due to the accumulation of abnormal mitochondria below the plasma membrane of the muscle fiber. These may extend throughout the muscle fiber as the disease severity increases. The mitochondrial aggregates cause the contour of the muscle fiber to become irregular, causing the "ragged" appearance. Besides muscle, what other tissues would you expect to suffer the most damage from a mitochondrial defect? (**a**) MERFF positive biopsy with diseased mitochondria staining red. (**b**) Muscle fiber irregularity clearly seen. (**a**) [Reprinted from Wikimedia. Retrieved from: https://en.wikipedia.org/wiki/Gömöri_trichrome_stain https://commons.wikimedia.org/wiki/File:Ragged_red_fibers_in_MELAS.jpg With permission from Creative Commons License 2.0: https://creativecommons.org/licenses/by/2.0/deed.en.] (**b**) [Reprinted from Wikimedia. Retrieved from https://commons.wikimedia.org/wiki/File:Ragged_red_fibres_-_gtc_-_very_high_mag.jpg. With permission from Creative Commons License 3.0: https://creativecommons.org/licenses/by-sa/3.0/deed.en]

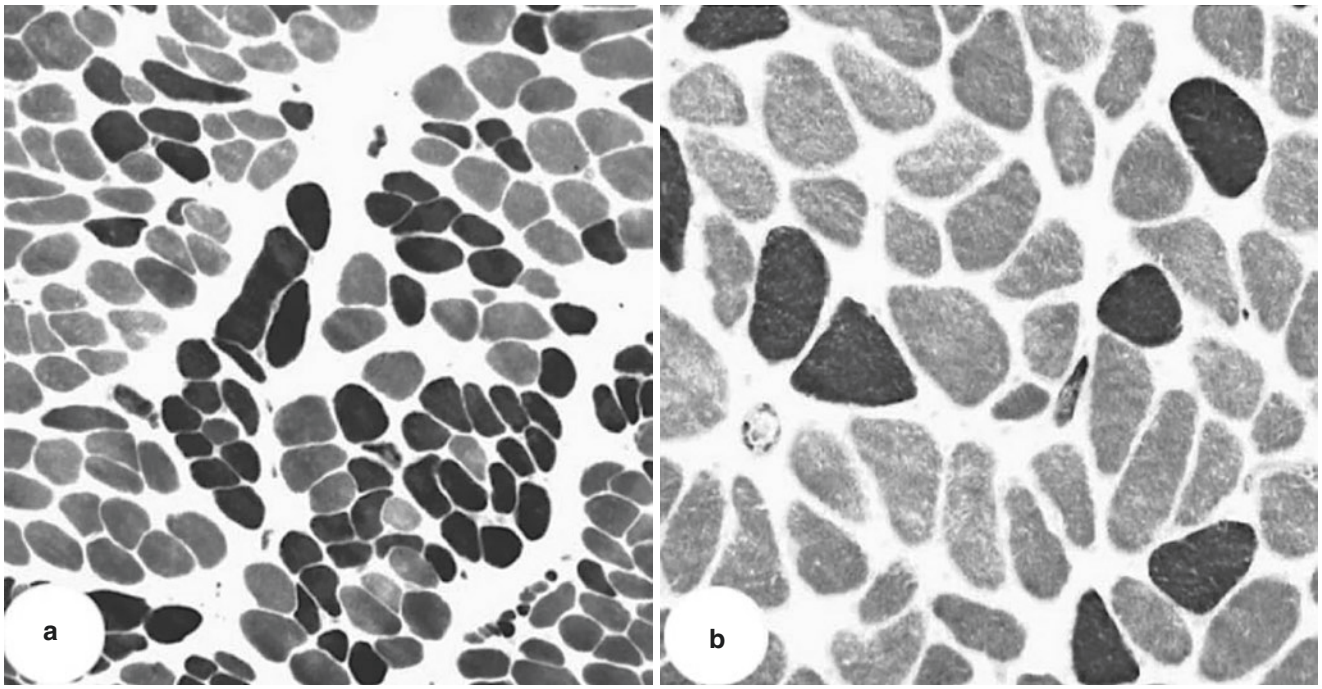

Fig. 18.57 Fiber type in cleft palate third arch Sm7 levator veli palatini. (**a**) LNP in child with cleft Type 1, 36.9% and Type 2, 63.1%. Fiber diameter (mean) 24.9 μm. There is a large proportion of fibrous tissue. (**b**) LVP in normal adult. Type 1, 74.9% and Type 25.1%. Fiber diameter (mean) 46.1 μm. Note: Infant LVP has reversed type 1/type 2 ratio and almost 59% smaller fiber diameter. Fiber diameter relates to degree of use. Light staining fibers = type 1 Dark staining fibers = type 2. [Reprinted from Lindman R, Paulin G, Stål PS. Morphological characterization of the levaator veli palatine muscle in children born with cleft palates. Cleft Palate Craniofac J 2001; 38(5):438–448. With permission from SAGE Publishing]

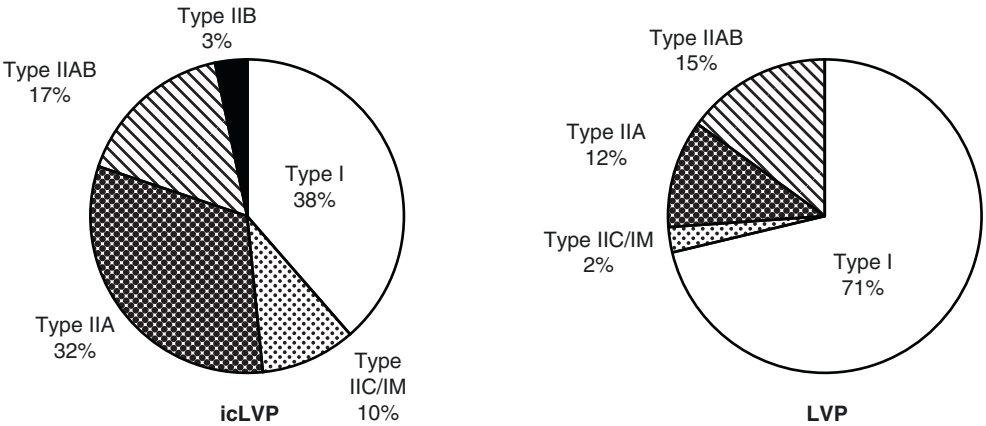

Fig. 18.58 Levator veli palatine in the cleft versus normal state. Cleft state in LVP characterized by 50% less type I fibers. [Reprinted from Lindman R, Paulin G, Stål PS. Morphological characterization of the levator veli palatine muscle in children born with cleft palates. Cleft Palate Craniofac J 2001; 38(5):438–448. With permission from SAGE Publishing]

of prerequisite for later fusion of the lateral lip element to the midline.

Metabolic Insufficiency

Metabolic demands of this rapidly proliferating tissue are undoubtedly high. Immediately before MxP fuses with the unified LNP/MNP complex, the LNP demonstrates a *burst of cell division that renders it vulnerable to insult.* Many possible mechanisms could depress the rate of cell proliferation of the LNP, resulting in the failure to fuse with the MNP; these include: (1) inadequate physical approximation of the processes, (2) Impaired epithelial break-down, and (3) impaired metabolism due to environmental toxicity defective cell programming.

Comparison of cleft formation in three strains of mice provides a useful model to separate out some of the vari-

ables. C57Bl/6J embryos have a normal growth pattern of the LNP and MNP, and a negligible incidence of clefts. A/J and CL/Fr embryos have cleft incidences of up to 12% and 36%, respectively. Both strains have alteration in MNP growth that is more parallel to the midline and therefore cannot fuse properly with the LNP. A dramatic *decrease in epithelial activity at the fusion site* is what sets the CL/Fr embryo apart, making it more susceptible to cleft formation than the A/J strain [63].

Cleft may result from *oxygen deprivation* to the nasal fields at this critical juncture. Hypoxia increases the incidence of CL/P in AJ mice. As FiO_2 drops from 21 to 10%, cleft incidence increases from 38 to 90% [47, 49, 50]. Smoking causes perturbations in placental blood flow. Carbon monoxide produced by maternal smoking decreases oxygen release by 42% causing hypoxia which can affect the developing embryo [64]. A Swedish study demonstrated a doubling in the incidence of clefts born to smoking mothers [65]. Hyperoxia can also be protective. CL/Fr mice born to mothers exposed to 50% FiO_2 have only a 10% incidence of clefts. The known susceptibility of A/J mice treated with phenytoin drops from 87% at room air to 25% at FiO_2 [48].

Vascular Insufficiency

Blood supply issues may also come into play. The distal-lateral zone of the A field lies immediately subjacent to the D field and mesial to the internal aspect of the B field. This A–B–D "apex" is a watershed between two vascular systems, between the most distal branches of the internal carotid artery and the most caudal and mesial branches of the external carotid artery. During this early development period, it should be borne in mind that the external carotid system is itself in formation. All facial structures not supplied by the internal carotid artery are initially served by branches of the stapedial artery system. This system must be replaced by means of aortic arch derivatives, selective portions of which coalesce to form the external carotid system [66, 67].

The point of vascular "switchover" leaves the nasal prominences particularly vulnerable to insult for two reasons. First, the transition is itself genetically determined, and errors in this process could occur. Second, extrinsically caused hypoxia could rob whatever "safety margin" the embryo possesses during the switchover. Conversely, the protective effect of hyperoxia in cleftsusceptible mice may apply here. Embryos with a statistically greater likelihood to sustain a vascular insult could be "tided over" by higher O_2 concentrations.

Simonart's Band

What is it that drives the production of the cutaneous Simonart's band? It does not arise from the premaxillary tissues. PMxB is in communication with the caudal tip of LNP which is composed of r2 neural crest. Let's postulate that metabolic activity at the alar base "revs up" the basal LNP to produce this protrusion. In some ways this is analogous to basal MNP when it spits out prolabial process. In any case, the "epithelial experiment" of Simonart's band is short-lived and all-or-nothing. Either it achieves fusion with the medial process or it does not. The success depends upon the physical distance and strength of the biochemical signal.

As we saw, this bridge quickly fills with mesenchyme. If lip development stops here we have a have a very high incomplete cleft. Mucosal fusion (not shown in our diagram) provides the template for DOO migration. The skin envelope fulfills the same function for SOO. Why does SOO stop at the philtral boundary? We can explain this as a question of "like versus unlike." The r2 skin abuts against r1 skin of the philtrum. SOO will along go as far as its template permits. So it simply makes contact with the subcutaneous mesenchyme of the philtrum. Meanwhile, DOO, unimpeded, proceeds blithely along the mucosa until it encounters its contralateral fellow.

In summation, experimental evidence suggests the following

- The closure process of the nose and lip involves a sequence of events, the site of which is located at the caudal aspect of the medial and lateral nasal processes. TS = Theiler stage.
- Physical size (mesenchymal mass) of the processes must put them within the *critical contact distance*.
- Epithelial breakdown along the seams of the processes is the prerequisite for fusion. This requires a diffusible morphogen, BMP4.
- LNP fusion to the MNP is the prerequisite for the migration of MxP mesenchyme medial to eventually unite with prolabium/premaxilla.
- LNP initiates contact with MNP.
  - Both the epithelium and mesenchyme of the LNP at the fusion site are activated *before* those of the MNP.
  - After fusion occurs (TS7), DNA labeling indices continue to decrease in both the LNP and MNP. These reach zero at TS l 1 for the MNP and TS13 for the MNP.
- Simonart's band: mesenchymal stabilization in these processes correlates with the formation of a mesenchymal bridge at TS12–TS13.

B

Unification of the Lip: Mesenchymal Migration

Lateral lip element migrates along the bridge bringing muscles with it. As more mesenchyme fills the envelope, the fusion process proceeds downward. As BMP4 arrives at the cutaneous border, epithelial breakdown and fusion ensue. Note that all the action is on the lateral lip side as the BMP4 is produced by the premaxillary field.

Intraorally during this time, the medial nasopalatine fields are undergoing posterior-to-anterior fusion. Mesenchyme is added progressively, as discussed in Chap. 14. At precisely the point that this "zipper" mechanism arrives at the incisive foramen, the palatal shelves are lifting up such that contact can be made. At that point medial nasopalatine proceeds forward into the primary palate. Thus, fusion of the secondary palate is anterior–posterior while that of the primary palate is posterioanterior.

- The "flow" of such mesenchyme is lateral to medial. Its timing is short (4 h).
- This period is one of great vulnerability to a number of potential environmental and genetic insults.

Pathophysiology of Cleft Lip/Palate Muscle

We have discussed at great length how developmental field model applies to craniofacial bone fields. Neuroangiosome failure leading to a reduction in mesenchymal volume is manifested as small or absent bone structures that produce smaller amounts of biochemical products, such as diffusible morphogens. We have seen how the feedback loop between bone morphogenetic protein 4 and sonic hedgehog regulates epithelial stability, thereby controlling fusion of neighboring mesenchymal structures, such as palatine shelf to vomer or lateral lip element to philtrum. But the BMP4/Shh mechanism is only one of many that must be operative. In the progressive loss of mesenchyme from PMxF to PMxB the local concentrations of multiple signals and growth factors are affected. In this important section, we shall look at selected aspect of the perioral musculature surrounding the cleft, first, in terms of anatomic organization and function, and second, in terms of histochemistry and ultrastructure. These studies further support the diffusible morphogen model.

- Diffusible morphogens from abnormal field affect multiple tissues, including muscle.
- The reduction in concentrations of these morphogens is highly localized to the submucosal tissues on both sides of the cleft.
- The concentration gradient normalizes distal to the cleft site, with consequent return of microanatomy and histochemistry to normal.
- Non-philtral prolabial tissues are abnormal.
- The fundamental goal of surgical repair is to reassign healthy developmental fields to normal anatomic relationships.

Muscle Anatomy and Function

Traditional anatomic concepts of the orbicularis as a monolithic layer are incorrect. These had led to any surgical publications in which the two muscle layers are dissected as full thickness flaps and sutured either directly or rearranged. Orbicularis is dynamic with two distinct functions: DOO is a sphincter and SOO acts as a dilator. In point of fact, the orbicularis is a layered structure with specific points of insertion, which explains the esthetic "drape" of the lip as well as its prehensile abilities. These layers give the pout of the lip and philtrum. Surgical approaches based on z-plasty muscle flaps and interdigitation can violate the architecture of the nasolabial complex.

The best way to conceptualize this anatomy is to combine the work of Park with that of Delaire, Precious and Nammoun, building on previous studies by Nairn and Nicolau [68–70]. Park's dissections show the orbicularis to possess a deep, sphincteric layer that traverses the entire lip beneath Cupid's bow and permits the lip to pucker. Contraction of DOO causes narrowing of the philtral columns. The deep layer has a flat, peripheral portion hugging the mucosa and an outwardly curving marginal portion: The marginal part does not lie flat but curls outward like the lip of a jug. Its form follows the mucous membrane of the lip as this everts onto the face to become the red lip margin [71] (Figs. 18.11, 18.59, 18.60, 18.61, 18.62 and 18.63).

Superficial to this plane of orbicularis is another superficial layer associated with the muscles of facial expression. *Widening of the philtral columns* results from contraction of this layer. Three-dimensional computed tomographic reconstruction of the lip demonstrate that the superficial orbicularis does not cross the midline but inserts into the lateral margins of the philtrum. Computed tomography could distinguish muscle formation but was unable to detect philtral development until after the second trimester. This discrepancy may reflect the relative insensitivity of the technique. This contradicts the previous work by Latham, who used layered Plexiglas tracings, a methodology which leads to false conclusion that fibers from a single-layer orbicularis oris crossed the philtrum to insert on the opposite side.

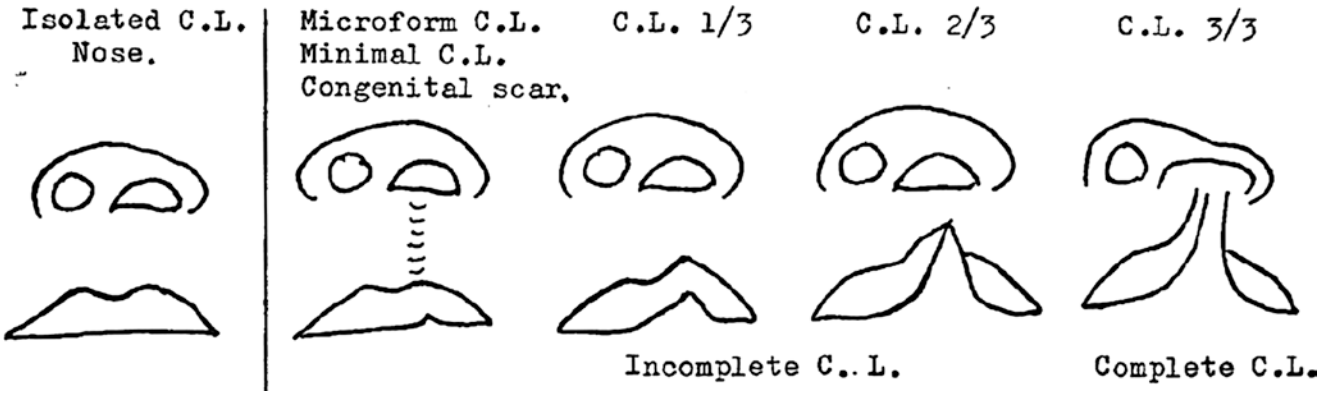

Fig. 18.59 Onizuka classification 1. Onizuka classification of microform clefts is compatible with DFR model. Diffusion of BMP4 as an inhibitor of Sonic hedgehog causes epithelial breakdown. PMx field deficiency results in reduced [BMP4} and therefore resistance of epithelium to fusion. Isolated Cl is defined by Mullein as the "minimicroform" which places emphasis on the lip rather than on the piriform fossa and the nose. [Reprinted from Onizuka T, Ho aka Y, Ayoyama R, Takahama H, Jinnai T, Ursi Y. Operations for microforms of cleft lip. Cleft Palate Craniofac J 1991;28(3): 293. With permission from SAGE Publishing]

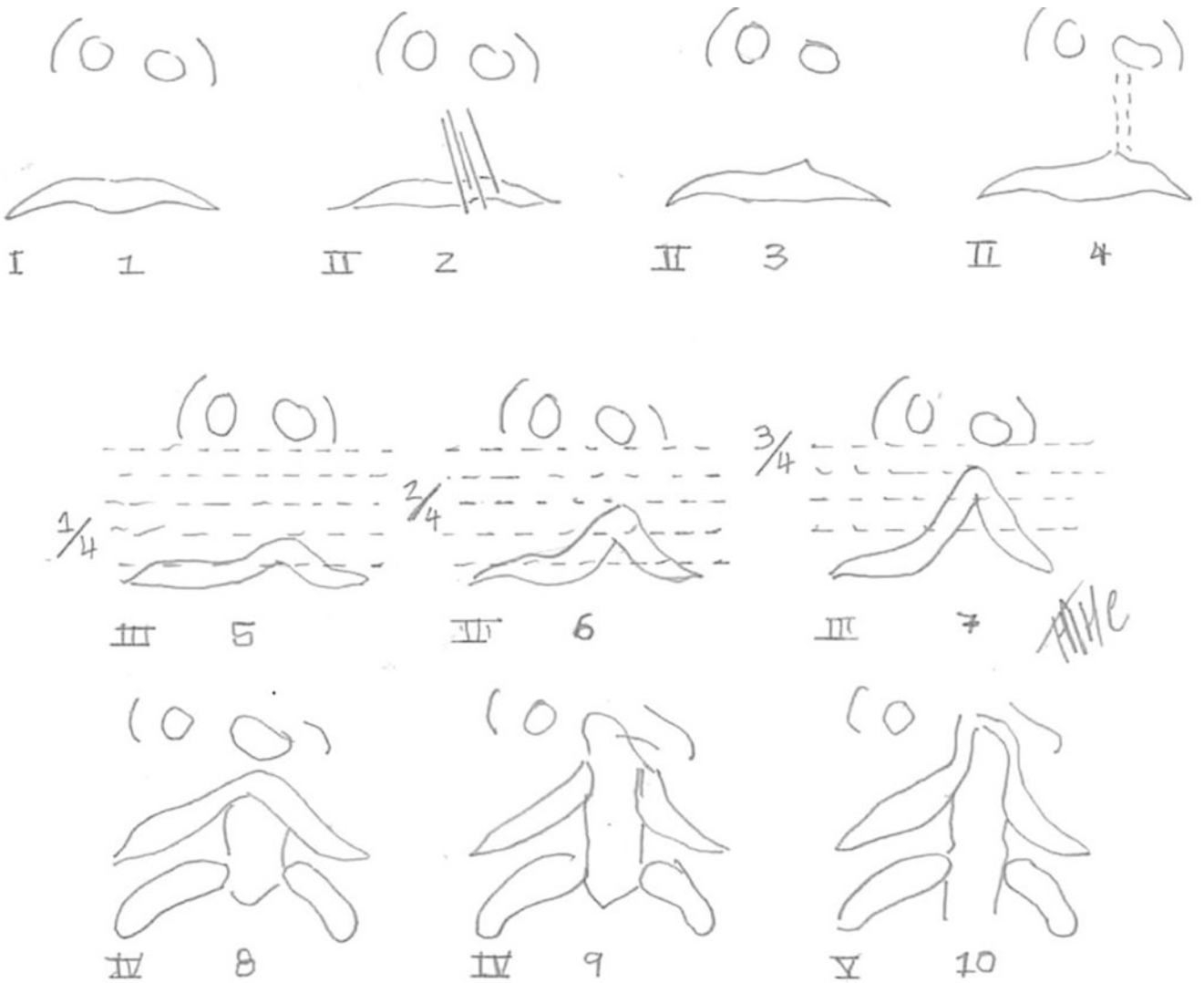

Fig. 18.60 Onizuka classification 2. See text. [Reprinted from Onizuka T, Ho aka Y, Ayoyama R, Takahama H, Jinnai T, Ursi Y. Operations for microforms of cleft lip. Cleft Palate Craniofac J 1991;28(3): 293. With permission from SAGE Publishing]

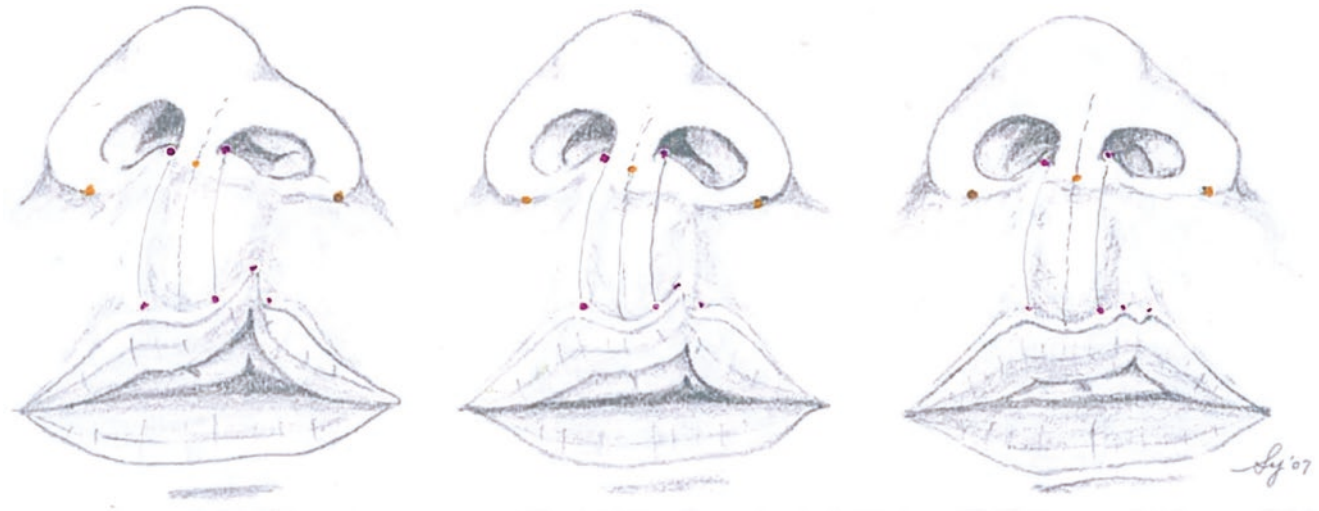

Fig. 18.61 DFR Mulliken classification. Mulliken classification. (Left) incomplete, (center) microform, (right) mini-microform (see text). Red dots (1) Distance from non-cleft side footplate of medial crus to Cupid's bow (13–2); (3) distance from cleft side footplate to Cupid's bow (12–3); maximum height of cleft taken by Mulliken as point 3. Note: DFR defined width of Cupid's bow 2–3 as the territory of the anterior ethmoid neuroangiosomes; it is the distance between the alar footplates (12–13). Orange dots indicate subnasale and the position of the alar bases, on the non-cleft side (4) and on the cleft side (10). Note as alar base displacement becomes more pronounces with increasing severity of the cleft. [Reprinted from Yuzuriha S, Mulliken JB. Minor-form, microform, and mini-microform cleft lip: anatomical features, operative techniques and revisions. Plast Reconstr Surg 2008; 122(5):1489–1493. With permission from Wolters Kluwer Health, Inc.]

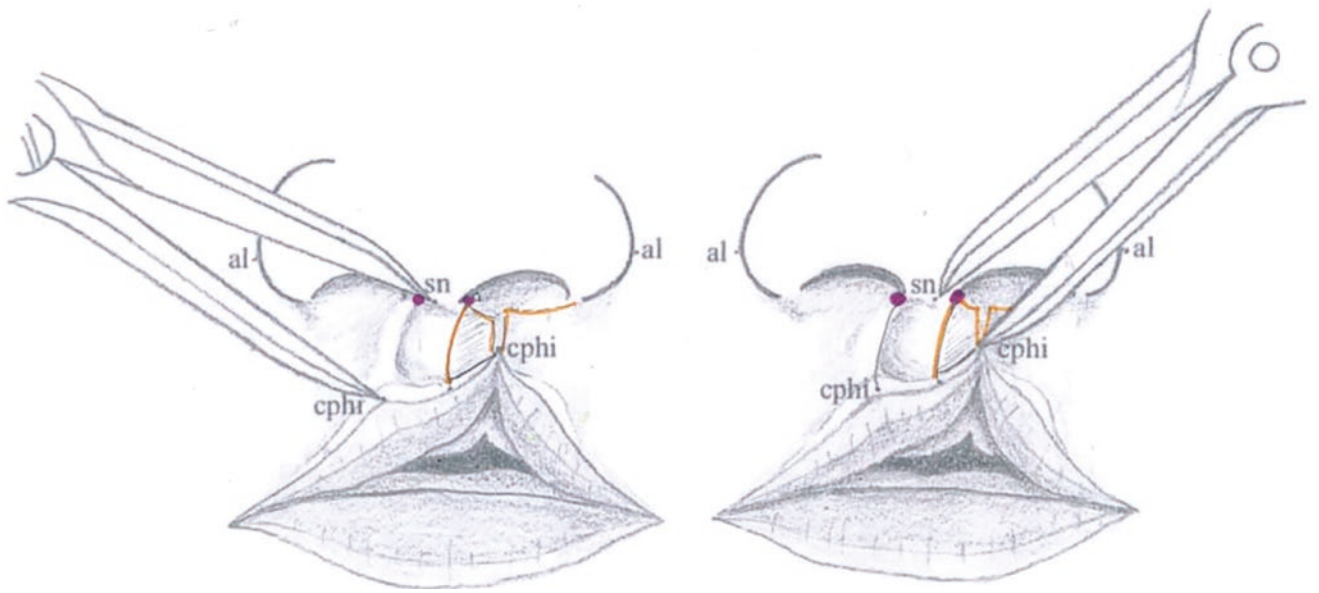

Fig. 18.62 Prolabium paradox. Caliper tip is placed on subnasale and shown to measure a difference in philtral height. Obvious difference between sn-cph non-cleft versus sn-cphi cleft. If caliper tip is placed on the alar footplates 13–2 = 12–3. Non-philtral prolabium, defined by the orange trapezoid, is full-thickness skin and subcutaneous tissue based on terminal branch of medial nasopalatine. It is advance into the columellar release and rotated into in the nasal floor. [Reprinted from Yuzuriha S, Mulliken JB. Minor-form, microform, and mini-microform cleft lip: anatomical features, operative techniques and revisions. Plast Reconstr Surg 2008; 122(5):1489–1493. With permission from Wolters Kluwer Health, Inc.]

Fig. 18.63 Residual nasal features of right-side microform cleft after repair. Cleft nasal deformity persists post repair: columellar deflection, footplate of medial crus tractioned downward and lies internal to the left side asymmetrical tip, airway reduced in size with compromise of the external valve. Lip shows asymmetry of orbicularis insertion into the right side of columellar base. [Reprinted from Yuzuriha S, Mulliken JB. Minor-form, microform, and mini-microform cleft lip: anatomical features, operative techniques and revisions. Plast Reconstr Surg 2008; 122(5):1489–1493. With permission from Wolters Kluwer Health, Inc.]

The layered orbicularis model provides a functional explanation of the philtrum. It is also compatible with work by Delaire et al. [21] demonstrating that oblique fibers inserted high into the midline near the anterior nasal spine could establish a drape for the lip. These fibers also intermingle with those of the paranasal complex. Joos and Friedburg used magnetic resonance imaging to study the relation of these muscles to the autonomic nervous system (ANS) in normal subjects and in cleft patients both pre- and postoperatively. The lateral muscle, particularly at the level of the spina nasalis, runs in a stepwise fashion dorsally through the nasal floor and is inserted into the nasal septum. This explains why in the cleft state the nasal septum always deviates to the healthy side, where the muscles are inserted in a ring-shaped distribution of the musculature in the anterior facial region. If the muscle ring is not closed ... the musculature of the mid-face contracts outward, and pulls the ala of the nose.

Recognizing the concept of function rings of perioral musculature, Delaire and Markus pioneered in developing the concept of early subperiosteal centralization of the musculature. Cleft repair is thus functional as well as anatomic. Its design should synchronize and facilitate a more normal subsequent facial development (cf Fig. 18.14).

The development and insertion of these muscles follows a strictly coordinated timeline. The overall "game plan" of facial muscle development is from deep to superficial, from lateral to medial [17]. Philtral formation occurs long after the lip has formed due to the late insertion of the SOO [72]. Intrauterine photographs of developing human fetuses demonstrate absence of a philtrum at 10 weeks [72, 73]. Between 12 and 16 weeks, Kraus' specimens demonstrate philtrum formation concomitant with full development of the nostrils and a true nasolabial fold. Delaire's schema of three perioral muscle "rings" develop in an order consistent with facial muscle embryology. The middle ring (the orbicularis oris) is complete at 12 weeks [74, 75]. At 16 weeks, the lip is united to the anterior–inferior septum and the anterior nasal spine; the median cellulous ligament of Delaire is present.

- **37 mm** Orbicularis oris appears but does not encircle the mouth until 58–80 mm.
- **58–80 mm** The levator labii et alequae nasi appears at 58 mm; it is fully inserted at 80 mm.
- **80 mm** The pars alaris of the nasalis is present at 80 mm and subsequently passes deep to the levator labii et alequae nasi to insert bone along the caudal rim of the piriform aperture.
- **142 mm** The depressor septi passes vertically from the caudal septum through the orbicularis to insert on the maxilla. Thus, the most midline and "septal" muscles form last.

A small but extremely important detail must be mentioned here. The proper insertion of the perioral and perinasal fibers is not truly "into" the septum. Rather, the fibers that mingle and make up the septopremaxillary "ligament" insert into the perichondrium of the anterior paraseptal cartilages. The ligament is hemispheric, U-shaped and extends into the interpremaxillary suture. Thus, the septopremaxillary "liga-

ment" is a fusion of fibers that insert into each half of the united mesial leaves of the r1 mesenchyme into which the septum develops [75].

Cadaver studies of nasolabial muscles by Wu in 4 aborted fetuses with cleft lip demonstrate several important points [76]. Muscle fibers on the lateral side of the cleft were thinner and more disorganized. Absent depressor septi nasi on the cleft side explain the traction of the columellar base to the normal side by remaining DSN. Pars transversalis of nasalis was confirmed to insert *lateral to the incisive fossa*, ascending to the dorsum to join the SMAS of the contralateral muscle. Pars alaris of nasalis has its insertion in the center of the incisive fossa. It bypasses the ala to terminate in the dermis above the lateral crus. On the cleft side nasalis fibers were observed to attach into the skin of the ala nasi and into the piriform fossa as well.

Anatomic and Histologic Studies of Cleft Lip Muscle

We begin with the historic work by Fará on cleft muscle using generalized non-selective vascular injection (via the common carotid) and cadaver dissection which were interpreted to show muscle fibers running upward along the cleft site. This was subsequently popularized by Millard and widely accepted, but turned out to be misleading due to fixation artifact. Fará did document in the normal lip anastomosis between columellar arteries and the superior labial artery. An arteriogram is presented showing the exclusive supply of the bilateral cleft prolabium by what we now know to be paired StV1 anterior ethmoids. Because the injections were non-selective, the developmental significance of this finding was missed.

Dado and Kernahan, using electrical stimulation and serial histologic sections, refuted the Fará model finding [77]. At the lateral cleft margin, instead of an upward pull of muscle fibers along the cleft margin (as predicted by Fará), they observed lateral contraction and puckering, indicating insertion into the skin. In histologic examination of a stillborn with complete unilateral cleft lip and palate, the muscle fibers were found to be sparse and hypoplastic with more abundant collagen staining. The immediate submucosal tissue had an abundance of connective tissue.

Heckler writing on 8 cases of microform cleft compared the degree of orbicularis disorganization with the dental defect, the size of the vermilion notch and with the nasal deformity. In each case, a vertical section was taken full-thickness through the scar and submitted for histology. The severity of orbicularis disorganization strongly correlated with the severity of the nasal findings.

De Mey used histologic section from 18 operative cases of unilateral cleft lip. They identified the bilaminar structure of orbicularis. In 4 incomplete clefts DOO, in association with mucosa was simply interrupted. Within the bridge above the cleft they found SOO to be distorted, with the degree of muscle distortion proportional to the degree of the nasal deformity, confirming Heckler's observations.

DOO and SOO were formally identified by Park in normal cadaver specimens. DOO extends from modiolus to modiolus and is continuous with buccinator. Its purpose is to seal the mouth as a constrictor. SOO extends more lateral to modiolus, comingling with adjacent facial muscles.

"When the mouth is pursed up, the vermilion becomes thickened as the marginal portion of the deep orbicularis oris muscle constructs. Simultaneous relaxation of the superficial part (allows) numerous perioral fine wrinkles (to become visible), accentuated the philtral columns and flattens the nasolabial folds. When the mouth is open, in contrast, perioral fine wrinkles and the philtral column are flattened as contraction of the superficial orbicularis oris muscle stretches the perioral skin."

In a stillborn with complete UCL Park found SOO on the non-cleft side to be undistorted and to insert directly into the nasal columella (and philtral column), again on the side of the normal nostril. On the lateral side, it was found to insert into the alar base. Importantly, fibers (attributed to SOO) were observed to be inserted into the *periosteum of the cleft side piriform fossa* (italics mine). These were surely those of the *nasalis complex* coursing along the superior margin of SOO at the level of the alar base fold.

Histochemistry of Muscle in Cleft Lip and Cleft Palate

The margin of soft tissue clefts constitutes a zone of altered development in which muscles from different embryologic origins, second arch orbicularis in cleft lip and third arch levator, palatopharyngeus and uvulus cleft palate show similar patterns of dystrophic change as seen in their histology, ultrastructure and histochemistry. Compared with normal facial muscle biopsies of cleft muscle are markedly different. Routine stains from specimens at the margin show disorganized fibers going in different directions. As the cleft margin is approached muscle fibers are reduced in number and the amount of connective tissue increases (Figs. 18.54 and 18.55).

- We must immediately note work by Solov'ev with the same findings but documenting a *reversion in muscle histology toward normal about* ***5 mm*** *lateral to the cleft margin*.

We now consider two studies by Schendel at Stanford which are absolutely pivotal and deserving of the greatest

attention. The first study [78] focuses on the Sm6 facial muscle, orbicularis, comparing muscle from the cleft margin on the cleft side (the prolabium) versus muscle from the margin of the non-cleft side (lateral lip). The second study evaluates a representative Sm7 muscle, the uvulus in two situations: CP, isolated cleft palate (implying a minimal to modest involvement of palatine bone P3 horizontal shelf) and CL/P, cleft palate involving the secondary palate and lip. In the latter case biopsies were able to distinguish the effects of P3 along on muscle development versus more extensive clefting into the maxillary hard palate fields.

- Recall that the secondary hard palate consists of three palatine bone fields, from anterior to posterior, P1–P3.
  - P1–P2 are incorrectly referred to the "maxillary" hard palate but these fields have a separate evolutionary origin. They form the lingual wall of the maxillary alveolus.
  - P3 is commonly considered the horizontal shelf of the palatine bone. Pathology of the lesser palatine neuroangiosome is confined to P3 and the anterior palatine aponeurosis.
  - P4, the ancient ectopterygoid, is no longer part of the mammalian hard palate, being displaced forward to become the medial pterygoid plate.

Terminology: CL, CP and CL/P

CL Cleft lip refers to a deformity of the lip and alveolus from the microform to complete cleft. Why should one include the alveolus? Because the bone stock of PMx is always involved, and, at the very minimum, a bone deficit of the piriform fossa is present, CL implies some degree of alveolar involvement, from a reduction in volume to a frank cleft. A quantitative deficit of the diffusible morphogen, BMP4 from P3 is responsible for failure of soft tissue unification.

CL/P In the literature, this condition implies a concomitant "hit" to both the lip and the secondary palate. With regard to the biochemical effect on the soft palate, the PMx field is too far removed from the soft palate; it is therefore irrelevant. *Any* form of isolated secondary hard palate cleft by virtue of reduced concentrations of BMP4, will affect the soft palate to a degree proportional to the bone defect.

CP This refers to the isolated defect of the soft palate without overt involvement of the hard palate. Recall that in CP, by definition, the specific field defect resides in P3. Once again, BMP4 diffusing backward through the soft tissues, is responsible for the soft tissue cleft in a gradient from posterior to anterior.

Cleft Side Versus Noncleft Side This out-of-date terminology makes a supposition that the cleft pathology somehow resides on the lateral side. To be sure, microform cleft shows only the depression in the lower lateral corner of the piriform fossa due to missing dysplastic or missing PMxF and PMxB. This is an obvious site for decreased BMP4. However, in complete clefts, the BMP4 available to the prolabial cleft margin comes strictly from PMxA. Thus, in terms of muscle development, morphogen deficit exists on both sides of the cleft but the reduction in concentration gradient is less severe on the prolabial side. Thus, it is more appropriate to make reference to the prolabial (noncleft) side and the lateral lip (cleft) side.

Cleft Lip Muscle (Sm6): Orbicularis

Sixty-eight muscle biopsies were taken from *unilateral cleft lip* patients at the time of surgery and submitted for histochemistry and electron microscopy. Fiber type was studied using the following enzyme-specific stains. Although not stated, it is reasonable to assume the DOO layer of orbicularis was biopsied, since SOO on the cleft side does not exist. Here is a summary of the stains used.

- Muscle fiber type
  - ATPase: attached to myosin
    Reaction at pH 9.4 shows type 1 (slow-twitch fibers)
    Reaction at pH 4.6 shows type 2 (fast-twitch fibers): 2a, 2b, 2c
- Mitochondrial location
  - NADH-TR: NADP-tetrazolium reductase is present mitochondria, sarcoplasmic reticulum, and T-tubules
  - SDH: succinic dehydrogenase is exclusive to mitochondria
- Neuromuscular end plates
  - Esterase is specific and indicates degenerating fibers

Table 18.1 Summary of muscle characteristics

Muscle	Origin	Fiber type		Fiber diameter μm	
		Type 1	Type 2	Type 1	Type 2
Extremity	Somites	69.7%	30.3%	23.5	21.4
Orbicularis normal[a]	Sm6	24.5%	75.5%	22.6	23.1
Orbicularis medial	Sm6	29.2%	70.8%	11.1	11.8
Orbicularis lateral	Sm6	17.4%	82.6%	8.9	8.9
LVP normal[b]	Sm7	74.9%	25.1%	46.1 (mean	
LVP CL/P	Sm7	36.9%	63.1%	24.9 (mean)	
Uvulus CP	Sm7	56.7%	43.3%	20.8	20.9
Uvulus CL/P	Sm7	62%	38%	10.16	7.4

[a]Data from [78–80])
[b]Data from [81]

- Z-band identification (can be displaced or degenerate in myelopathies)
  - Gomori trichrome stains collagen

Results from studies by Schendel, de Chalain and Lindman are summarized chart appended below (Table 18.1).

In the normal state, fiber types vary by embryonic origin. The ratio of type 1 compared with type 2 fibers in somitic muscle is 69.7% vs 30.3%. In normal Sm6 muscle the ratio is 24.5% vs 75.5%. In normal Sm7 muscle the ratio is similar to somites, 74.9% vs 25.1%. Recall that the somite system represents the transformation of Sm8 the S1.

- Perhaps the genetic switchover applies to Sm7 as well.

Schendel noted that the orbicularis is abnormal along the cleft margins on both sides compared with the normal. Furthermore, the cleft state has differential effects on the prolabial side versus the lateral lip side. Regarding fiber type, there was no difference on the prolabial size but the lateral side had significantly fewer type 1 fibers. Fiber size (mean) on the prolabial side versus the lateral side 52% and 42% of normal, respectively.

Electron microscopy using Gomori stain showed large numbers of abnormal mitochondria pushing apart the muscle fibers. Instead of being at the periphery of the muscle fibers, the mitochondria were clumped together in the center. They had an unusual shape with abnormal cristae. Glycogen was seen accumulating between the fibrils (Fig. 18.56).

Furthermore, both the Gomori and NADH stains demonstrated large numbers of "ragged red" fibers (RRF). This term refers aggregations of abnormal mitochondria in the sub-sarcolemma of the muscle fibers. RRF is characteristic of myoclonic epilepsy (MERRF, based on the ragged red fibers).

Evidence previously cited regarding metabolism of lateral nasal process tissue on the cleft side in mice indicates *deficient energy production*. A metabolic defect reflected in the mitochondria was hypothesized to be responsible for inadequate muscle migration and development. It should be noted that orbicularis muscle immediately lateral to the cleft site begins to normalize. Solov'ev performed similar studies in Russia and found smaller fibers at the cleft margin with a *reversion in muscle histology toward normal about 4–5 mm lateral to the cleft margin*. This is approximately the width of the non-philtral prolabium.

The model of a biochemical defect leading to changes in cellular metabolism provides a background for findings at the University of Pittsburgh [74] obtained by studying orbicularis anatomy in 29 fetuses, including 9 with cleft lip/palate. Using 3-D CT scanning of section and documented a difference in the speed of development. When compared to the normal time sequence (vide supra) orbicularis oris muscle lagged behind 3.5 weeks, thus affecting the superficial muscle ring and labial muscle ring. They postulated this to be causative for distraction of the premaxillary away from the midline as proposed by Delaire.

- This mitochondrial hypothesis does not explain generalized changes in histology nor does it relate muscle embryogenesis to surrounding bone fields.

Important supportive work by De Chalain evaluated orbicularis biopsies from normal children with lip lacerations versus patients with isolated cleft lip and cleft lip associated with cleft alveolus (a more severe affection of the PMx field).

Sm6 orbicularis in both normal and cleft states was shown to have a fiber type and size profile different from both somitic muscle and from Sm7 palate muscle. Cleft muscle demonstrated hypoplasia, disorganization and clusters of abnormal mitochondria. Ragged red fibers were *not* observed.

- Data for normal orbicularis from this are included with those from Stanford in Table 18.1.

Cleft Palate Muscle (Sm7): Levator Veli Palatini, Palatopharyngeus, Uvulus

Histochemical evaluation of palatal muscle offers similarities and differences. Recall that, with exception of tensor veli palatini from first arch and Sm4, all remaining soft palate muscles originate from Sm7 and therefore come from a different homeotic environment that orbicularis being of second arch origin from Sm6. Findings of fiber type in normal and cleft palate children were reported in Russian in 1988 by Khamidov.

Lindman, working independently from Stanford characterized 11 biopsies of levator veli palatini from children undergoing palatoplasty, using the following histochemical stains: mATPase for fiber classification, NADH-TR to assess mitochondrial oxidation, and Gomori trichrome stain to image cell morphology, membranes and nuclei. Two of 11 were isolated soft palate clefts (P3), and the remainder were clefts involving the secondary palate as well (P2–P3 or P1–P3). On general histology, LVP fibers were loosely packed with types 1 versus 2 at 38% and 72%, respectively. This pattern indicates predominance of fast-twitch response. Interestingly this distribution reverses in adults (Figs. 18.57 and 18.58).

Doménech-Ratto [82] and Cohen et al. [83] documented soft palate morphogenesis in normal fetal specimens. Sm4 tensor veli palatini appears concomitant with the rest of the muscles of mastication with Sm7 muscles maturing later: levator, palatoglossus, palatopharyngeus and uvulus. Bone synthesis followed a similar pattern: mandible, medial pterygoid plate, lateral pterygoid plate and hamulus. Subsequently Cohen et al. [84] noted in 4 cases with cleft palate developmental delay in myogenesis. Interestingly, 3 speci-

mens had a very low amount of myoblasts in Sm7 LVP, while Sm4 TVP remained resistant with myoblast volume comparable with normal.

- An abnormality exists in the early development of soft palate muscles.
- These finding persist throughout fetal life and are present at time of palatoplasty.
- **Note** Similarity in behavior between Sm6 orbicularis in the cleft lip and Sm7 uvulus in cleft palate.

  – In both second arch and third arch muscle fields, a defect in an underlying bone field creates a morphogen deficit which causes a slower rate of development and smaller fiber size.

Why muscle fibers of TVP resistant, whereas those of the levator sling are not? Recall that the bone deficit in P3 follows a gradient inverse to its development. In the cleft state, the rectangular horizontal plate becomes a triangle: bone is missing medially and posteriorly. Laterally P3 at the orbital plate remains normal in volume. BMP4 from P3 diffuses front-to-back along the soft palate edges; i.e. considerably medial to the location of tensor. Additional P3 morphogens critical for muscle development may follow the same pathway.

- Bone deficit of P3 in the medial horizontal plate creates a morphogen deficit which could affect myogenesis in the levator sling.
- The bone volume of P3 is unchanged near TVP thus it is not exposed to a morphogen deficit.

Schendel et al. [80] applied the same methodology used for the cleft lip study to 30 biopsies of the uvulus muscle obtained from 16 patients undergoing primary palatoplasty: 7 cases were isolated soft palate clefts and the remainder were combined with cleft lip in which one side of hard palate was normal and the other was deficient in size. Histochemistry was performed using the same stains as before.

Biopsies of Sm7 muscles showed a different fiber pattern that those from orbicularis, having a much higher percentage of slow fibers. Furthermore, there quantitative differences noted for uvulus specimens from isolated cleft palate versus CL/P. Recall that for soft palate clefts CP there is no "cleft side." But for CL/P there is a cleft side and its anatomy will reflect the great degree of morphogen deficit.

Chapters 14 and 16 presented extensive evidence demonstrating that differences in the biology of soft palate clefts are utterly dependent on pathology in the hard palate platform. Specifically, isolated CP occurs in the context of involvement of the P3 field, i.e., the horizontal plate of the palatine bone. The presentation of isolated CP worsens when the mesenchymal defect advances into the P2 field of the hard palate, even when no obvious bony cleft is visible. Soft palate cleft in the presence of an open hard palate cleft is even more severe. In all these cases, diffusion of BMP4 is responsible for the failure of epithelial fusion. The uvulus is the last site to receive the morphogen and the first to fail when it is inadequate. We shall now consider the Stanford palate data in view of the following principles.

- The greater the degree of palatine bone field involvement, the more severe is the deficit of BMP4 available to the soft palate.
- This universal law of diffusible morphogens applies to all other growth factors produced by the P3 field.
- If development of uvulus muscle is dependent on such morphogens it will be more hypoplastic in cases of CL/P that in isolated CP alone.

Uvulus from isolated CP demonstrates differences from normal orbicularis. There are significantly more type 1 slow-twitch and less type 2 fast-twitch fibers (56.1%/43.3%) compared to normal (29.2%/70.8%). Fiber size of uvulus was much larger than in orbicularis, 20.8 μm versus 11.1/11.8 μm, but comparable to that of skeletal muscle. Interpretation these data must consider differences in origin of the muscles involved.

- Tensor veli palatini, the sole first arch muscle of the soft palate Sm4, arises from Sm4
- Orbicularis is a second arch muscle originating from Sm6
- Palatopharyngeus is a third arch muscle that arises from Sm7

Uvulus specimens from CL/CP when compared with those from CP show similarities and difference. Fiber size for uvulus in the isolated cleft palate is roughly comparable to that of skeletal muscle. It is roughly twofold greater than in cases involving the secondary palate.

- The morphogen effect on the uvulus muscle fiber diameter is inversely proportional to the degree of deficiency in the palatine bone fields.

Finally, mitochondrial stains, both NADH and Gomori trichrome, reveal in the uvulus specimens, of CL/P an abnormal accumulation of mitochondria the center of the muscle, similar to that observed in the orbicularis specimens. These mitochondrial also show the "ragged red" phenotype. In contrast uvulus from CP did *not* show mitochondrial pathology. What could explain this difference? Fiber size is small for both CL and CL/P in both instances whereas CP fibers are much larger. Perhaps a relationship exists between the process that results in reduced fiber size and abnormal mitochondria.

These finding corroborate previous observations by Khamidov in which electron microscopy of CL orbicularis and CL/P palate muscle showed abnormal muscle fibers and mitochondria. Note they did not obtain biopsies from CP patients. Furthermore, patients did not appear to "grow out of" this condition as older children (age 12) showed worse pathology.

Lazzari's group reported similar dystropic changes in Sm6 orbicularis but their study documents changes in Sm7 palatopharyngeus as well. Biopsies were taken at the margins at the time of primary repair cleft lip (7) and cleft palate (20), cleft lip patients (6) presenting for secondary surgery involving takedown of the original repair were also biopsied. Enzymes were the same as Stanford, save SDH and esterase. Orbicularis from both sides of the cleft was taken at unilateral lip repair. Biopsies of superior constrictor and palatopharyngeus were taken at palate repair. Orbicularis did *not* include pathological fibers such ragged red mitochondria but disorganization and fibrosis were documented.

Summary of Histochemical Data

- Second arch Sm6 orbicularis has a fiber diameter similar to somitic skeletal muscle in the normal state.
- Under conditions of cleft (PMx defect) fiber orbicularis diameter becomes 50% smaller on the medial side and 60% smaller on the lateral side.
- Third arch Sm7 uvulus has a fiber type and fiber diameter similar to somitic skeletal muscle in both the normal state and in isolated soft palate cleft (only P3 is affected)
- When hard palate cleft is added (P2 affected), uvulus fibers in the soft palate become 50–67% smaller.

Conclusion

In the cleft state, muscle fibers along both the "cleft-side" lateral lip and along the "non-cleft side" non-philtral prolabium are abnormal for at least 5 mm of distance.

- Lateral lip element muscle should be pared.
- NPP flap, usually about 5 mm wide, should be transferred into the nasal floor.

Clinical Studies of Microform Cleft

Historical Perspectives

Clinical descriptions of minimal cleft are a relatively recent phenomenon in the literature. In 1935, Broderick[101] described hidden radiologic findings in patients with an asymmetric nose and/or a philtral scar. The 1964 case report by Brown of an isolated cleftlip nasal deformity is generally credited as being the first formal description of minimal cleft in the English literature: "The nostril deformity may be an integral part of the cleft-lip syndrome and not secondary to it." This was followed by reports from Stenstrom and Thilander in 1965 and Tulenko in 1968 [85, 86].

Based on previous work by Huffman and Lierle, Brown made a number of important observations [87]. (1) The alar cartilage was held in a faulty position-thereby being forced into distortion; it was *not intrinsically abnormal*. (2) Cleft represented an *asymmetric growth* state. (3) Alar form was somehow linked to the configuration of the *nostril floor*. Reflecting an understandable focus upon the obvious, Brown's explanation focused on a single anatomic variable: the alar cartilage: "The consideration of the case presented and of the embryology of the face suggests that this is another defect of mesoderm, a primary defect of the alar cartilage, and not secondary to developmental abnormality of the lip or alveolus."

That the cleft-lip nose is derived from malformed or deficient cartilage is a *misconception* that has been previously reviewed by this author [88]. In five minimal clefts, Boo-Chai and Tange dissected out the alar cartilages, finding them to be "normal in size and shape, but displaced [10]. It is, therefore unlikely that the condition is due to an intrinsic defect within the cartilage." Stenstrom came to the same conclusion: "We can see no reason to interpret the nasal deformity as a consequence of inherent abnormality of the alar cartilage .... It is more reasonable to regard cleft-lip noses as secondary deformities."

- Nasalis misinsertion as a primary cause was not appreciated for many years. Because the emphasis in the early literature was on appearance, not function, early contributors missed the connection between the normal insertion of nasalis and its relocation to the nostril sill and piriform fossa. All that was missing would have been, in the words of Millard:
  - "Know the beautiful normal."

Dentoalveolar Deficits

Dental considerations in minimal clefting have been noted by many surgeons. Although the palate and arch appeared normal in Brown's case, radiographs revealed an unerupted left lateral incisor (no. 7) and a "minimal" cleft of the alveolus and hard palate. Twenty-one minimal clefts at Columbia-Presbyterian Hospital were studied by Cosman and Crikelair [1]. Dental records from 16 of these cases showed a 100% incidence of incisor anomalies. Radiographs of seven patients demonstrated an alveolar bone defect in six cases despite an apparently intact alveolar arch. All eight case Heckler's series had similar findings.

The orthodontic literature documents patterns of dental anomalies associated with clefts [89, 90]. That these could occur in the absence of an overt cleft was demonstrated in fetuses by Kraus in 1966. Johnson applied these concepts in 4 cases: "The cleft is therefore a symptom of a disorder affecting the whole process of development of the fissural areas and particularly the dental lamina. The presence or absence of a cleft is not the sole criterion for concluding that an error... has taken place."

Stenstrom and Thilander summarized the situation as follows: "It seems as if a developmental disturbance in the lateral incisor region can manifest itself in various ways according to its intensity from a slight disturbance of the tooth germ to its most serious form, a cleft. Since nothing has been forthcoming which can clarify the cause of the defective lateral incisor in an otherwise ideal bite ... it is reasonable to assume that, as it is of the same order as cleft lip nasal deformities, it should be regarded as a *microform* of a cleft manifestation."

- The locus of the cleft is the lateral incisor zone of premaxilla, from which projects the frontal process. The neural crest defect manifests itself not only in the bone but in the dental unit as well.

Orbicularis Abnormalities

The anatomy of the orbicularis oris in minimal clefts has likewise received attention. Orbicularis muscle fiber disorientation is associated with increasing degrees of cleft nasal deformity. Furthermore, the maximum area of disarray was found in those sections taken from the nasal floor and upper lip.

As has been previously discussed, the orbicularis oris in the upper lip is anything but sheet-like. It has deep and superficial components; the oblique fibers of the latter have much to do with the "drape" of the lip. Paranasal levator insertions make important contributions to the geometry of the alar bases, whereas the nasalis insertions determine the curvature of the nostrils. Stenstrom and Oberg recognized that pathologic muscle insertions (or lack thereof) into the nose and septum could play an important role in determining septal, columellar, and alar cartilage configuration in cleft [91]. In two minimal cases, Stenstrom and Thilander [85] noted "obvious defects in the part of the pars alaris of musculus nasalis which holds the nasal wing in against the columella." Restoration of muscle anatomy to the midline is the basis for the Delaire-Joos subperiosteal "functional cheilorhinoplasty [92].

- Attributing a cleft (minimal or otherwise) to a defect in the orbicularis oris (or to any combination of muscles) proved to be an *intellectual dead end*. The biggest drawback in muscle analysis had been the failure to separate out nasalis from orbicularis. When this is inadvertently anchored to the midline, nasalis, a dilator of the airway is converted to a *constrictor*.

Credit for recognition of the nasal floor as "ground zero" for cleft formation surely goes to Cosman and Crikelair, as they correctly identified the locus of the deficiency zone to exist *beneath the plane* of the nostril floor. This zone extends (sagittally) from beneath lip epithelium anteriorly, under nasal floor, posteriorly through the alveolar arch, and terminates at the incisive foramen. What no one anticipated was the existence of the frontal process of premaxilla, which is the primary cause for the misshapen piriform margin.

Heckler observed that the extent of deformity in minimal clefts depends on the severity of the nasal deformity is correct. Greater degrees of premaxillary deficit affect the insertion sites of the nasalis muscle above the canine and lateral incisor causing it to insert pathologically into the nasal floor and piriform fossa. The most striking findings in microform cleft are therefore in the nose. Microform by definition, has an intact lip. What we can see is the quantitative reduction in BMP4 reaching the surface of the skin from below creating a furrow as Cupid's bow.

Onizuka Classification

The concept that microform clefts exist as part of the spectrum of clefting was first advanced by Boo-Chai and Tange: "There may exist a subgroup of the cleft lip deformity in which there is a typical cleft lip nasal deformity with a clinically intact lip. *We believe that they (microform clefts) represent the first link in the progression of severity of the cleft lip syndrome*" [10].

Onizuka expanded on the idea to define the anatomic differences separating various types of clefts (Figs. 18.59 and 18.60). In this classification:

- Minimal (microform) clefts are first degree (isolated nasal deformity) and second degree (upper/lower vermilion border notching, cutaneous striae).
- Incomplete clefts are classified as third degree, having (1) notching of the pars marginalis of the orbicularis oris, which affects both upper and lower vermilion borders; and (2) cutaneous shortening of the ipsilateral philtral column—the degree of the latter being defined as a proportion of total philtral height.

The Onizuka classification should be studied with care for the following reasons: It distinguishes between the variations of minimal cleft presentations. It places minimal clefts into a visible context with other cleft forms. It is visually simple and accurate. It is remarkably compatible with the DFR model.

Class I and Class II: Cleft Nose + Normal Lip

Here, a partial deficit in PMxF affects the insertion sites of nasalis

- Onizuka no. 1 cleft. The most terminal manifestations occur in the development of the most medial and caudal aspect of the SOO. Here the incisal fibers penetrate vertically through the otherwise intact SOO to insert on the vermilion. Note that there is no discontinuity of DOO fibers across the vermilion; the DOO is fully formed by this time.
- Onizuka 2 has a foreshortening of these fibers which causes the vermilion to be elevated; an isolated notch in the lower border of the vermilion results. The white roll is intact.
- Onizuka 3 represents the failure of the caudal margin of the SOO to insert properly into the philtral margin (the lateral border of the A field). The upper border of the vermilion appears notched: white roll discontinuity is present.
- Onizuka 4 occurs when the entire length of the SOO fails to insert at the philtral margin. A cutaneous stria (plural striae) is present; the SOO is seen as a muscle bulge lateral to the pseudophiltrum.

Class III: Cleft Nose + Incomplete Cleft Lip

These represent failure at fusion of lateral lip element with philtral prolabium. Full-thickness notching of the cleft border results. Onizuka subdivides this process into nos. 5, 6, and 7 reflects the fact that the flow of tissue from B to A across the D/C bridge is not an all-or-nothing phenomenon but is a spectrum. The apparently greater "disorientation" of muscle fibers at the cleft margin, seen with more severe degrees of clefting, reflects their development within the confines of a distorted functional matrix at that site. The orbicularis fibers do not "turn to run parallel" to the cleft margin as described by Fará [19]. They simply conform to the preexisting envelope.

Class IV: Cleft Nose + Complete Cleft Lip

As previously discussed, *step* 2 involves failure of the B field to make contact with the D/C "bridge." A complete cleft of the lip, usually (but not necessarily) involving the alveolus, results. The abortive cutaneous D/C bridge, without muscle fibers, is later represented as a cutaneous "Simonart's band." This situation is represented by Onizuka as a no. 8 cleft; this recognizes the importance of Simonart's band as an integral part of the clefting model. Full-fledged *step 1* failure represents the complete separation of the D and C fields, again usually accompanied by an alveolar cleft. This is an Onzuka no. 9 cleft (class IV). A no. 10 cleft includes involvement of the hard palate internal to the alveolus.

Mulliken Classification

Yuzuriha and Mulliken's review of 393 patients with unilateral incomplete cleft lip disclosed 59 with lesser-form variants. These were divided into three categories: incomplete (20), microform (28) and mini-microform (11) the characteristics of which are as follows. Note my addition of features involving the alveolus and nasalis (Figs. 18.61, 18.62 and 18.63).

Incomplete Form

- Defect of the vermilion-cutaneous junction of >3 mm above normal peak of Cupid's bow (on the non-cleft side). [Delta Cupid's bow >3 mm]
  - DOO is discontinuous across the cleft
  - SOO discontinuous below notch, dysplastic or not inserted above the notch
- Vermilion deficient/dysplastic on medial (non-cleft) side
- Muscle depression along philtral column exacerbated by pout
- Cutaneous groove
- Significant nasal deformity
  - Misinsertion of nasalis (both heads)
- Alar base displacement >2 mm
- Alveolar
  - Bone deficit nasal floor significant
  - Alveolar cleft and dental abnormalities are common
- Surgical strategy [93]: modified rotation-advancement with single-limb z-plasty inserted into a slot between the vermilion-skin and vermilion-mucosa, i.e., the wet-dry mucosal border. Alar base repositioning along with lateral lip element

Microform

- Defect of vermillion-cutaneous point <3 mm above normal peak of Cupid's bow (on the non-cleft side); [Delta <3 mm]
  - DOO is continuous across the cleft

  - SOO below notch is discontinuous; above the notch, it is malinserted or dysplastic
- Vermilion deficient/dysplastic on medial (non-cleft) side
- Muscular depression along philtral column but no defect on pucker
- Nasal deformity less: hemicolumella almost equal, the nostril sill has a depression in it
  - Nasalis misinsertion
- Alar base minimally displaced 2 mm
- Alveolus
  - Bone deficit nasal floor
  - Alveolar cleft may be present and/or dental abnormality
- Surgical strategy [93]: single-limb z-plasty at both the wet-dry mucosal border and at the nostril sill. Alar base repositioning is by elliptical excision or v–y advancement

Mini-microform

- Vermilion notch with continuity to the white roll
  - DOO continuous
  - SOO continuous but dysplastic
  - Cupid's bow peaks are equal, vermilion border with skin is discontinuous
- Peaks of Cupid's bow are both level [Delta = 0]
- Free mucosa margin is notched
- Muscle depression seen mostly beneath the nostril sill
- Nasal deformity is subtle: just a depression in the nostril
- Alveolar bone
  - Deficit minimal
  - Alveolus may have a notch and/or dental abnormality
- Surgical strategy [93]: simple excisions in the vermilion and in the nostril sill

Surgical Management of the Incomplete Cleft

As described above, most of literature regarding the microform cleft has emphasized its anatomic features, with par-

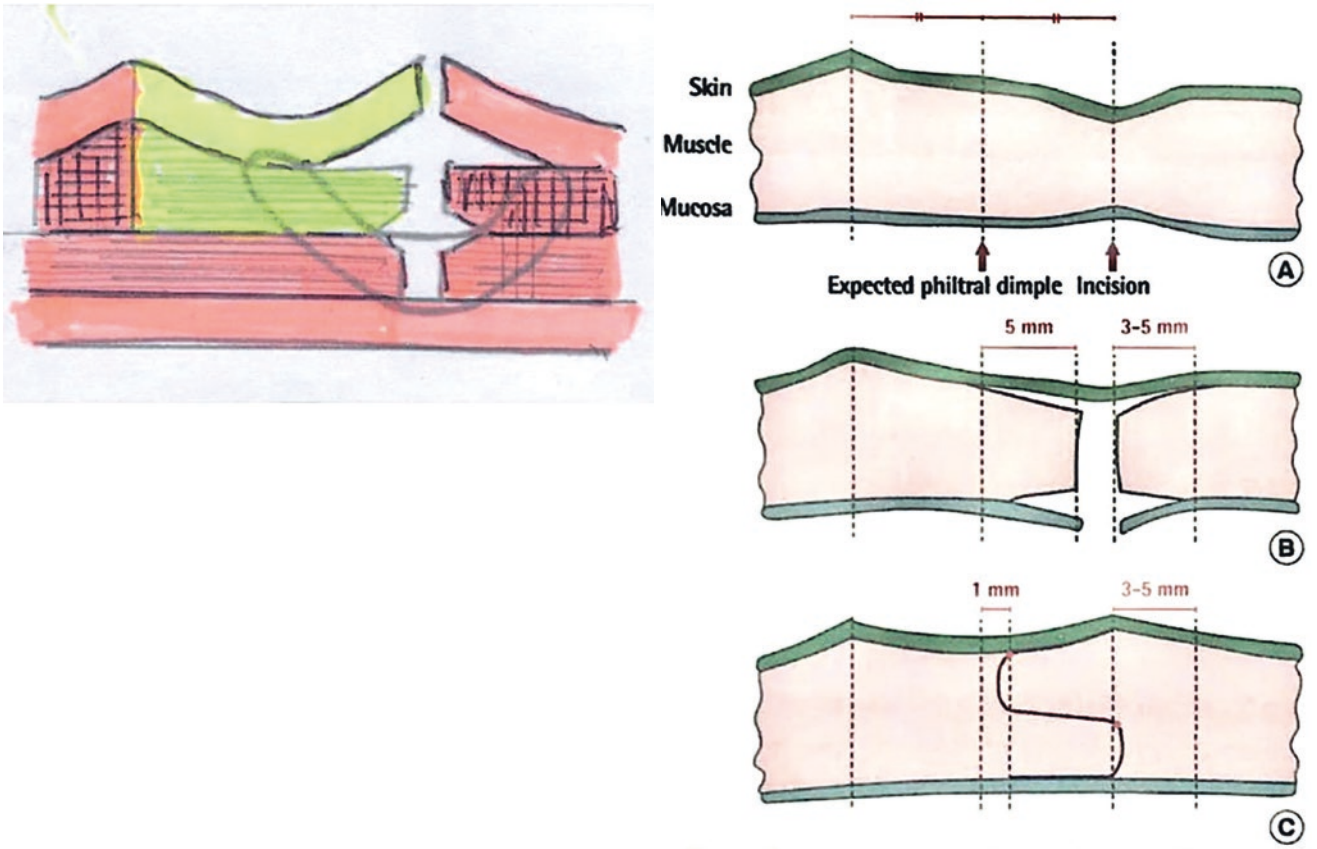

Fig. 18.64 Philtral reconstruction using monolitihic orbicularis as a block. Left: [Reprinted from Kim S, Kwon J, Kwon G-Y, Choi TH. Dynamic reconstruction of the philtrum using coronal muscle splitting technique in microform cleft lip. J Craniofac Surg 2014; 25(3):742–745. With permission from Wolters Kluwer Health, Inc.] Right: [Reprinted from Kim MC, Choi DH, Bae Sg, Cho BC. Correction of minor-form and microform cleft lip using modified muscle overlapping with a minimal skin excision. Archives of Plastic Surgery (Korean Society of Plastic Surgery). 2017; 44(3): 210–216. With permission from Creative Commons License 4.0: http://creativecommons.org/licenses/by-nc/4.0/]

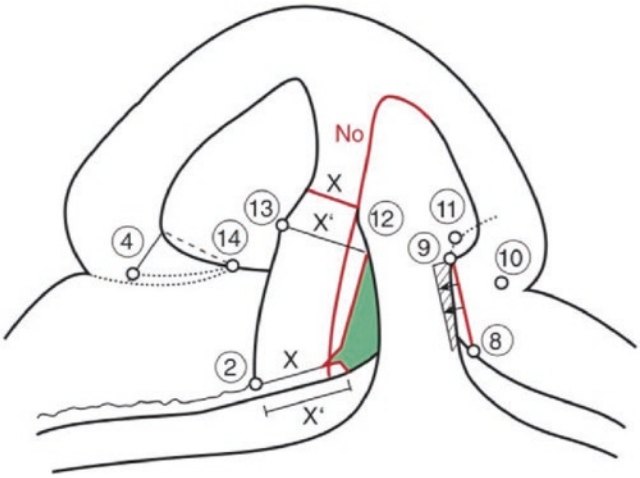

Fig. 18.65 Basic concepts of DFR: markings. See Chap. 19 for details. Width of columella (x); width of philtral prolabium (x') = 12–13; width of Cupid's bow at white roll = 2–3 – 12–13*: height of normal philtral column = 13–2; height of cleft-side philtral column—12–3, height of lateral lip = 8–9. *Difference $x' - x$ is 1–2 mm. This allows for a back-cut for final height adjustment. Normal nostril sill is an isosceles triangle. Base = width of the alar at point 4. Limbs = 4–14. Cleft-side nostril sill is marked the same way beginning at point1 10. Tip of the triangle found internally rotated. When the sill is rotated outward to normal position the space can be fill with NPP or inferior turbinate flap, anteriorly-based. [Courtesy of Michael Carstens, MD]

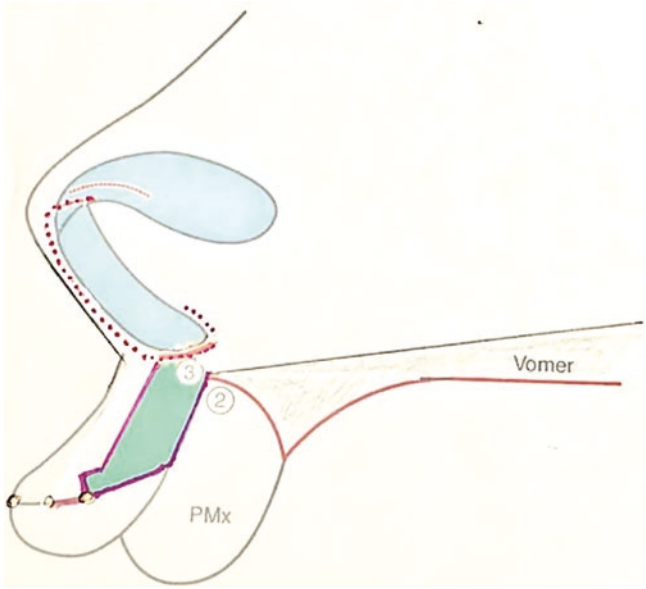

Fig. 18.66 Basic concepts of DFR: medial dissection. Separation of NPP (green) from PP is indicated by red incision lines. Vascular supply to PP from medial nasopalatine is at point 3. Posterior incision ascends to just below the footplate. One then makes a decision depending on how one intends to manage the medial crus and nasal tip. Recall that medial crus is displaced downward and backward as marked by its footplate, point 12 (not shown). Medial crus must be elevated into equality with other side for proper tip support. This can be done in one of two ways:

- Separate skin-cartilage flap, known as *lateral columellar chondrocutaneous flap* (LCC). This requires a skin only incision (orange) just below the footplate. Through this a curved scissors can hug the medial crus all the way to the tip. Spreading at the incision will advance the LCC while leaving the pedicle undisturbed. Spreading around the base at point 3 will give the "shoulder" of PP mobility. At the same time as it is rotated into the nasal floor the "shoulder" can be advanced medially and sutured higher up to fill in the gap created by the upward advance of LCC. Note the should of PP should be mattress-sutured to the other side so it won't pull on LCC
- Lateral columellar incision (red dots) can be brought under the nostril as an "open-closed" rhinoplasty. From point 2 an incision in the membranous septum (red dots) creates a large "bucket handle" flap, the NPP-LCC which can be advance in its entirely upward with PP rotated into the nasal floor. The scar is unnoticeable and exposure to the nasal tip is extensive for suture control of the ipsilateral dome

[Courtesy of Michael Carstens, MD]

ticular emphasis on the nasal deformity. Operative techniques have centered on management of lip height, the creation of a philtral column, muscle repair and repositioning of the alar cartilage. Respiratory function in these patients has not received attention. Of these issues, those specific to the microform cleft are prolabial, symmetry, philtral height and muscle repair. This section is not intended as a comprehensive review (Kim and Cho do a nice job) but to comment on technical details as they conform or at variance with developmental anatomy. Illustrations are focused on general design for the three variants: incomplete, microform and micro-microform. The reader is referred to Chap. 19 for a full presentation of DFR technique (Figs. 18.64, 18.65, 18.66, 18.67, 18.68, 18.69 and 18.70).

The Prolabium

The true philtral prolabium (PP) is the paired neuroangiosome of V1 and StV1 anterior ethmoid arteries. Its subcutaneous mesenchyme is r1 neural crest. The width of PP is equal to that of the columella or (a bit more generously) the distance between the footplates of the medial crura. The optical illusion of the "prolabium" has led to attempts to lower the cleft-side border using rectangular flaps [95], triangular flaps (Tennison), and rotation advancement [6, 96–99]. These techniques are reviewed in Losee and Kirschner. Recently in vogue is complex geometric technique proposed by Fisher [22]. Being unaware of the existence of the non-philtral prolabial field these techniques relay on manipulation of available tissues immediately adjacent to the cleft. What's more, as previously discussed, these marginal tissues are intrinsically affected by the same abnormal biochemical signals (the BMP4/Shh loop) involved in fusion failure as the cleft margin. One does not encounter normal philtral tissue until one reaches the correct neuroangiosome.

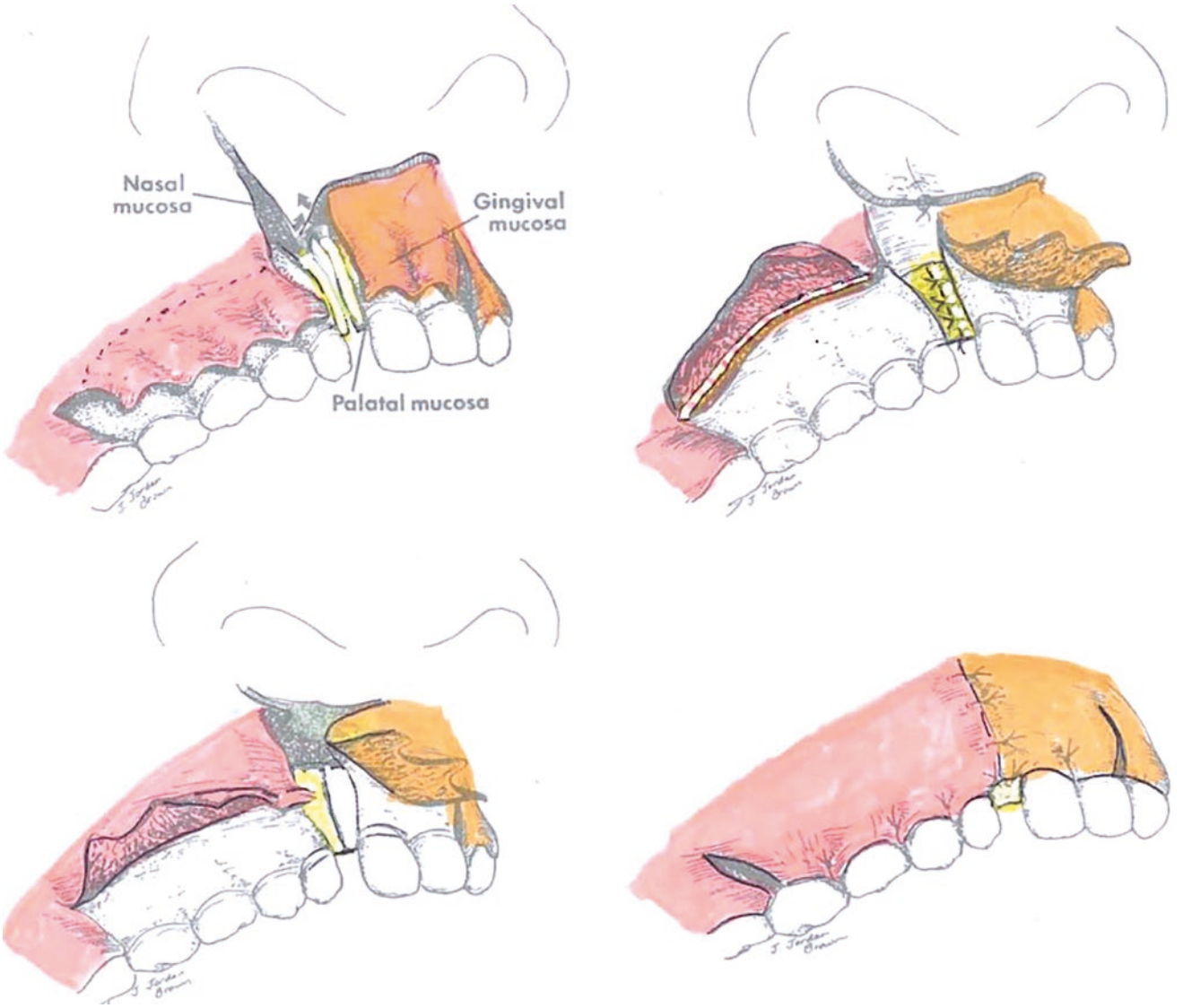

Fig. 18.67 Sliding sulcus mucoperiosteal flaps for closure of alveolar cleft. *Upper left* m S flap, maxilla (pink) is StV2 infraorbital and ECA facial. It is mobilized via pericoronal incision with a back-cut up the buttress. Dotted lines indicated periosteal releasing incision on the other side. S flap premaxilla and contralateral maxilla (orange) has additional supply from StV2 anterior ethmoid. Maxillary alveolar cleft flap (yellow) is greater palatine. Premaxillary alveolar cleft flap (white) is. *Lower left*: nasal floor elevated, flaps elevated. *Upper right*: nasal floor closed, back wall sutured, periosteal releasing incision (white line red dots) mobilizes 1–2 dental units. *Lower right*: closure [94]. [Reprinted from Cohen M, Figueroa AA, Aduus H. The role of gingival mucoperiosteal flaps in the repair of alveolar clefts. Plast Reconstr Surg 1989; 83(5): 812–819. With permission from Wolters Kluwer Health, Inc.]

- **In sum** All conventional prolabial dissections accomplish their purpose but at varying degrees of compromise to normal anatomy.

In 2000, based on vascular injection studies in fetuses, I first recognized the embryonic distinction between the philtrum and its surrounding tissues [3]. At the time, I was unaware of the Padget's work on stapedial system and its implications. Nevertheless, these findings lead to the development of an embryologically based model of the philtrum and prolabium which was translated into the *functional matrix cleft repair*. This concept demonstrated immediate and simplifying clinical results, including the use of the non-philtral prolabial flap for nasal floor reconstruction. It took me another 2 years before I could marry up the basic science with the surgical technique [28]. Neuroangiosome-sparing prolabial dissection has proven applicable across the spectrum of clefts, including incomplete and minimal presentations.

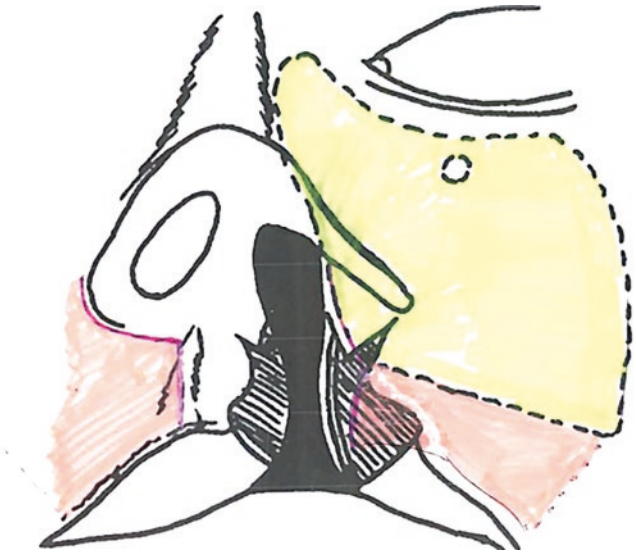

Fig. 18.68 DFR subperiosteal dissection. Delaire dissection plane (yellow) DFR dissection plane (pink) incision line (violet) mucoperiosteum is incised along the alveolar cleft border. This creates a "pocket" above gingival border that extends all the way back to the buttress. At that point an optional full-thickness incision through mucoperiosteum can allow the pocket to further advance as a large bipedicle flap suspended from the orbit above and the gingiva below. DFR undermining is no circumferential around the infraorbital bundle. The neurovascular axis is readily visualized during elevation of the periosteum. The combined incisions sweep upward around the piriform margin to gain access to the nasal bone and the sub-SMAS plane. On the non-cleft side, the mucoperiosteum is incised through a mini-incision just below piriform fossa with lateral elevation as well. Care is taken to sweep the periosteum around the non-cleft piriform margin, elevating the alar base and the nasal floor on that side. [Reprinted from Markus AF, Delaire J. Functional primary closure of cleft lip. British J Oral Maxillofac Surg 1993; 31(5): 281–291. With permission from Elsevier]

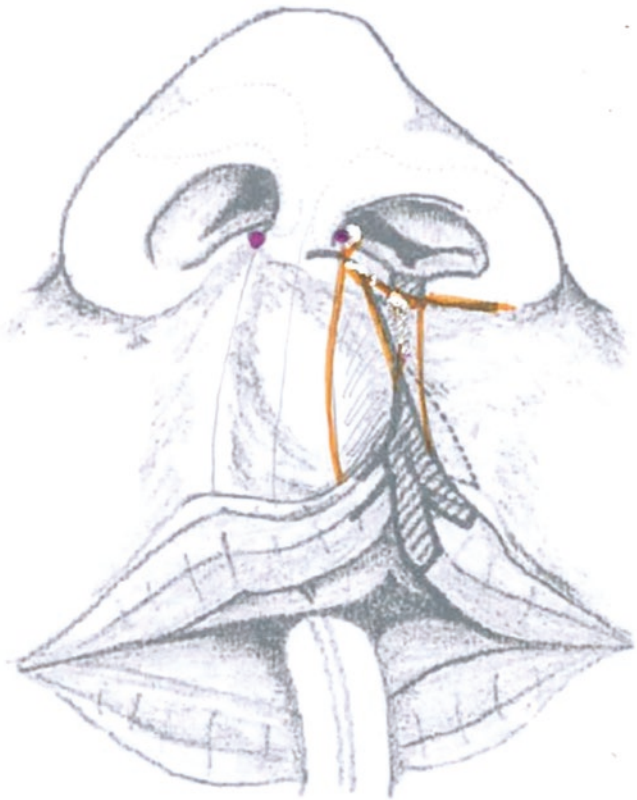

Fig. 18.69 Incomplete cleft DFR. Management consists of DFR subperiosteal mobilization, opening the lip with judicious use of NPP as full thickness flap (which can be thinned), and nasalis dissection. Immediate skin over the scar is discarded. [Adapted from Yuzuriha S, Mulliken JB. Minor-form, microform, and mini-microform cleft lip: anatomical features, operative techniques and revisions. Plast Reconstr Surg 2008; 122(5):1489–1493. With permission from Wolters Kluwer Health, Inc.]

Philtral Column

Creating an aesthetic projection of the ipsilateral philtral column has given rise to a variety of techniques, ranging from skin manipulation, buried dermal grafts and muscle rearrangements. Anatomic traps include (1) failure to recognize the distinct functional components of orbicularis as both sphincter (DOO) and dilator (SOO); (2) misinsertion into dermis rather than r1 mesenchyme; and (3) problems arising from the intrinsically faulty nature of the muscle itself at the cleft margin.

Fascia graft to bulk up the philtrum was reported by Park. The long-term results may be unstable due to absorption.

Reports by Kim and Kwon illustrate the issues of considering the orbicularis to be a single structure. The diagram presents what purports to be bilateral v–y advancement flaps suture together to throw the philtral column into relief. From a mechanical standpoint this works. However, the different embryonic tissues (indicated by colors) show a mismatch. Nonetheless, although not aware of the mesenchyme below the philtral skin, this repair effectively sutures SOO to r1 correctly (Fig. 18.64a).

Cho's group used an intraoral incision excise ½ of the r1 mesenchyme under the philtrum and interpose it with an equal resection of DOO from the cleft side [100]. The two flaps are advanced and overlapped such that SOO now occupies 50% of the territory beneath the philtrum (Fig. 18.64b).

Muscle Repair

Cho reported an intraoral approach to microform with dermal suturing of the lateral flaps [100]. Scar is avoided. However, if nasalis malfunction is present this approach will not provide the exposure needed to dissect out the muscle. The intraoral approach was made further complex by Derosiers who split the orbicularis into three muscle slips from each side and interposed them in a basket-weave manner. Although this thickened the philtral column interdigitation lead to predictable long-term scarring.

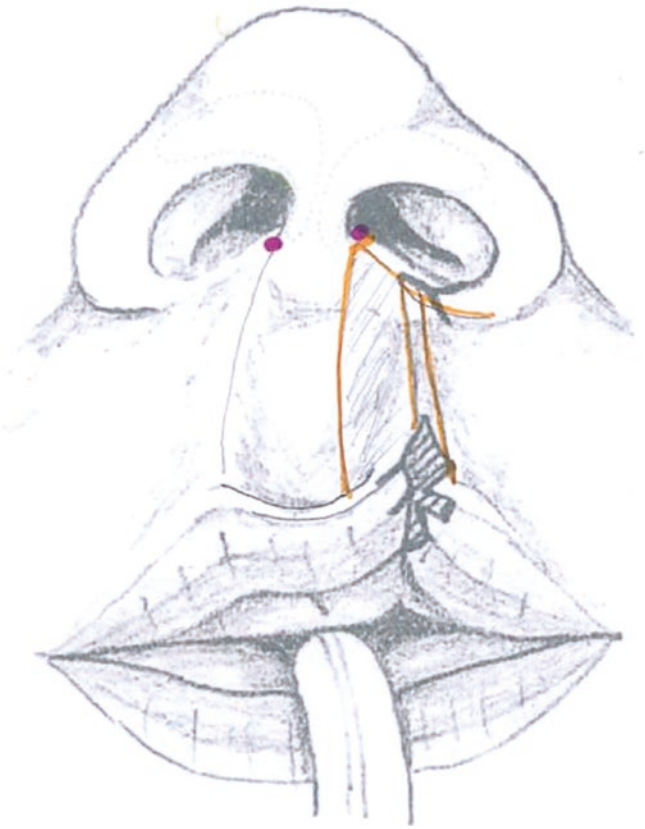

Fig. 18.70 Microform cleft DFR. Management presents variations with the incomplete form. Superiosteal mobilization is the same Lip can be opened completely or just down to DOO. This will give easy access to the nasalis without compromising normal structures. NPP incisions and medial crus elevation are the same but the NPP flap can be thinned considerably. [Adapted from Yuzuriha S, Mulliken JB. Minor-form, microform, and mini-microform cleft lip: anatomical features, operative techniques and revisions. Plast Reconstr Surg 2008; 122(5):1489–1493. With permission from Wolters Kluwer Health, Inc.]

Muscle manipulation via intraoral excision reaches perhaps its most complex in the technique reported by Ningbei Yin which attempt to reconstruct orbicularis according to two lines of tension, the nasal floor and philrum. The flaps are cut full-thickness with no separation of DOO and SOO. Alar part of nasalis is included in the orbicularis insertion into the root of the columella. Functional assessment for nasal breathing was not reported but nasalis was likely converted into a constrictor.

Mulliken Repair Sequence

Yuzuriha and Mulliken describe a logical surgical strategy to deal with the progression of clefts from the most subtle "mini-microform" to the standard microform to the incomplete variant. Using a caliper, they determined the distance from subnasale to the peaks of cupid's bow on the non-cleft and cleft sides. A difference greater than 3 mm is the indication to use rotation advancement. If less than 3 mm, two unilateral z-plasties are used. In both the incomplete and the microform clefts, alar base advancement is described, necessitating at times a v–y advancement. Nasal function is not addressed. The technique is excellent, but from the standpoint of developmental field reassignment, I would make the following points.

- Prolabial dissection errs based the classic misconception of the meaning of the Cupid's bow point. We know well that the philtrum expands with time. Conventional designs simply take the non-philtral prolabial tissue off the table as a reconstructive option for the nasal floor where it is needed most. Cupid's bow width inter-footplate distance is aesthetically pleasing. If short, at the very most a single 1–2 mm interposition flap above the white roll works nicely (Fig. 18.44).
- Subperiosteal dissection makes alar base relocation incredibly easy. v–y advancement simply not needed.
- Elevation of the nasal floor from its depressed condition is not described.
- Elevation and repositioning of the medial crus is not described. This can be done just one passes backwards beneath the footplate of medial crus (vide infra).
- Airway management with nasalis dissection is possible using the Mulliken incisions in all three variants. It had simply not been addressed.
- ***Note*:** In Mulliken measurement system, the position of the alar footplates was not considered. By using subnasale as the central point, they missed the fact that the cleft-side columella is retracted downward and inward into nasal introitus.
  - "What you see depends on where you sit."

Developmental Field Reassignment and Incomplete Cleft

Historical Perspective

In the past, the surgical approach to the microform cleft has focused on its skin-muscle presentation (especially the absent philtral column) and on the alar cartilage. Procedures have ranged from skin excision to full-thickness rotation-advancement, to complex muscle flap interdigitation. Various forms of tip rhinoplasty have been reported.

Without the benefit of the multiplanar orbicularis anatomy as currently known, some writers questioned the knee-jerk use of rotation advancement. Curtin queried: "Our personal experience with the microform cleft lip deformity is that the full thickness of the orbicularis muscle is not affected

and a through and through incision of the lip in the repair is not necessary. Since modifications of the straight-line repair have been successful in correction of the minimal deft lip deformity, why was it necessary to use the rotation-advancement flap repair in some of the cases?" Millard also reported the use of a simple excisional technique and a straight-line incision in a minimal cleft: "It is interesting to note the correction, which necessitated all other aspects of rotationadvancement with refinements, extensions and adjuncts, still did not require rotation."

That microform clefts have varying manifestations was documented by the extensive series of Tolorova. Onizuka described an individualized operative strategy that addresses the components minimal cleft: (1) alar rim, (2) notching of Cupid's bow, (3) notching of the vermilion free margin, (4) abnormal skin striae and (5) combined deformities.

Superficial rearrangements of skin and vermilion using w- and z-plasties are used for the first three problems. Creation of a philtral column in the fourth problem is achieved by dissection of a vertically oriented "central muscle flap" that is transferred laterally beneath an undermined lateral advancement flap; in so doing, the philtral column is "bulked up." Were this really the case, Millard's categorical critique would be justified: "An attempt at creating a philtral column by undermining skin and gathering it to a fold with sutures tied over stents usually does not maintain great improvement after removal of the sutures." In reality, Onizuka's technique does not depend on "gathering the skin." The success of the procedure lies in the degree to which the differential sutures reconstruct the anatomic insertion of the superficial orbicularis oris to the dermis of the lateral margin of philtrum.

Submental-vertex views from Onizuka's series disclose centralization of the columella and elevation of the deft-sided alar base to achieve symmetry with the noncleft side. His use of muscle suspension sutures is very accurate. But herein lies an ***embryologic error***. The key to alar base repositioning was not subperiosteal release. Instead, restoring communication between the "lateral muscle flap" (pars alaris of the nasalis) and the anterior nasal spine was described as the key objective key. The use of a non-subperiosteal release of the alar base is misleading. An increasing degree of piriform deformity make soft-tissue correction less optimal (and more likely to relapse). Furthermore, as previous stated, *nasalis is not designed to be inserted into the midline*. It requires separation from orbicularis and reassignment over the canine. This detail is crucial for the reconstruction of the cleft airway.

Assessment of the Microform Cleft

Patients presenting with minimal cleft deformities require extra care in assessment. Although they seek attention for a disturbance in their facial features, they may be rather vague as to the nature of their problem. They may report complaints such as: "I have a scar on my lip." "My dentist sent me." "I don't like my nose." "I look funny in photographs" or "I can't pucker up my lips to blow the flute." When the patient is informed as to the true nature of his or her condition, they may react with shock, embarrassment or denial. Being cognizant of this, the surgeon should discuss the matter with tact. Because the anatomic details are subtle, helping the patient to see cause-and-effect of their problem may be difficult. Photographic examples of other minimal clefts may be helpful for the patient at this juncture.

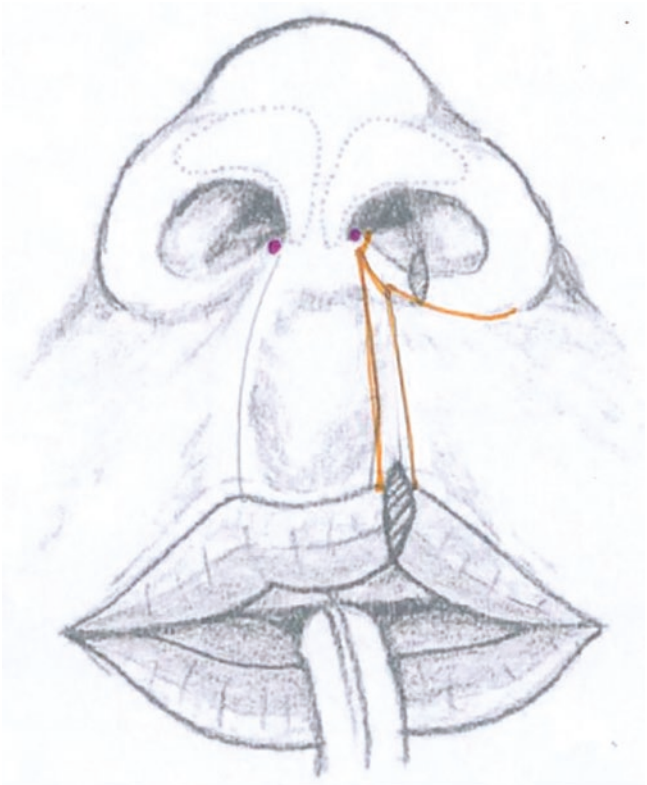

Fig. 18.71 Mini-microform DFR. Subperiosteal mobilization. PP is almost normal with very little NPP. NPP flap cutaneous only. Incision under the footplate only. Separate rim incision as needed for tip control of the ipsilateral dome. If nostril sill deformity is minimal it need not be mobilized and NPP can be discarded. Nasalis dissection is done through the nostril sill incision and the muscle is dropped through that same incision behind orbicularis, retrieved into the mouth by a small buccal sulcus incision, and secured to the periosteum and sulcus over the canine. [Adapted from Yuzuriha S, Mulliken JB. Minor-form, microform, and mini-microform cleft lip: anatomical features, operative techniques and revisions. Plast Reconstr Surg 2008; 122(5):1489–1493. With permission from Wolters Kluwer Health, Inc.]

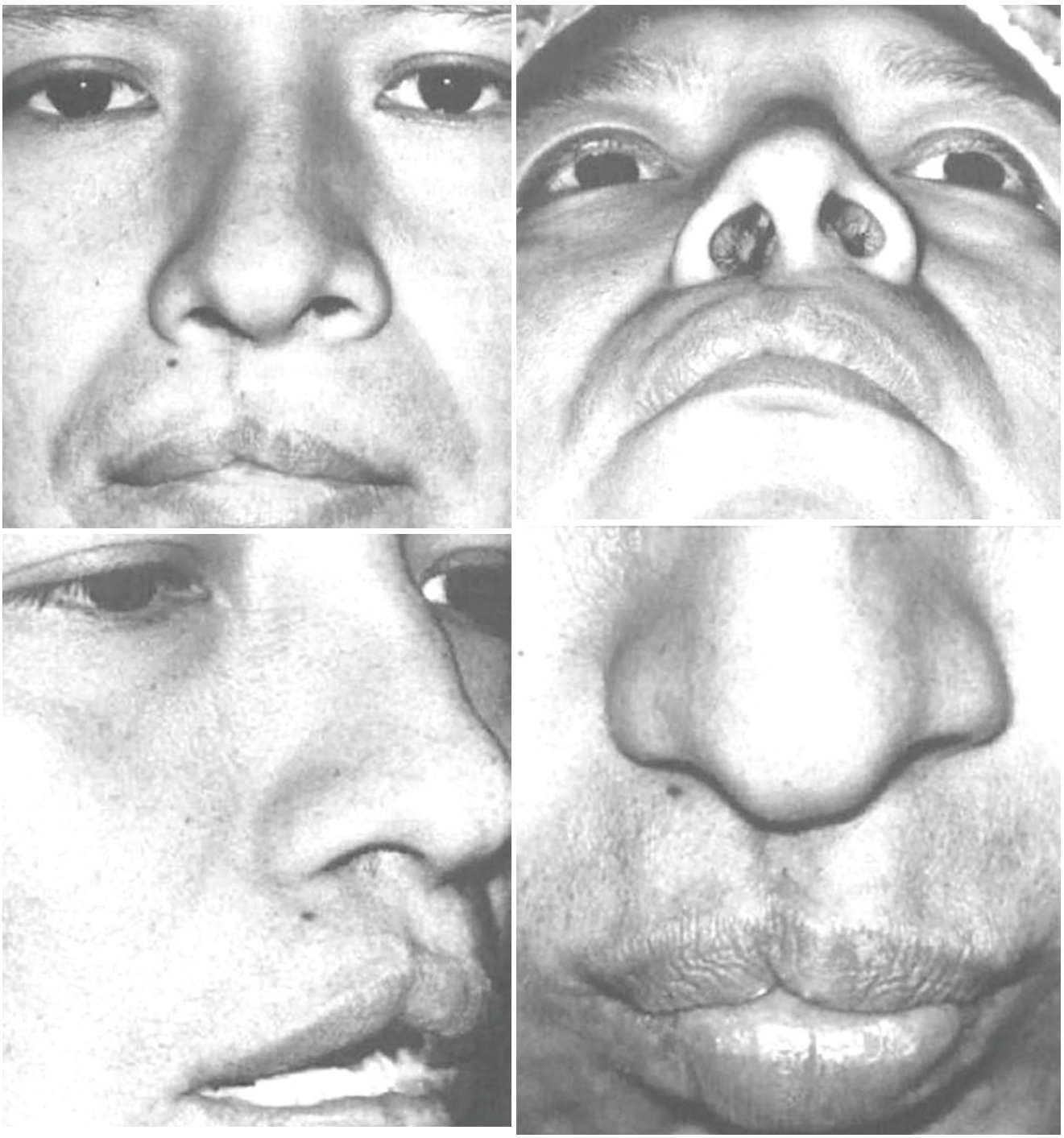

Fig. 18.72 DFR repair of microform cleft 1. In this early case, I did not do a nasalis repair. Medial crus was elevated with a bucket handle incision. The dead-space was filled with a composite chondrocartilage graft taken from the ipsilateral ear with a dermatology punch and the secured to the contralateral side, with a mattress suture. [Courtesy Michael Carstens, MD]

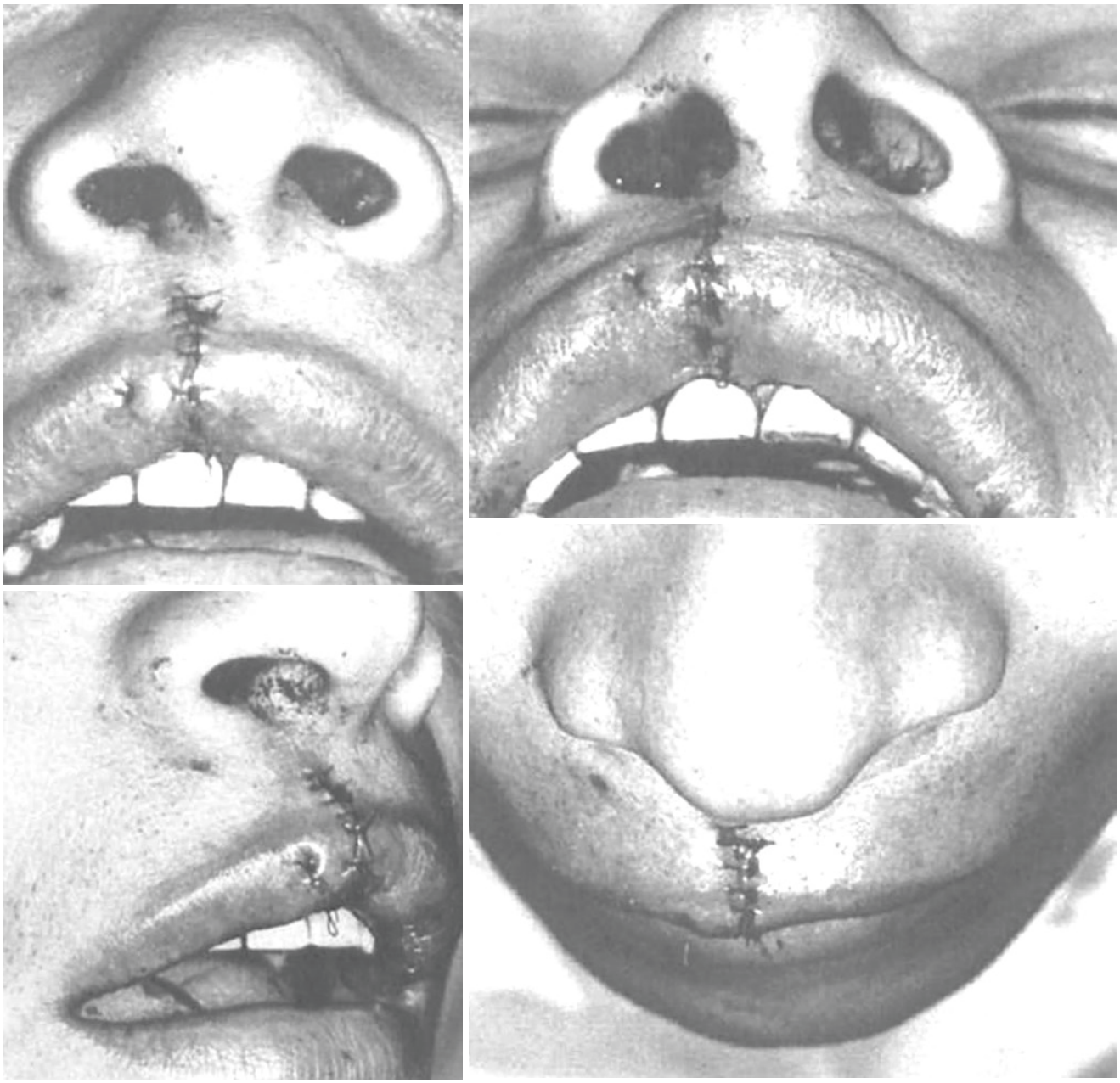

Fig. 18.73 DFR repair of microform cleft 2. Note change in symmetry of the nasal tip, alar base and nostril sill achieved with wide subperiosteal release. [Courtesy Michael Carstens, MDs]

Minimal clefts vary in severity. Some patients may present with a nostril deformity, whereas others possess a vermilion notch, cutaneous groove or muscle bulge. An individualized surgical approach should be designed for each patient according to his or her anatomy and desires. Not every deficit need be addressed. What the surgeon perceives as obvious may be of little significance to the patient. For this reason, the exact anatomic details of the cleft should be clearly understood by the patient so that proper informed consent can be obtained.

Nasalis function should also be tested. Comparison of alar motion can be made standing above with the patient seated and from the submental vertex position.

Problem-Directed Surgical Technique (Figs. 18.65, 18.66, 18.67, 18.68, 18.69, 18.70, 18.71, 18.72 and 18.73)

A depression or notch in the floor of the nose combined with a deformity of the piriform rim are the sine qua non of the

forme fruste cleft. The nasal mucosa and the alar base have settled into the bony depression and must be released subperiosteally. If no significant insufficiency of the lateral vestibular wall exists, this is all that is required.

The relationship of the alar base to the septum can be redefined with permanent suture placed connecting the base (taking care to stay superficial to the nasalis) to the anterior nasal spine. With adequate superiosteal release, this maneuver is seldom required.

Incision and Subperiosteal Release

The incision design used to accomplish the above depends on the degree of lateral displacement of the alar base. Separation of this variable from the anteroposterior and craniocaudal displacement of the piriform rim can be assessed in the office by placing a finger or cotton swab under the alar base in the sulcus and gently lifting it up. If the elevation achieved in this manner is inadequate, a lateral tethering effect of the ala by the periosteal sleeve over the face of the maxilla exists.

Access to the piriform fossa can be gained by a transverse incision in the mucoperiosteum from the anterior nasal spine beyond the canine fossa. Nasalis muscle will eventually be re-inserted at this point. This produces a broad mucoperiosteal flap that exposes the entire floor of the nose and gives access to the piriform fossa. The periosteum beneath the alar base is elevated. More alar release can be gained using a curvilinear scoring incision through the periosteum around the alar base. This gives additional exposure to the piriform fossa.

Lateral tethering of the alar complex to the anterior face of the maxilla requires a more extensive release but no change in incision design. From the level of the piriform rim, subperiosteal elevation can be directed laterally to the buttress. This elevation stops at the level of the attached gingiva. If further release is needed, an oblique counter-incision is made in the mucoperiosteum along the buttress.

The precision of this approach allows for entry into the fossa (which may drop sharply downward away from the rim itself) without injury to the mucoperiosteum of the nasal floor. Tears at this step may later cause a retethering of the alar complex via scar contracture and are worth avoiding.

Elevation of the Nasal Floor and Volume Restoration

When the alar base is completely released, the true nature of the piriform deficiency becomes apparent. In young children with active bone growth potential, the periosteal elevation will stimulate osteogenesis and support for the alar base may self-correct by the functional matrix reconstruction alone. In adults, actual piriform augmentation may be required. Using the trephine technique (Champy, Walter Lorenz Inc., Jacksonville, FL, U.S.A.), harvest of iliac crest cancellous bone is rapid and relatively noninvasive. A more elegant solution is a small amount of demineralized bone with or without morphogen rhBMP-2, thus eliminating the need for graft may be eliminated altogether.

- In adolescents and adults in whom piriform growth has cease, augmentation beneath the alar base may be required.

Reinsertion of Nasalis Muscle

If a significant amount of alar cartilage tethering is present, the insertion of nasalis should now addressed. This requires dissecting out its two heads. Recall that: (1) lateral head is inserted just beneath the nostril sill; and (2) medial head is inserted into the piriform fossa itself. The two head come together as they wind around the alar base and over the lower lateral cartilage to insert into the SMAS at the nasal dorsum.

Dissection of lateral head entails an external incision in the nostril sill and anterior alar base of 2.5 cm. It does not extend laterally around the alar base. The plane is immediately subcutaneous, above the nasalis. As one proceeds inward, dissection is continued above the *superficial aspect* of the muscle and below the vestibular lining, elevating the latter all the way into the piriform fossa and just beyond the inferior turbinate. The piriform elevation establishes the plane over the *superficial aspect* of medial head of nasalis as well.

In the incomplete cleft, getting below lateral head of nasalis is easy. One can grasp the muscle with a forcep and release it from the superior margin of superficial orbicularis. The two muscles have a different orientation and are easy to identify. One then follows the *deep aspect* of the nasalis around the alar base. At that point the plane is no longer deep to nasalis but *lateral* to it. You proceed upwards to above the alar cartilage. Traction on the lateral head will demonstrate an opening of the airway.

In the microform variant, nasalis dissection is straightforward if the lip is opened completely. If the lip is opened just through the SOO, the plane leading to nasalis is directly visualized as well.

In the mini-microform deformity the dissection is more subtle, as the lip is closed. One must proceed through the existing nostril sill incision, transect the nasalis. And then, putting the muscle on tension with a forcep, dive below it and, with a curved Stevens or Foman scissors, one advance laterally right the way around the alar base. You will then be able to traction the lateral head through the nostril sill to see if your release is adequate.

Dissection of the medial head is now completed through the intraoral incision. Medial head lies with the piriform fossa extending about 2–3 cm inside it. Recall that the vestibular lining has already been reflected away from the *superficial aspect* of head. What one now does is go is release the *deep aspect* of the medial head from the bony wall fossa

by means head by proceeding in the superiosteal plane within the fossa. You can thus "fish" the medial head out of the fossa. A short strongly-curved elevator, such a McKenty or a Molt, works well here.

At this point both heads of nasalis are identified. Through the nostril sill incision, spread through the fibers of orbicularis to deliver the lateral head downward into the piriform fossa. Both muscle heads can be treated as a single entity. Place suture of 4–0 vicryl or PDS through the sulcus, taking periosteum as well directly above the canine. Mattress the suture through the nasalis and return it into the mouth. This will re-establish the normal insertion above the canine fossa. Do not tie this suture until completion of the operation. It is just a place-holder. Excessive tension will traction the alar downward.

- *Nota bene*: It the surgeon is reluctant to use an external incision, the medial head in the piriform fossa can be sought and anchored. This may be functionally useful but the normal anatomy is incompletely restored without retrieving the lateral, more superficial head of the muscle.

Nasal Tip Asymmetry

The microform nasal tip may range from essentially normal to a full-blown deformity associated with the complete unilateral cleft. Management principles of the alar cartilage are no different in minimal cleft than in the more severe forms.[7] What should be emphasized in the minimal cleft is that access to the lateral crus of the lower lateral cartilage can be readily gained by the intraoral exposure. One proceeds by subperiosteal dissection along the outside of piriform rim and up over the dorsum: this puts one in the sub-SMAS plane, i.e., below nasalis. A concomitant rim incision puts one above the SMAS. Finally, blunt dissection of vestibular lining (Talmant maneuver) as described in Chap. 18 allows vestibular lining to be mobilized. When the alar complex is elevated from the piriform rim, the plane of the vestibular complete liberation of the lateral crus from the constraining influence of nasalis is an essential component for long-term tension-free repositioning of the tipdefining element. It is therefore important for the surgeon to take advantage of these exposures gained by this technique to accomplish this goal. Various forms of fixation have been described but probably this simplest is long-term stenting with this flexible silicone sheeting.

Vestibular Lining: Deficient or Displaced?

Comment *For some time, I thought that the lining was somehow short and the external vestibular release and addition of tissue using grafts or the inferior turbinate flap would solve the problem. This was a misconception on my part. The vestibular lining is not deficient, it is mismatched to its overlying soft tissues. Depending on the degree of nasal deformity, a Talmant release that bluntly frees the lining from the piriform altogether, may be required.*

- *I include the paragraphs below as examples of ideas **not** to try.*

"If the deficiency at the cleft site is more severe, superiosteal elevation alone will not be sufficient to release the alar complex. An incision in the lateral wall of the vestibule made in parallel to the nasal floor and terminating at the anterior aspect of the caudal margin of the inferior turbinate will accomplish a full release. The deficit site thus created can be replaced with full-thickness skin graft [101], composite conchal graft deficit [102], or a flap from the inferior turbinate [103–105]. The latter offers distinct advantages: (1) It relates directly to the deficit; (2) The donor site is unobtrusive; and (3) Although the palate is not cleft, intraoral subperiosteal exposure of the piriform fossa makes this flap relatively accessible for harvest."

"If the nasal vestibule exhibits an additional deficiency in the anteroposterior dimension, a releasing incision in parallel with the rim as described by Millard 129 may be required. Once again, the mucosal paring flap can be relied on to fill the deficit. The resultant oronasal fistula is clinically insignificant, acquiring, over time, the dimensions of a pinhole."

Nostril Sill

The nostril sill in a severe unilateral cleft can be readily designed based on the normal side. It is roughly an isosceles triangle, the base of which is equal to the thickness of the alar wall, *x* (usually about 4 mm), as measured inward from point 4. The anterior limb is 4–14. The posterior limb is drawn from point 14 back to *x*. After making the marks do not cut the flap: nasalis dissection comes next. If you cut the flap first, the muscle dissection is made more difficult.

The nostril sill is a skin and subcutaneous flap. Just below it lies nasalis. As stated previously, by dissecting subcutaneously all the way into the nasal vestibule as afar as inferior turbinate, one will stay quite nicely on top of nasalis. You can then dive beneath it down to the bone of piriform fossa to bet the remainder of the muscle. Once this is done, go ahead and cut the nostril sill flap.

Outward rotation of the nostril sill flap will put it in place to form the external border of nasal floor. It does not reach all the way to columella. Don't try to force it, as this will tighten the nostril. Instead, place the NPP behind the nostril sill, let them fall into place and suture accordingly.

There is obviously a full-thickness gap created by reassignment of the nostril sill. NPP alone may not reach the way. Keeping mucosa attached to the tip of NPP is not a

great idea as it interposes unlike tissue into the lateral nasal floor. Moreover, the blood supply is uncertain. A 100% reliable solution is an anteriorly-based inferior turbinate flap.

The above comments apply to the incomplete cleft but become progressively less important in the microform variant. Here, a simple interposition of the NPP skin flap behind nostril sill is sufficient. In minor degrees of cleft, the nostril sill can be left in situ, undisturbed.

Vermilion Border

Notching is a common presentation of the microform cleft. The issue at hand is the pars marginalis of the DOO as described by Park and Ha. The most caudal muscle curls forward beneath the vermilion, terminating at the white roll. Here it abuts the caudal margin of the SOO, which dead-ends at the white roll as well. The sequence of facial muscle development follows a deep-to-superficial and lateral-to-medial pattern. Three-dimensional computed tomographic reconstruction of the philtrum demonstrates that the pars marginalis of the DOO is continuous across Cupid's bow, whereas the SOO inserts into the r1 FNP mesenchyme of the philtrum. The abutment between r1 and r4 SOO creates the philtral columns. The vermilion notch, located just below the philtral column, represents a failure of the DOO to achieve full union at this site. Correction of the notch is accomplished using a *deepithelialized triangular muscle flap* pared from the lateral margin and inserted into a tunnel beneath the medial margin as described by Guerrero-Santos et al. [106]. This may need to be accompanied by a *zplasty of the vermilion* itself further within the lip. If so, the incision lines should be staggered so as not to create a contraction.

Philtral Column

When the superficial orbicularis oris fails to properly insert into the philtrum notching occurs. This is best appreciated when the patient is asked to pout the lip. When the DOO contracts, the philtral columns are pushed together; discontinuity of the SOO is revealed as a muscle bulge lateral to the pseudo-philtrum. In the same manner, SOO contraction reveals the lack of adequate cutaneous development across the philtrum. When viewed from below, the normal philtral column, albeit flattened, is still discernible. The pseudophiltrum merely flattens out, revealing the lack of support beneath it.

Should the patient desire correction of this problem, no option exists but to open the lip-partially. The thinned-out cutaneous skin of the philtral column is excised. Philtral skin is elevated with a knife from r1 mesenchyme, thus giving one an edge for suturing. The S00 is also undermined about 5 mm. SOO is then tacked to r1 mesenchymal "shelf" beneath the philtrum, and the edges everted. Re-closure of the skin shows "bulked up" philtral column.

- In patients with negligible muscle asymmetries, simple excision and closure of the philtrum column with everting sutures will suffice.

Final Thoughts: How Mechanism Affects the Clinical Applications Developmental Field Reassignment Surgery

- Thou shalt not subdivide or otherwise mutilate a neuroangiosome.
- Replace like with like, whenever possible, by reassigning fields to their correct embryonic relationship.
- Do not include metabolically challenged or embryonically-incomplete tissues in critical reconstruction sites.
  - The non-philtral prolabium must be taken out of the lip and used to support the columella and restore the nasal floor.
- Surgery in of congenital defects in infancy is a four-dimensional equation: growth will occur.
- Mesenchymal stem cell populations are the engine of facial growth.
- A cardinal principle of surgery should be the restoration of stem cell populations to their rightful place in space such that they will produce tissues over time where nature intended them to be.

Pathogenesis of Clefts: The Neuromeric Model

We come now to our final discussion, the heart of this chapter: the developmental sequence leading to the anatomic pathology of the cleft deformity. Let's summarize it up front as a formula; we shall then consider it component parts in sequence.

The Formula of Cleft

Lesion at level of arch formation > neuroangiosome failure > field defect with loss of mesenchymal mass > consequences: (1) physical and (2) biochemical

- Physical/mechanical
  - Critical contact distance between fields is exceeded: fusion failure
  - Effect on surrounding normal fields: distortion
- Biochemical: morphogen failure [BMP4]
  - Epithelial function: fusion failure
  - Muscle binding sites: aberrant insertions
  - Muscle differentiation

Presentations of Cleft Lip and Palate

Cleft lip, in all its forms, is caused by a mesenchymal deficiency in the premaxilla, first affecting the frontal process (PMxF) and then progressing to the lateral incisor zone (PMxB). In rare instances, the central incisor zone is affected as well, either as an isolated entity or in the total loss of the hemi-premaxilla. The cause is insufficient development of the StV2 neuroangiosome, medial nasopalatine artery. The consequences are physical and biochemical. This are best seen in the microform variant, where PMxB remains intact

- The physical effects of deficiency involving PMx and PMxB are as follows;
  - When the volume of PMxB is reduced such that the *critical contact distance* between the premaxillary alveolus and the maxillary alveolus is exceeded, normal fusion cannot take place.
  - All clefts have varying degrees of bone insufficiency. These affect surrounding bone and soft tissue structures. The ipsilateral normal nasal bone can be flattened. Premaxilla can be torqued away from midline. The scooped-out piriform fossa or in the thing of alveolar bone housing the lateral incisor causes the vestibular lining to be pulled down into the cleft site and the alar base to be anchored in a lateralized and posterior position.
- The mesenchymal deficiency also means a *quantitative reduction in diffusible morphogens* which are intrinsic to the process of membranous bone synthesis. These substances move through the overlying soft tissues from above downward and from deep to superficial with varying physiologic effects.
  - BMP4 deficit potentiates the activity of Shh in the surface epithelium, thus preventing fusion from below-upward and from superficial to deep.
  - BMP4, diffusing in the same way, affects the maturation of bone at the insertion sites of nasalis into the incisive fossa and canine fossa, forcing it to relocate to the piriform fossa and the nostril sill.
  - An unidentified morphogen controls development of overlying orbicularis oris muscle. The effect of this deficit is seen along the margins flanking either side of the cleft. As one moves away from the margin (beginning at about 5 mm), normalization of the orbicularis is seen.

Cleft palate, in all its forms, is caused by a mesenchymal deficiency in four bone fields, medially in the vomer and laterally among the three palatine bone fields, P1–P2–P3. In the first case, the cause is a progressive knockout of collateral branches from the medial nasopalatine axis which proceeds with increasing severity from posterior to anterior. In the second case, the cause is also a progressive knockout, first hitting the lesser palatine axis to P3 and subsequently the collateral branches from the greater palatine axis to P2 and P1.

- The physical effect of mesenchymal deficiency is twofold.
  - If the *shelf width* is reduced sufficiently in P1 or further backward in P2 such that the distance between the hard palate and vomer exceeds the critical contact distance, normal fusion cannot occur.
  - When *shelf length* is reduced, as takes place in P3, the palatine aponeurosis is foreshortened, thereby causing the third arch Sm7 muscle sling to be displaced forward into pathologic contact with the posterior shelves of P3.
- The reduction in diffusible morphogens exerts similar effects.
  - BMP4 deficit along the epithelial border prevents normal fusion.
  - An unidentified morphogen affects development of the levator sling but not tensor because the neighboring bone stock of P3 is normal.

Cleft nasal deformity in all its forms, involves (1) a mesenchymal defect in the frontal process of premaxilla and (2) some degree of disturbance in the insertion of nasalis. The latter may even precede the former. Nasal deformity is universal in all premaxillary deficiency states. The spectrum of its presentation is directly related to the lip defect. Every component of the nasal envelope is involved.

- *Columella* is determined by muscle insertions and by the position of the premaxilla.
  - The base of the columella is shifted to the non-cleft (normal) side due to abnormal muscle insertion and the position of the premaxilla. The more complete the cleft, the more deviation occurs. Even though the orbicularis complex is normally inserted in the incomplete form, the force vector is less than on the normal side. Note that in complete CL depressor septi nasa is absent on the affected side.
  - The remainder of columella and nasal tip are angulated toward the cleft side; this is due to the tethering of the nasal skin envelope.
  - In cleft states with a complete alveolar defect, premaxillary may be twisted toward the opposite side; this will flex the caudal septum and columella to the non-cleft side.
- *Septum* has two deflections, making it S-shaped.
  - Anteriorly it is deviated toward the normal nostril anteriorly.
  - Posterior deflection is present about ½ way back is into the cleft nasal passage. The is due to the greater cross-sectional surface area on the cleft side. Hydraulic pressure exerted by fetal breathing of non-compressible amniotic fluid is elevated within the normal airway forcing posterior septum into the cleft.
- *Nasal skin and vestibular lining* is stretched out to fit into the piriform fossa defect. The "program" for lower lateral cartilage is retained. Blunt dissection upward from piriform fossa (Talmant maneuver) will liberated the lining allowing for more stable repositioning of the alar cartilage.
- *Alar cartilage* is normal in size and shape.
  - Lateral crus conforms to a more lateralized position due to mechanical deformation of its lining "program." It is also locked down by the abnormal force vector of overlying nasalis.
  - Medial crus is pulled downward by insufficient bone stock. Its footplate is universally displaced, it can be located about 3 mm down and 3 mm behind the footplate on the normal side.
- *Alar base position* is lateralized due to a combination of muscle insertion and, with complete primary palate cleft, the deflection of maxilla both lateral and posterior. This can reach extremes as in the bilateral clefts.
- *Nasalis* muscle fails to insert into its intended binding sites above the canine and lateral incisor fossae. In the absence nasalis no other muscle attachments are located at those sites. The developmental cause is likely due to lack of morphogen signal from the underlying bone of PMxB which are responsible for activating the binding sites. Nasalis is forced to make other arrangements into the skin of the nostril sill and into the piriform fossa.

These principles are perfectly illustrated by a secondary repair of a right unilateral minimal cleft. The repositioning of the soft tissue is accomplished by developmental field technique combined with wide bilateral subperiosteal elevation of the midface envelope extending downward to include bilateral mucoperiosteal advancement flaps (Figs. 18.72 and 18.73). The result is a centralization of previously displaced soft tissue fields on both sides of the cleft.

Neuromeric Model: *Volume Deficit* Affects Bone and *Morphogen Deficit* Affects Soft Tissues

The spectrum of the *incomplete naso-labial-maxillary clefts*, by definition with an *intact secondary palate*, constitutes a **Rosetta Stone of the embryo** that enables us to decode the secret language of clefts, thus gaining insight into how their anatomic features come about. What's more, the neuromeric model extends far beyond the oral cavity to encompass multiple congenital conditions of the head and neck. So… let's recap the central tenets of what we have learned in sequence, from the general to the specific.

Homeotic Genes: The Universal System of Axis Determination

The first task in the construction of a body plan in all vertebrate embryos consists of axis definition. This is fundamental to the nervous system, the master CPU (central processing unit) to which tissues of the body are "wired." Throughout this text we have seen how homeotic genes, both those of the *original HOX genes* from r3 backwards and *non-HOX homeotic genes* from r2 forward, determine the boundaries and the anatomic contents of all neuromeres. This system is presented in Chaps. 1 and 2. Chapter 5 relates the evolution of the neuromeric system into its final iteration as per Puelles and Rubenstein. Alterations in the homeotic code result in specific tissue defects, i.e., the "knockout" model.

Pharyngeal Arches are Constructed from Paired Rhombomeres

Endodermal, mesodermal and neural crest tissue specific to r2–r11 are assembled into five pharyngeal arches. Each arch thus contains tissues from two distinct homeotic combinations. Specific sectors of the arches are defined by a universal system of Dlx genes.

- The original system of multiple branchial arches in jawless fishes morphed into the 7-arch system of sarcopterygian fishes immediately prior to tetrapods. Over the course of evolution the sixth and seventh arches are represented by neuromeres sp1–sp4.
- In mammals this means that tissue derivatives from c1 to c4 have two fates: between the modern structures of the

neck and primitive derivatives of the arch system, such as sternocleidomastoid and trapezius.
  – It is possible that the esophagus may represents a genetic unit spanning from sp1 to sp8.

Neuroangiosome are Programmed by Genetic Zones in the Arches

Pharyngeal arches are divided into specific zones by the Dlx gene system [107, 108]. Each arch has a designated neurovascular axis that subdivides to supply each Dlx zone or subzone as its unique neuroangiosome. First arch and second arch, because they were reassigned in evolution from respiratory structures to jaws, have a unique vascular composition.

- First arch divides into original mesodermal components, such as branchial chewing muscles related to the oral cavity and "modern" (with placoderms) non-branchial bone fields that produce the maxillary-zygomatic complex and the oro-nasal cavities.
  – Mesodermal (branchial) derivatives are supplied by a single branch of ECA, now known as the internal maxillo-mandibular axis.
  – Neural crest (non-branchial) derivatives are supplied by branches of the stapedial system which are annexed by internal maxillary.
- Second arch has two fates: (1) its anterior zones are fully incorporated into the first arch to form a "sandwich" with (2) remaining myoblasts migrate widely to cover the entire head. Blood supply therefore consists of four distinct branches from ECA.

Neuroangiosomes Have Paired Growth Cones

The neural growth cone produces vascular endothelial growth factor (VEGF) while the vascular growth cone elaborated nerve growth factor (NGF). Both growth cones contain stem cell precursors, pericytes, with differing homeotic origins. Reciprocal interaction between the growth cones takes place within the genetic environment of surrounding mesenchyme.

- Tissue defects (clefts) are caused by failure of a neuroangiosome or of its subsidiary branch. This can occur for two reasons
  – Stem cell failure at the growth cone
  – Abnormal interaction between the growth cones and signal from the surrounding mesenchyme

Neuroangiosome Failure Causes Local Field Defects

Embryonic fields, by definition, is supplied by a specific neuroangiosome. Fields may be homogeneous (e.g. inferior turbinate) in which case the axis has breaks into multiple coequal branches. Other fields, such as premaxilla have several subcomponents which develop in a sequence. In this case the branches of the axis will subdivide to supply each one individually but in a specific order reflecting their temporospatial maturity. Mesenchyme housing the central incisor is laid down first and receive the first-order branches of the axis. Lateral incisor mesenchyme is laid down not next; it receives the second-order branches. The most distal field, the frontal process, arises from PMxB and is supplied last and is therefore vulnerable to axis failure.

Resin casts of vascular injections by Amin in normal mouse palates versus spontaneous cleft palate (both unilateral and bilateral), are very instructive [109]. This report documents in normals a difference in density between the nasal side of the hard palate and the oral side of the hard palate: lateral nasopalatine axis is a smaller circulation joined by transpalatal anastomoses to the greater palatine axis. Furthermore, the medial border of the palatal shelves demonstrated terminal dilatations. Under normal conditions GPA from P1 continues into the premaxilla where it anastomoses with medial nasopalatine.

In the spontaneous cleft group, elevation of the palatal shelves was delayed. Moreover, the extension of the plexus to the medial borders of the shelves on the cleft side showed leakage of resin, indicating *underdeveloped and defective arteries*.

- **In UCL/P, altered development of capillary beds is observed in the nasopalatine region, i.e., the premax-**

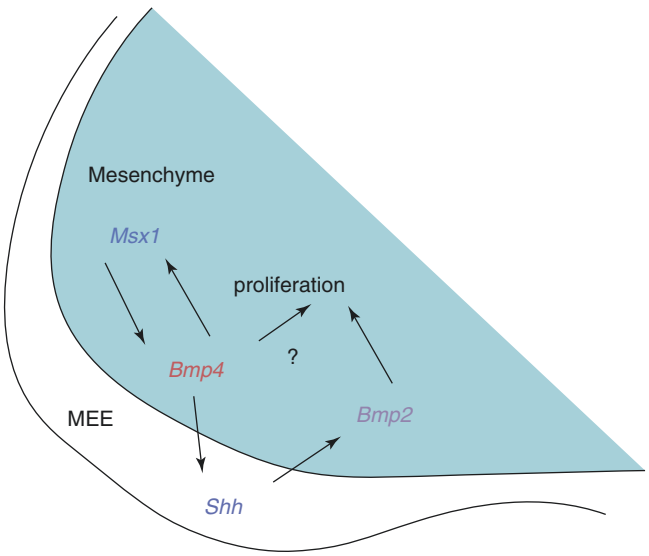

Fig. 18.74 BMP4 and sonic hedgehog (SHH) regulate epithelial fusion. A model for a genetic pathway integrating *Msx1*, *Bmp4*, *Shh*, and *Bmp2* in the epithelial–mesenchymal interactions that regulate mammalian palatogenesis. In this model, it is proposed that in the anterior palatal shelves, mesenchymally expressed *Msx1*, which can be induced by *Bmp4*, is required for *Bmp4* expression in the palatal mesenchyme. Mesenchymally expressed BMP4 maintains *Shh* expression in the MEE and Shh in turn induces *Bmp2* expression in the mesenchyme. BMP2 functions to induce cell proliferation in the palatal mesenchyme, which leads to palatal growth. [Reprinted from Zhang Z, Song Y, Zhao X, et al. Rescue of cleft palate in Msx-1 deficient mice by transgenic Bmp4 reveals a network of BMP4 and Shh signaling in the regulation of mammalian palatogenesis. Development 2002; 129:4135–4146. With permission from Company of Biologists]

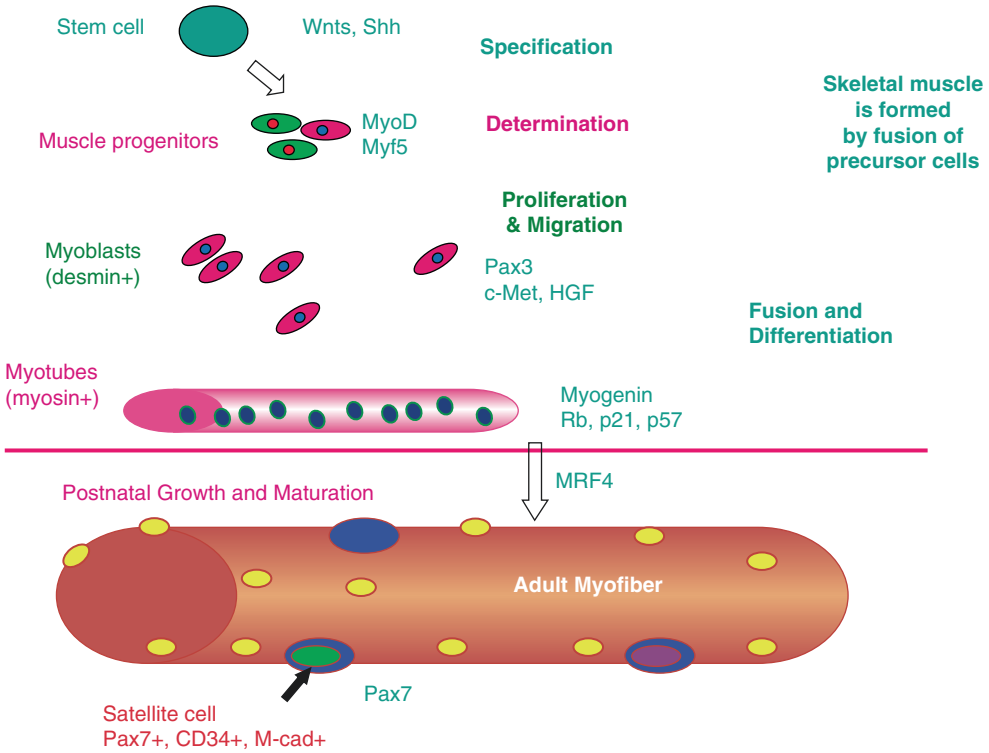

Fig. 18.75 Skeletal muscle embryogenesis 1 BMP4 acts primarily on Myf5. Formation of skeletal muscle tissue involves progressive commitment to the myogenic fate and fusion of myoblasts to form multinucleated myofibers. Specification of myogenic cells from early embryonic stem cells occurs under environmental influences (Wnts, Shh). Subsequently, the expression of MyoD/Myf5 in proliferating muscle progenitors commits them to a muscle fate and expression of muscle-specific proteins such as desmin. Cell cycle arrest, fusion of determined myoblasts into myotubes, and activation of differentiation-specific genes such as myosin are regulated by the MRFs in conjunction with cell cycle regulators. Maturation of myotubes into large myofibers progresses postnatally. Satellite cells (mononucleated muscle precursors) are associated with myofibers and marked by Pax7 expression. [Reprinted from Sachidanandan C, Dhwan J. Skeletal Muscle Progenitor Cells in Development and Regeneration. Proc Indian Nat Sci Acad 2003; 69(5): 719–740. With permission from Springer Nature]

illa. The alternation is ipsilateral in UCLP and affects the entire premaxilla in the BCLP.

Being a "Mesenchymal Midget" has Consequences

When, through neurovascular failure, a developmental field loses one or more of its component sub-field (such as PMxF) or simply experiences a deflation in volume, three things occur: (1) change in shape, (2) reduced production of otherwise normal morphogens, and (3) possible production of abnormal morphogens.

- Shape changes alter the anatomy of otherwise normal partner structure. Plagiocephaly elevates the eyebrow. A scooped-out PMxB lowers the nasal floor or causes a rotation of the lateral incisor.
- Morphogen deficit can lead to cleft formation or failure of muscle binding sites to "turn on the landing lights."
- Abnormal morphogens can cause structural alterations in surrounding tissues. Muscle in the *immediate environment* (5 mm) of the cleft margin shows abnormalities of muscle fibrils and mitochondria. Faulty signal from any of the four zones of parietal bone can cause synostosis in the adjacent suture.

Pathogenesis of Cleft: Molecular Mechanism

A Deficit in [BMP4] is the Common Denominator of Soft Tissue Pathology at the Cleft Margin

From its site of origin in the bone fields of premaxilla BMP4 diffuses through the soft tissues from above downward and from deep to superficial until reaching the margins of prolabium and lateral lip element. Thus, the cleft site is the most distal and the most vulnerable to a reduced or absent concen-

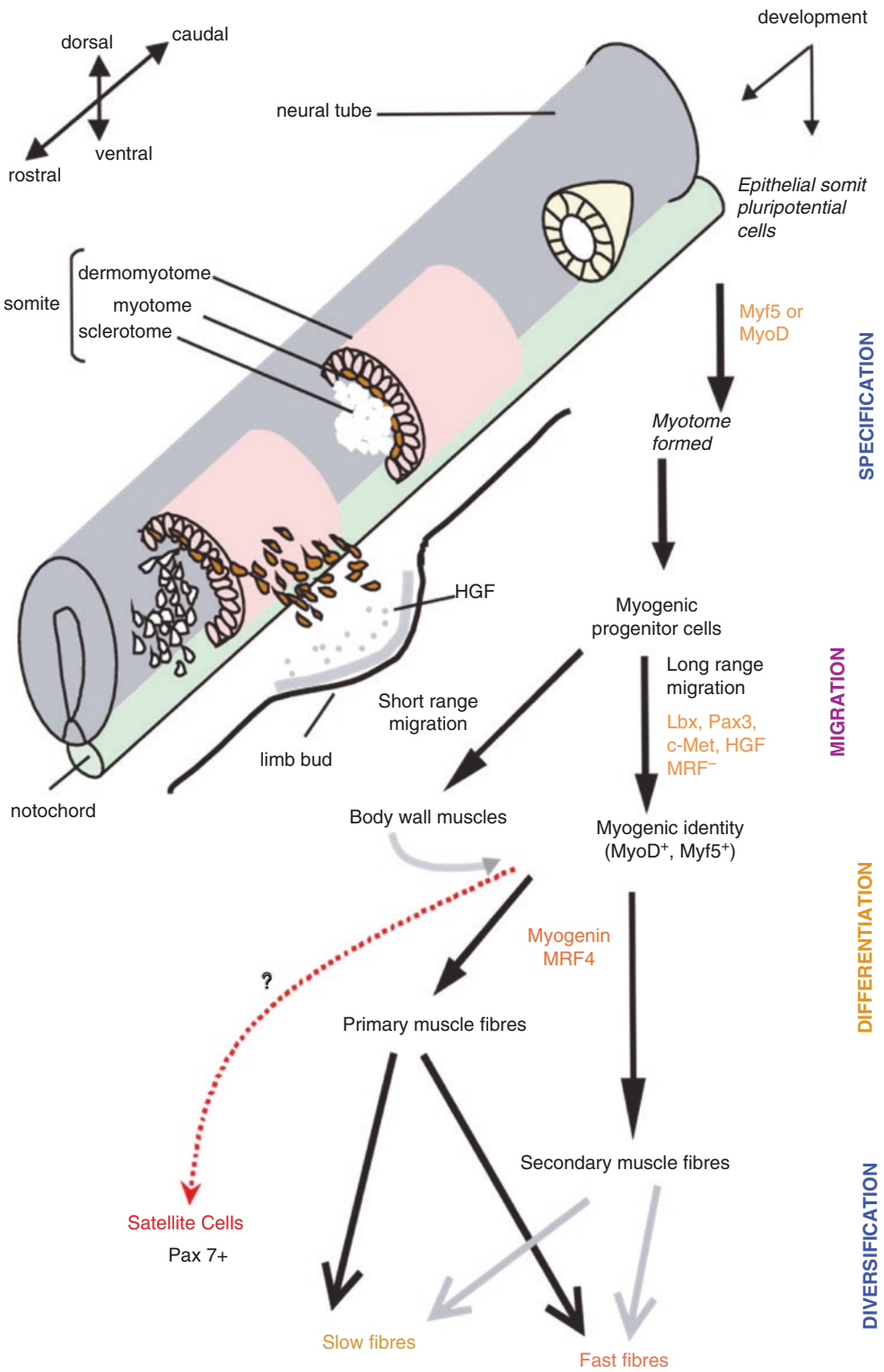

Fig. 18.76 Skeletal muscle embryogenesis 2 BMP4 acts primarily on My5. Schematic representation of somite development indicates the relative location of somites with respect to the axial neural tube and notochord. Although the somite is the source of many cell types (cartilage, muscle, skin), this schematic emphasizes the genes involved in the determination and differentiation of myogenic precursors. Interestingly, muscle progenitors from somites at different axial levels are influenced by different environmental cues. For example, muscle progenitors from somites positioned at the level of the developing limb bud, are induced by HGF to migrate long distances and form the limb muscles. These cells are marked by a distinct set of genes that are not expressed by the precursors of body wall muscles that migrate only short distances. Fusion and differentiation occur in two temporal waves to form primary and secondary myofibers that subsequently mature and diversify into fast and slow fiber types with distinct patterns of myosin expression. Neural signals influence fiber diversification. [Reprinted from Sachidanandan C, Dhwan J. Skeletal Muscle Progenitor Cells in Development and Regeneration. Proc Indian Nat Sci Acad 2003; 69(5): 719–740. With permission from Springer Nature]

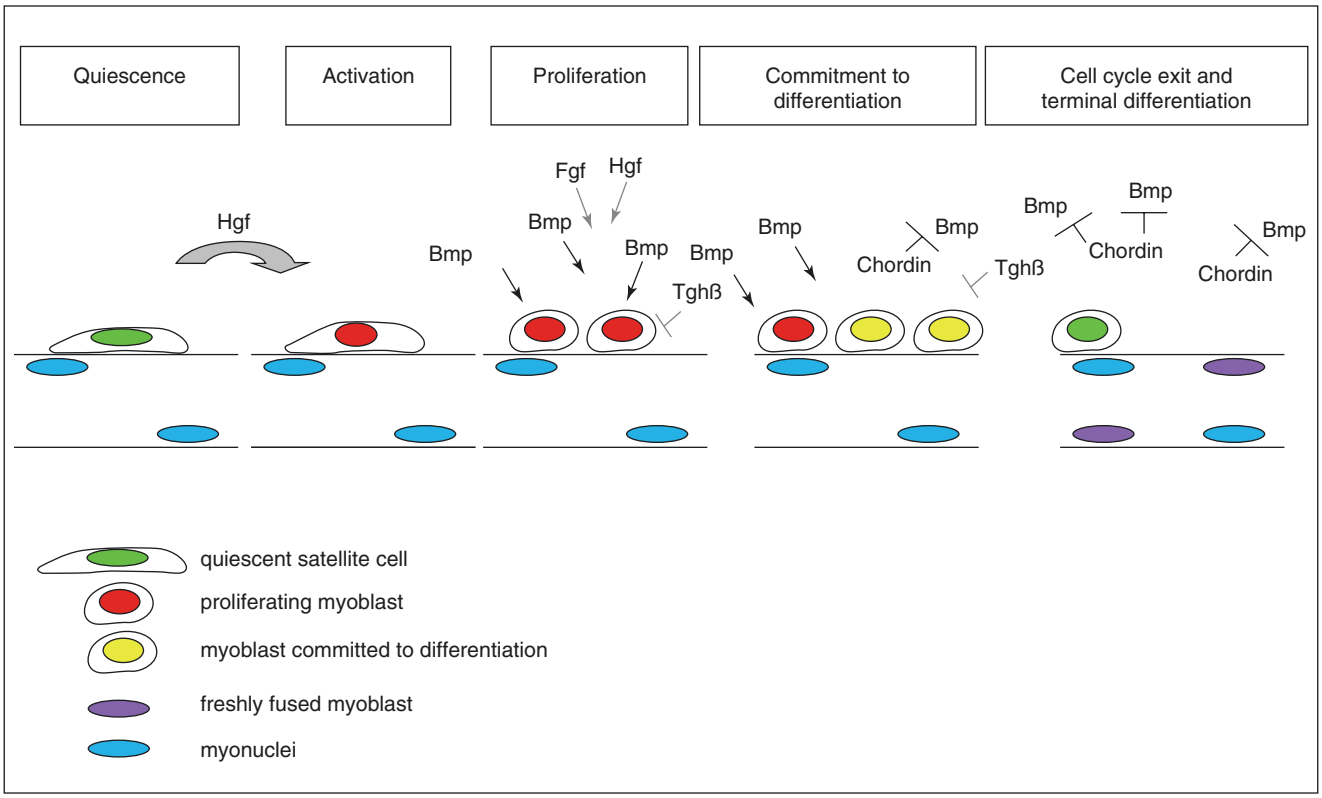

Fig. 18.77 BMP signaling during satellite cell differentiation. Quiescent satellite cells (green) do not respond to BMP signals. Upon activation, satellite cells express MyoD and respond to BMP signals with phosphorylation of p-Smad (red) and reduced differentiation. After satellite cell descendents are committed to differentiate (yellow) they express Myogenin and subsequently the BMP inhibitor Chordin. Upon inhibition of BMP signaling, myoblasts exit the cell cycle, fuse into myotubes and undergo terminal differentiation (purple). Postmitotic myonuclei (blue) irreversibly loose the competence to respond to BMP signals. [Reprinted from Friedrichs M, Wirsdöefer F, Flohé SB, Schneider S, Wuelling M, Vortkamp A. BMP signaling balances proliferation and differentiation of muscle in satellite cell descendents. BMC Cell Biol. 2011; 12:26–43. With permission from Springer Nature]

tration of BMP4. The effects of BMP4 deficit on epithelial surfaces (previously discussed) are highly localized and explain fusion failure at the cleft margins. Also highly localized are muscle abnormalities as documented above. These are similar in both lip and palate muscles: decreased number of muscle fibers, disorganization (failure to properly assemble), abnormal predominance of type II (fast twitch) fibers. BMP4 has a regulatory role at multiple steps in myogenesis (Figs. 18.74, 18.75, 18.76 and 18.77).

- **Conclusion**: *the epithelial and muscle abnormalities at the cleft site evidence the morphogen BMP4 plays central role in the pathogenesis of cleft lip*.
- **Conclusion (see below):** BMP signaling regulated muscle development in the postnatal period by controlling stem (satellite) cell dependent growth of myofibers and the generation of an ongoing reserve of adult muscle stem cells.

How does this work? Let's organize our discussion as follows. First, we will look at the basic properties of BMP4. We then consider the stages of myogenesis and how it is regulated. As we shall see, BMP4 impacts on multiple steps in this process. Satellite cells are stem cells within muscle. They are responsive to BMP4 so we will need to define them. Myogenesis has three phases through development: embryonic, fetal, and perinatal (adult); cleft margin muscle fits into the transition between the first two, beginning around Carnegie stage 20.

BMP4: A Brief Introduction

Bone morphogenetic protein 4, produced by the *BMP4* gene located on chromosome 14q22–q23 and is a member of the transforming growth factor beta superfamily. It is produced at all neuromeric levels of the dorsal notochord and plays a protean role in the formation of the embryonic axis. From the ventral notochord, and opposition to BMP4 is sonic hedgehog.

Later in embryogenesis BMP4 becomes inhibited by dorsal gene expression and assumes a ventralizing role for mesoderm.

BMP4 is responsible for determining the non-neural fate of overlying ectoderm. It affects the development of multiple tissues, including the eye, angiogenesis, the musculoskeletal system and the ureteric bud. Additional roles in craniofacial development include generation of new neurons (stem cell effect) in the subventricular zone of the ventricles; and the control of apoptosis affecting r1 neural crest which is responsible for unification of the nose and centralization of the orbits. See review by Wang et al. [110].

Martin showed histologic changes in "subepithelial" clefts consistent with fibrosis. Ultrasound now demonstrates this as a hypoechoic interruption in an otherwise hyperechoic (black) band corresponding to orbicularis. Demonstrating ultrasound were used.

The Three Phases of Skeletal Muscle Development

Primary myogenesis is embryonic. This population is controlled by *Pax3*. It refers to the formation of the first multinucleate fibers from embryonic precursors the fuse together, creating a scaffold. This phase lasts in mice until E14.5 or approximately Carnegie stages 19–20. Recall that the primary fibers are predominantly type 1.

- Facial skeletal development takes place prior to this time.
- Thus, the effects of decreased [BMP4] are present during embryonic myogenesis.

Secondary myogenesis is fetal. Population control is from *Pax7*. Fetal progenitors add on to the scaffold. They favor type 2 (fast-twitch) fibers. This final differentiation consists of three steps.

- *Exit from the cell cycle*: Myoblasts "decide" to stop proliferating
- *Alignment*: Myoblasts recognized one another and clump together
- *Fusion*: Meltrins, metalloproteinases play a crucial role
  - Primary myoblasts form slow-twitch muscle type 1 fibers
  - Secondary muscle fibers develop with innervation and form fast-twitch type 2 fibers

Tertiary myogenesis is perinatal and stabilizes in the adult. When myogenesis is complete both Pax3 and Pax7 are no longer required thus BMP4 no longer plays a role. In the case of muscle repair after trauma, BMPs again are important for satellite cell activation but via an entirely different mechanism, using chordin as antagonist.

Genetic Regulation of Myogenesis: A Play in 6 Acts

The overall process of myogenesis consists of 6 steps—based on the somite model. Key genes are listed. We shall see them again when discussing where and how BMP4 affects the process. Some familiarity with these genes is worthwhile, trust me! Chai and Pourquíe provide a very comprehensive review.

Note: A homeobox is a sequence of DNA 180 base pairs in length in genes involved in morphogenesis. These genes produce homeodomain proteins have a helix–loop–helix configuration to binds to segments of DNA and unlocks them

- *Delamination from the somite* (PAX3, c-Met) Departure from the dermomyotome is controlled by PAX3 via its induction of c-Met. Failure totally blocks entry into the migration pathway.
  - Control of delamination from somitomeres Sm1 to Sm7 is unclear because PAX3 is not expressed in facial muscles.
- *Migration* (c-Met/HGF, LBX1) Myoblasts move into position in the limbs according to dorsal and ventral signals.
  - c-Met alone is expressed by epithelium whereas c-Met in association with hepatic growth factor is expressed in mesoderm. Cell survival along the migration pathway is dependent on c-Met/HGF.
  - LBX1, ladybird homeobox 1, regulates the actual migration of myoblasts into the limb. It acts unopposed in the hindlimb but the forelimb has separate ventral signals. Thus in the absence of LBX1 flexor muscles develop in the forelimb while the hindlimb is sterile.
  - Control of migration into the orbit and pharyngeal arches from somitomeres is unclear. From levels r8 to r11 tongue muscle migration is distinct from migration of pharyngeal constrictors and laryngeal muscles.
- *Proliferation* (PAX3, c-Met, MOX2, MSX1, Six, My5, MyoD) Myoblasts have to expand in number becoming myocytes.
  - MOX2, mesenchymal homeobox 2 controls expansion of the myoblast pool globally in the hindlimb, causing it to shrivel; in the forelimb only certain muscles are affected. How this gene in the pharyngeal arches is unknown.
  - Myf5, myogenic regulatory factor 5, is a homeobox gene; it is the earliest in a series of MRFs (myogenic regulatory factors). MyoD belongs to the same family and is Myf5 drive myoblasts to commit to skeletal muscle lineage. Under experimental conditions MYF5 can force undifferentiated mesenchymal cells such as

fibroblasts into a muscle. A block in Myf5 causes complete absence of muscle.
  - MyoD, myogenic differentiation factor 1, regulates the committed state of muscle cells. It acts in concert with the more important Myf5. MyoD resides in satellite cells at low levels (vide infra) but gets turned on in response to trauma. MyoD is important for the expression of fast-twitch, type 2 fibers.
  - MSX1, Msx homeobox protein 1, is implicated in cleft palate. Cases of Msx1 deficiency have be "rescued" by BMP4 [111]. This implicates BMP4 in the production of MSX1.
  - SIX1, Sineoculis homeobox homolog 1, is the homolog of the Drosophila eyeless gene. It is involved in the neuromuscular junction. As we shall see, innervation of muscle is necessary for its expansion. SIX1 is required for hypaxial muscles, i.e. muscles of the pharyngeal arches.
- *Determination* (Myf5, MyoD) refers to the final phenotypic expression of skeletal muscle. Assuming the myoblasts have proliferated their conversion into skeletal muscle depends upon proper function of both of these factors.
- *Differentiation* (Myf4, Myf6, MyoD) myocytes now mature.
  - Myf4, myogenin, is required for the fusion of myocytes to either form new fibers or add on to existing one. If permits muscle fibers to grow before the terminal differentiation event.
  - Myf6, herculin, controls differentiation of myotubes in skeletal muscle (not smooth muscle).

Stem Cell Regulation: General Characteristics

Skeletal muscle stem cells ("reserve" cells) have two fates: (1) they serve as precursors of skeletal muscle or (2) they maintain a self-replicating population. Stem cells are found intercalated between the sarcolemma and the basement membrane. Because of their peripheral location they acquired the name "satellite" cells, These cells are small, with few organelles and a high nucleus-to-cytoplasm ratio. Satellite cells can fuse directly to underlying muscle fibers, thus augmenting their nuclei. They can also form new fibers. In the adult stage these stem cells are quiescent but they respond to trauma by first proliferating as myoblasts and then undergoing division.

Satellite cells of non-craniofacial muscle express both PX3 AND PAX6 while craniofacial muscles express only PAX6. In the dormant state, satellite cells express CD34 (typical for baseline mesenchymal stem cells) and Myf5 (indicating stable muscle function). When activated by BMP4, satellite cells initially express the PAX genes but these quickly give way to MyoD and Myf4 (myogenin), indicating ongoing fusion. In general, BMP upregulation *maintains satellite cells in a proliferating state*, thereby expanding the numbers of cells and fibers. Once the cells decide to differentiate, they upregulate Chordin which shuts down BMP as a negative feedback loop to support terminal differentiation [112].

Two experimental situations illustrate this concept

- Noggin has been used to block BMP in utero. Under these conditions, postnatal histology shows decreased satellite cell proliferation and decreased muscle fiber growth (Stantzou 2017).
- *Fibrodysplasia ossificans progressive* is an experiment of nature which shows what happens to muscle stem cells under conditions of abnormally high BMP signaling. The response is quantitative; they are driven to an osteogenic fate thus producing ectopic bone as in Shore et al. [113].
  - **Note**: This is precisely what takes place when rhBMP2 recruits MSCs and converts them into bone (see Chap. 20).

Muscle Stem Cells: Main Population Versus Side Population

Skeletal muscle has more than one type of stem (satellite) cell [114]. A main population (MP) and a side population (SP). SP cells express BMP4 which induces in the MP cells BMP receptor 1a (BMPR1a). The protein Gremlin 1 (Grem1) acts as an antagonist for TG-Beta signaling molecules, specifically blocking BMP2 and BMP4. It is essential for limb bud development. Grem1 is produced by MP cells as a response to the BMP4 stimulus, acting as a negative feedback loop to shut down the process. It has been shown the BMP4+ cells coexist with BMPR1a+ cells in the interstitial cells of muscle.

BMP4 causes cells that are BMPR1a+ to proliferate but has no effect on stem cells that are BMPR1a−. Furthermore, BMP4 inhibits transcription of the gene *MyoD*, which is responsible for causing muscle cells to pull out of the cell cycle and undergo terminal differentiation. As long as BMP4 is active the muscle population expands. Under normal conditions:

- Muscle SP cells cause proliferation of myogenic precursors via BMP4.
- This produces an expansion of the embryonic muscle population to reach its final state prior to shutdown.
- Gremlin stops this process, bringing muscle proliferation to an end.

Cleft Lip Muscle: Why Is It the Way It Is?

Early myoblasts must choose between continued proliferation and differentiation into multi-nucleate myotubules. BMP4 is the potential driver. The myoblast at the margin of the prolabium and maxillary process are the most distal from the "radio signal" of BMP4. They receive the transmission last. Their blood supply is the most distal as well. BMP2, BMP4 are all important for the maintenance of vascular endothelium [115, 116]. What happens to this milieu if the [BMP4] is pathologically reduced?

Muscle fibers within 5–10 mm of the cleft site undergo premature shutdown of proliferation due to morphogen deficit

- Decrease in number of muscle fibers
- Failure of fibers to correctly assemble, leading to disorganization
- Muscle fibers are 50% reduced in diameter
- Interstitial tissue remains in a primitive, fibrotic state
- Reduced number of blood vessels due to BMP4-related endothelial dysfunction

Conclusion

In this chapter, the microform and its variants have served as a Rosetta Stone to help us decipher the secret language of clefts. Using the neuromeric model, we have followed the consequences of a deficit in the premaxilla from local manifestations involving the hard tissue platform to its distal soft tissue effects. In so doing, the stage is now for a final consideration of the complete form of the nasolabial cleft in the chapter that follows.

The soft tissue pathology of the cleft nose is dependent in every way upon the bone platform due to inadequate development of the premaxilla, both in terms of how its soft tissues of the nasal envelope are anchored and how muscles acting on the alar based and lateral nasal wall are anchored. The principles of surgical management are:

- Wide subperiosteal dissection, both within the piriform fossa and nasal vestibule and external all the way to the nasal bones to correctly reassign tissues to their correct relationships
- Correction of the septum, as indicated
- Restoration of the airway by reassigning nasalis to its functionally correct insertion
  - Separate nasalis from orbicularis anchor it to canine, *not* to the midline

The soft tissue pathology of cleft lip takes place in a limited zone of tissue in close proximity to the cleft site characterized by reduction in BMP4 concentration below a critical level required for epithelial stability, normal myogenesis, and microvascular development. The principles of surgical management are as follows:

- Wide subperiosteal mobilization
- Developmental field dissection of the prolabium
- Exclusion of embryologically damaged tissue from the repair site
- Restoration of the nasal floor

Addendum: Alveolar Cleft Closure (with DFR Modification)

Non-DFR flaps are shown in the original illustration with nasal floor closure using nasal mucosa flaps from below as a blind procedure. Under *DFR protocol* the nasal floor is addressed at primary lip repair (6 months) with the backwall and floor created by AEP at 18 months. If the nasal floor has not been closed, prior repair was non-DFR. Secondary lip repair is done with nasalis dissection and water-tight closure.

Step 1 *Upper Left*: Mucoperiosteal flap (r2, pink) gingivoperiosteoplasty flaps (sliding sulcus flap) is mobilized via pericoronal incision with a back-cut up the buttress. The S flap is supplied by medial and lateral branches of StV2 infraorbital and by overlying ECA facial artery. The dotted lines indicate the level of a counter-incision that will be made along the undersurface of the flap. Mucoperiosteum of premaxilla (orange) has also a mixed blood supply from StV1 anterior ethmoid, from StV2 medial nasopalatine, and from StV2 medial branch of infraorbital. Periosteal flap on maxillary side (yellow) is supplied by greater palatine. Periosteal flap on the premaxillary side (white) has a variable blood supply. If the cleft is unilateral, it receives StV2 greater palatine + StV2 medial nasopalatine and back flow from StV1 anterior ethmoid. If the cleft is bilateral, it is perfused by the latter two arteries only. Note the cut shown between lateral incisor and canine on the non-cleft side. In DFR this is usually unnecessary for two reasons: (1) the non-cleft flap can be mobilized in a similar manner. (2) A similar periosteal releasing incision. Bilateral S flaps can cover a total of up to 4 dental units without tension. Dissection time is fast and bloodless, under 5 min per flap.

Step 2 *Upper right*: backwall flaps are sutured, maxillary (yellow) to premaxillary (white). The counter-incision along

the undersurface of the S flap is indicated by a white line with red dots. The incision is placed at the level of the buccal sulcus. Although the S flap is mobilized over the entire face of the maxilla, the counter incision frees the alveolar component to translate with ease, with no tethering from above.

Step 3 Mesial translation of maxillary S flap (pink) and premaxillary S flap (orange). Dead space for the flaps is transferred to the first or second molar.

Step 4 Final closure with bone graft/rhBMP2 in place. Incision at premaxillary–maxillary junction on the non-cleft side is not necessary.

Commentary: Karoon Agrawal

The Embryologic Basis of Craniofacial Structure: Developmental Anatomy, Evolutionary Design, and Clinical Applications

Michael Carstens

(Editor in New York: Michelle Tam. Publisher: Springer Verlag)

The world is progressing very fast, and the knowledge is expanding exponentially in breadth and depth; we need to keep pace. This book will be a milestone in the understanding of developmental anatomy, of its evolutionary origin and its clinical applications, especially in reference to the occurrence of facial clefts.

Mr. Michael Carstens is a big name in India. He is a great friend of the Indian Plastic Surgery community and is an honorary member of our Indian Societies. He has visited our country multiple times and has participated in many academic meetings to present his innovative work. He has tirelessly encouraged our scientific community for doing research and making innovations with newer techniques of cleft repair.

I cannot forget my encounter with Mr. Mike for a debate on "Alveolar Extension Palatoplasty" popularized by him. He was speaking in favor, and I was speaking against. In spite of the outcome of the debate, we became great admirers of each other. We kept exchanging our thoughts at regular intervals. The more I interacted with him, the more I realized that this man was born with a mission as he has dedicated his career to solve the jigsaw puzzle of the origins of facial clefts. His concept relates to the stapedial artery not as a single entity, but as a complex system making a relationship between failure of individual stapedial branches as a causation of facial clefts is unique and impressive.

I was surprised by a personal call from Mike for writing a foreword of his book being published by Springer-Verlag, and I am here to do justice to his request. I consider it a great privilege to be asked to write a foreword and express my assessment of this work.

A Note from Dr. Carstens

Karoon Agrawal

For over four decades, Dr. Karoon Agrawal, Professor of Plastic Surgery at the National Heat Institute of New Delhi, India, has been a thought leader with extensive contributions to both cleft lip/palate and hypospadias. A tireless academician, he has also proven himself to be a glutton for punishment on two accounts: first, he is the editor of a six-volume treatise published with Thieme covering the entire specialty; and second, he willingly committed to review this book from cover to cover, contributing careful and in-depth comments. For the time and effort this required, I sincerely hope that his wife will forgive me. Karoon cuts a fine-featured, slender, and scholarly figure, accompanied by a warm smile and restless intellect. He is also a first-class debater, which I discovered to my discomfiture. We were summoned by the Indian Society for Cleft Lip and Palate to debate on the relative merits of alveolar extension palatoplasty versus the traditional concept of cleft palate repair. Right off, I knew that it was a dangerous proposition … no mortal could expect to approximate Karoon's surgical experience. But I had not counted on his sense of humor. There, upon the screen, with his very first slide, in front of the entire audience, was a picture of a crouching King Kong in the posture of a sumo wrestler with my face pasted on top! I suppose it was intended as a backhanded compliment about AEP, but at the time I wanted to crawl in a hole. Anyway, the discussion was lively and the whole audience loved it. Later on, as the journal editor for the ISCLP, Karoon invited me to contribute to a special issue to present the developmental science of palatoplasty. Although it was like pulling teeth, he was patient with me and the result was two articles that eventually formed the blueprint for Chapters 14–17. Karoon's gentle but persistent questioning forced me to focus on mechanism and good writing. I can say, in retrospect, that the content of the chapters are as much his thinking as my own. As both colleague and friend, Dr. Karoon Agrawal represents the very best of Indian plastic surgery, a gift for which I will always be indebted.

This book is a treasure trove for all embryologists, anatomists, cleft clinicians, as well as researchers. The chapters are designed remarkably well, keeping in mind the interests of the readers and beneficiaries. Chapters 1–5 are on the basic concepts; Chaps. 6–13 cover specific anatomic entities (such as bone, fascia and the orbit), Chaps. 14–19 are on the pathologic anatomy and basis of repair of cleft lip and palate and Chap. 20 on BMP is speculative, which I enjoyed the most. The content reflects the unparalleled thought process of a man who has spent all his lifetime thinking, analyzing, and writing about neuroembryology and functional anatomy of the head and neck.

Although the explosion of knowledge in craniofacial surgery coupled with advances in science and technology has improved our clinical outcome, little attention has been given to expanding our understanding of basic anatomic principles. Reading through the chapters of this book, it seems that there are many basics which are still unexplored. This work is an attempt to unravel many such mysteries, not only in clefts, but also in synostosis, orthognathics, and absence or excess of structures in the orbit, nose, neck, and brain. Even the rationale for structures we take for granted, such as the fascial layers, sutures and foramina are explored. All this is clinically relevant. Better understanding of the development of the anomalies will pave the way for better prevention and management strategies.

While going through the chapters, one will be awed by the amount of information that Mike has for all the readers. How he imbibed so much in his lifetime is difficult to fathom. The embryology and pathogenesis of CLP (hard palate, soft palate, and lip/nose complex) are remarkable chapters. At the same time, I do not intend to belittle the relevance of other chapters. No stone is left unturned.

This analysis of principles of development of craniofacial structures is extraordinary. A great amount of research has been done to prepare the manuscript. This is of immense value to every embryologist, anatomist, researcher, and clinician.

Creation of a single-author book of this magnitude is a gigantic task. Mike has spent years working toward the creation of this. Into it he has poured all his knowledge and research, along with his innovative thoughts. I admire his effort. This book is a must-have in the reference section of every institute's medical library and a must-read for every member of the cleft care team.

Karoon Agrawal, MS, MCh

Consultant Plastic Surgeon, National Heart Institute

Member of Smile Train Global Medical Advisory Board

Former Director Professor and Head of Burn, Plastic & Maxillofacial Surgery

VMMC & Safdarjung Hospital, New Delhi, India

Editor: Textbook of Plastic Reconstructive, and Aesthetic Surgery

References

1. Cosman B, Crikelair GF. The shape of the unilateral cleft deformity. Plast Reconstr Surg. 1964;35:484–93.
2. Carstens MH. Correction of the bilateral cleft using the sliding sulcus technique. J Craniofac Surg. 2000a;11(5):137–67.
3. Carstens MH. Functional matrix cleft repair: a common strategy for unilateral and bilateral cleft lip. J Craniofac Surg. 2000b;11(5):437–69.
4. Hinrichsen K. The early development of morphology and pattern of development of the face in the human embryo. Advances in anatomy, embryology and cell biology 98. New York: Springer; 1985.
5. Curtin J. Clinical evaluation of microform cleft lip surgery (discussion of article by Thomson and Delpero). Plast Reconstr Surg. 1984;75:804.
6. Heckler FR, Oesterle LG, Jabaley M. The minimal cleft lip revisited: clinical and anatomic considerations. Cleft Palate J. 1979;16:240.
7. Thomson HG, Del Pero W. Clinical evaluation of microform cleft lip surgery. Plast Reconstr Surg. 1984;75:800–3.
8. Johnson D. Some observations on certain developmental dentoalveolar anomalies and the stigmata of cleft. Dent Pract Dent Res. 1967;17:435.
9. Olin WH. Orthodontics in cleft lip and palate. In: Grabb WC, Rosenstein SW, Bzoch KR, editors. Cleft lip and palate. Boston: Little Brown; 1971. p. 599–615.
10. Boo-Chai K, Tange I. The isolated cleft lip nose: report of five cases in adults. Plast Reconstr Surg. 1968;41(35):28–34.
11. Trott JA, Mohan N. A preliminary report on one-stage open tip rhinoplasty at the time of lip repair in bilateral cleft lip and palate: the Alor Setar experience. Br J Plast Surg. 1993;46:215.
12. Nammoun JD, Hisley GS, Hucthins GN, Van Der Kolk C. Three dimensional reconstruction of the human philtrum. Ann Plast Surg. 1997;38:202–8.
13. Park CG, Ha B. The importance of accurate repair of the orbicularis oris muscle in the correction of unilateral cleft lip. Plast Reconstr Surg. 1995;96:780.
14. Martin RA, Jones KL, Benirschke K. Extension of the cleft lip phenotype: the subepithelial cleft. Am J Med Genet. 1993;47:744–7.
15. Martin RA, Hunter V, Neufeld-Kaiser W, Flodman P, Spence MA, Furnas D, et al. Ultrasonographic detection of orbicularis oris defects in first degree relatives of isolated cleft lip patients. Am J Med Genet. 2000;90:155–61.
16. Marazita ML. Subclinical features in non-syndromic cleft lip with or without cleft palate (CL/P): review of the evidence that subepithelial orbicularis oris muscle defects are part of an expanded phenotype for CL/P. Orthod Craniofac Res. 2007;10:82–7.
17. Gasser RF. The development of the facial muscles in man. Am J Anat. 1967;20:357.
18. Fará M. Anatomy and arteriography of cleft lips in stillborn children. Plast Reconstr Surg. 1968;42:29.
19. Fará M. Anatomy of unilateral and bilateral cleft lip. In: Bardach J, Morris HL, editors. Multidisciplinary management of cleft lip and palate. Philadelphia: WB Saunders; 1990. p. 134–43.
20. Gamba-Garib D, Petrocelli-Rosai J, Sathler R, Okada-Ozaka T. Dual origin of maxillary lateral incisors: clinical implications in patients with cleft lip and palate. Dental Press J Orthod. 2015;20(5):118–25. https://doi.org/10.1590/2177-6709.20.5.118-125.sar.
21. Delaire J, Precious S, Gordeef A. The advantage of wide subperiosteal exposure in primary surgical correction of labial maxillary clefts. Scand J Plast Reconstr Surg. 1993;22:710.
22. Fisher DM. Unilateral cleft lip repair: an anatomical subunit approximation technique. Plast Reconstr Surg. 2011;116:61–71.

23. Stark RB. Development of the center of the face with particular reference to surgical correction of bilateral deft lip. Plast Reconstr Surg. 1958;21:177–92.
24. Peter K. Atlas der Entwicklung der Nase und des Gaumen beim Menschen, rnit Einsdlluss der Entwicklungsstorungen. Jena: Gustav Fischer; 1913.
25. Veau V, Recamier J. Bec-de-Lievre: Formes CliniquesChirugie. Paris: Masson et Cie; 1938. p. 6.
26. Rohrich RJ, Gunter JP, Friedman R. Nasal tip blood supply: an anatomic study validating the safety of the transcolumellar incision in rhinoplasty. Plast Reconstr Surg. 1995;95:795.
27. Song R, Liu C, Zhao Y. A new principle for unilateral complete deft lip repair: the lateral columellar flap method. Plast Reconstr Surg. 1998;102:1848.
28. Carstens MH. Functional matrix cleft repair: principles and techniques. Clin Plast Surg. 2004;31:159–89.
29. Cohen D, Goitain K. Arhinia. Rhinology. 1986;24:287–92.
30. Cohen MM, Sulik KK. Perspectives on holoprosencephaly: Part II. Central nervous system, craniofacial anatomy, syndrome commentary, diagnostic approach, and experimental studies. J Craniofac Genet Dev Biol. 1992;12:196–244.
31. Patel H. Holoprosencephaly with median cleft lip: clinical, pathological, and echoencephalographic study. Am J Dis Child. 1972;214:217–21.
32. Probst FP. The prosencephalies: morphology, neuroradiological appearances, differential diagnosis. New York: Springer; 1979. p. 29–30.
33. O'Rahilly R, Muller F. Developmental stages in human embryo, publication 637. Washington, DC: Carnegie Institution of Washington; 1987. p. 175–302.
34. Streeter GL. Developmental horizons in human embryos: description of age groups XV, XVI, XVII, and XVIII, being the third issue of a survey of the Carnegie collection. Contrib Embryol Carnegie Inst. 1948;32:13–203.
35. Latham RA. The pathogenesis of the skeletal deformity associated with unilateral cleft lip and palate. Cleft Palate J. 1969a;6:404–14.
36. Latham RA. The septopremaxillary ligament and maxillary development. J Anat. 1969b;104:584.
37. Latham RA. The developmental deficiencies of the vertical and antero-posterior dimensions in the unilateral cleft lip and palate deformity. In: Georgiade NG, Hagarty RF, editors. Symposium on the management of cleft lip and cleft palate and associated deformities. St. Louis: CV Mosby; 1974.
38. Latham RA. The structural basis of the philtrum and the contour of the vermilion border: a study of the musculature of the upper lip. J Anat. 1976;121:151.
39. Semb G, Shaw WC. Simonart's band and facial growth in unilateral clefts of the lip and palate. Cleft Palate Craniofac J. 1991;28:40.
40. Enlow DH. Facial growth. 3rd ed. Philadelphia: WB Saunders; 1990.
41. Moss ML. The functional matrix concept and its relationship to temporomandibular joint dysfunction and treatment. Dent Clin N Am. 1983;27(3):445–55.
42. Sasaki A, Takeshita S, Publico AS, Moss ML, Taneka E, Ishino Y, Watanabe M, Tanne K. Finite element growth analysis of the craniofacial skeleton in patients with cleft lip and palate. Med Eng Phys. 2004;26(2):109–18.
43. Avery JK, Happle JD, French HC. Development of the nasal capsule in normal and cleft palate formation. Cleft Palate Bull. 1957;7:8–11.
44. Hairfield WM, Warren OW. Dimensions of the cleft nasal airway in adults: a comparison with subjects without cleft. Cleft Palate J. 1989;26:9–13.
45. Jirasek JE. Atlas of human prenatal morphogenesis. Boston: Kluwer; 1983.
46. Kosaka K, Hama K, Eta K. Light and electron microscopic study of fusion of facial prominences. Anat Embryol (Berl). 1985;173:187–201.
47. Millicovsky G, Johnston MC. Maternal hyperoxia greatly reduces the incidence of phenytoin-induced cleft lip and palate in A/J mice. Science. 1981a;212:671.
48. Millicovsky G, Ambrose JL, Johnston MC. Developmental alterations associated with spontaneous cleft lip and palate in CL/Fr mice. Am J Anat. 1982;164:129.
49. Millicovsky G, Johnston MC. Active role of embryonic facial epithelium: new evidence of cellular events in morphogenesis. J Embryol Exp Morphol. 1981b;63:53–66.
50. Millicovsky G, Johnston MC. Hyperoxia and hypoxia in pregnancy: simple experimental manipulation alters the incidence of cleft lip and palate in CL/Fr mice. Proc Natl Acad Sci U S A. 1981c;9:4723.
51. Poelmann RE, Vermeij-Keers C. Cell degeneration in the mouse embryo: a prerequisite for normal development. In: Muller-Berat N, editor. Progress in differentiation research. Amsterdam: North Holland; 1976. p. 93–102.
52. Gaare JD. Cell degeneration during the fusion of the nasal processes in mice. Anat Rec. 1976;184:407.
53. Gaare JD, Langman J. Fusion of nasal swellings in the mouse embryo: surface coat and initial contact. Am J Anat. 1977a;150:461–475.
54. Gaare JD, Langman J. Fusion of nasal swellings in the mouse embryo: regression of the nasal fin. Am J Anat. 1977b;150:477–499.
55. Gaare JD, Langman J. Fusion of nasal swellings in the mouse embryo. DNA synthesis and histological features. Anat Embryol (Berlin). 1980;159(1):85–99.
56. Figueroa AA, Pratt RM. Autoradiographic study of macromolecular synthesis in the fusion epithelium of the developing rat primary palate in vitro. J Embryol Exp Morphol. 1979;50:145–54.
57. Wilson DB, Hendrickx AG. Quantitative aspects of proliferation in the nasal epithelium of the rhesus monkey embryo. J Embryol Exp Morphol. 1977;38:217–26.
58. Smuts MS. Concanavalin A binding to the epithelial surface of the developing mouse olfactory placode. Anat Rec. 1977;188:29–38.
59. Gui T, Osama-Yamashita N, Eto K. Proliferation of nasal epithelium and mesenchymal cells during primary palate formation. J Craniofac Genet Dev Biol. 1993;13(4):250–8.
60. Warbrick JG. The development of the nasal cavity and upper lip in the human embryo. J Anat. 1960;94:351–62.
61. Juriloff DM. Genetic analysis of the construction of the AEJ. A congenetic strain indicates that nonsyndromic CL(P) in the mouse is caused by two block with epistatic interaction. J Craniofac Genet Dev Biol. 1995;15:l–12.
62. Osumi-Yamashita N, Asada S, Eto K. Distribution of F-actin during mouse facial morphogenesis and its perturbations with cytochalasin D using whole embryo culture. J Craniofac Genet Dev Biol. 1992;12:130–40.
63. Johnston MC, Millicovsky G. Normal and abnormal development of the lip and palate. Clin Plast Surg. 1985;12:521.
64. Longo AD. Carbon monoxide in pregnant mother and fetus and its exchange across the placenta. Ann N Y Acad Sci. 1970;174:131.
65. Ericson A, Kallen B, Westerholm P. Cigarette smoking as an etiologic factor in cleft lip and palate. Am J Obstet. 1979;135:348.
66. Congdon ED. Transformation of the aortic arch system during the development of the human embryo. Carnegie Contrib Embryol. 1922;14:46.
67. Feinberg RN, Scherer GK, Auerbach R. The development of the vascular system. Basel: Karger; 1991.
68. Nairn RJ. The circumoral musculature. Br J Plast Surg. 1975;36:141.
69. Nicolau PJ. The orbicularis oris muscle: a functional approach to its repair in the cleft lip. Br J Plast Surg. 1983;36:141–53.

70. Precious D, Delaire J. Surgical considera tions in patients with cleft deformities. In: Bell WH, editor. Modern practice in reconstructive and orthognathic surgery. Philadelphia: WB Saunders; 1992.
71. Joos U. Muscle reconstruction in primary cleft lip surgery. J Craniomaxillofac Surg. 1989;17:8.
72. Monie IW, Cacciatore A. The development of the philtrum. Plast Reconstr Surg. 1962;30:313–20.
73. England M. Life before birth. Chicago: Year Book Medical Publishers; 1996.
74. Mooney MP, Siegel MI, Kimes KR, et al. Anterior paraseptal cartilage development in normal and cleft lip and palate human fetal specimens. Cleft Palate J. 1994;31:239–45.
75. Ross RB, Semb G, Shaw WC. Simonart's band and facial growth in unilateral clefts of the lip and palate. Cleft Palate Craniofac J. 1991;28:40.
76. Wu J, Yin N. Anatomy research of nasolabial muscle structure in fetus with cleft lip: an iodine staining technique based on microcomputed tomography. J Craniofac Surg. 2014;25(3):1055–62.
77. Kernahan D, Dado DV, Bauer BS. The anatomy of the orbicularis oris muscle in unilateral cleft lip based on a three dimensional histological reconstruction. Plast Reconstr Surg. 1984;73:875–9.
78. Schendel SA, Pearl RM, De'Armond SJ. Pathophysiology of cleft lip muscle. Plast Reconstr Surg. 1989;83(5):777–84.
79. de Chalain T, Zuker R, Acklery C. Histologic, histochemical and ultrastructural analysis of soft tissues from cleft and normal lips. Plast Reconstr Surg. 2001;108(3):605–11.
80. Schendel SA, Cholon A, Delaire J. Histochemical analysis of cleft palate muscle. Plast Reconstr Surg. 1994;94:919–23.
81. Lindman A, Paulin G, Stal PS. Morphological characterization of levator veli palatini muscle in children born with cleft palate. Cleft Palate Craniofac J. 2001;38:438–48.
82. Doménech-Ratto G. Developmental peripheral innervation of the palate muscles. Acta Anat. 1977;97:4–14.
83. Cohen SR, Chen L, Trotman CA, Burdi AR. Soft palate myogenesis: a developmental field paradigm. Cleft Palate Craniofac J. 1993;30:441–6.
84. Cohen SR, Chen LL, Burdi AR, Trotman C-A. Patterns of abnormal myogenesis in human cleft palates. Cleft Palate Craniofac J. 1994;31(5):345–50.
85. Stenstrom SJ, Thilander BL. Cleft lip nasal deformity in absence of cleft lip. Plast Reconstr Surg. 1965;35:160–6.
86. Tulenko JF. Cleft lip nasal deformity in the absence of cleft lip: a case report. Plast Reconstr Surg. 1968;41(1):35–7.
87. Huffman WC, Lierle DM. Studies on the pathologic anatomy of the unilateral hare-lip nose. Plast Reconstr Surg. 1949;4:225–34.
88. Carstens MH. Correction of the unilateral deft lip nasal deformity using the sliding sulcus procedure. J Craniofac Surg. 1999;10:346–64.
89. Dixon D, Newton I. Minimal forms of the cleft syndrome demonstrated by stereophotogrammetric surveys of the face. Br Dent J. 1972;132:183.
90. Ranta R. A review of tooth formation in children with cleft lip/palate. J Orthod Dentofac Orthop. 1986;90:11.
91. Stenstrom SJ, Oberg TRH. The nasal deformity in unilateral cleft lip. Plast Reconstr Surg. 1961;28:295–305.
92. Horswell JBB, Pospisil OA. Nasal symmetry after primary cleft lip repair: comparison between Delaire cheilorhinoplasty and modified rotation-advancement. J Oral Maxillofac Surg. 1995;53:1025.
93. Yuzuriha S, Mulliken JB. Minor form, microform, and minimicroform cleft lip: anatomical features, operative techniques, and revisions. Plast Reconstr Surg. 2008;122(5):1489–93.
94. Demas P, Sotereanos GC. Closure of alveolar cleft with corticocancellous block grafts and bone marrow: a retrospective study. J Oral Maxillofac Surg. 1988;46(8):682–7.
95. Le Mesurier AB. Harelips and their treatment. Baltimore: Williams & Wilkins; 1962. p. 80–100.
96. Lehman JA, Artz JS. The minimal cleft lip. Plast Reconstr Surg. 1976;58:306.
97. Millard DR. Cleft craft. Vol. I: the unilateral deformity. Boston: Little Brown; 1976a. p. 229–377.
98. Millard DR. Cleft craft. Vol I. The unilateral deformity. Boston: Little Brown; 1976b. p. 456–7.
99. Thaller SR, Lee T. Microform cleft lip associated with a complete cleft palate. Cleft Palate J. 1995;32:247.
100. Cho BC. New technique for correction of the microform cleft lip using vertical interdigitatation of the orbicularis oris muscle through the intraoral incision. Plast Reconstr Surg. 2004;114:1032–41.
101. Mcindoe A, Rees TD. Synchronous repair of secondary deformities in cleft lip and nose. Plast Reconstr Surg. 1959;24:150–62.
102. Matsuo K, Hirose T. Secondary correction of the unilateral cleft lip nose using a conchal cartilage graft. Plast Reconstr Surg. 1990;86:991–5.
103. Kimes KK, Siegel MI, Mooney MP, et al. Relative contributions of the nasal septum and airways to total nasal capsule volume in normal and cleft lip and palate fetal specimens. Cleft Palate J. 1988;25:282–7.
104. Noordhoff MS, Chen YR, Chen KT, et al. The surgical technique for the complete unilateral cleft lip-nasal deformity. Oper Tech Plast Reconstr Surg. 1995;2:167–74.
105. Noordhoff MS. The surgical technique for the unilateral cleft lip-nasal deformity. Taipei: Noordhoff Craniofacial Foundation; 1997.
106. Guerrero-Santos J, Ramirez M, Castenda A, et al. Crossed denuded flap as a complement to the Millard technique in the correction of the cleft lip. Plast Reconstr Surg. 1971;48:506–8.
107. Depew MJ, Lufkin T, Rubenstein JL. Specification of jaw subdivisions by DLX genes. Science. 2002;298(5592):381–5. https://doi.org/10.1126/science.1075703.
108. Depew MJ, Simpson CA, Morasso M, Rubenstein JL. Reassessing the DLX code: the genetic regulation of branchial arch skeletal pattern and development. J Anat. 2005;207(5):501–61.
109. Amin N, Ohasi Y, Chiba J, Yoshida S, Takano Y. Alterations in vascular pattern of the developing palate in normal and spontaneous cleft palate mouse embryos. Cleft Palate Craniofac J. 1994;31(5):332–44.
110. Wang RN, Green J, Shi LL, et al. Bone morphogenetic protein (BMP) signaling in development and human diseases. Genes Dis. 2014;1:87–105.
111. Zhang Z, Son Y, Zhao X, Zhang X, Fermin C, Chen Y-P. Rescue of cleft palate in *Msx1*-deficient mice by transgenic BMP4 reveals a network of BMP and SHH signaling in the regulation of mammalian palatogenesis. Development. 2002;129:4135–46.
112. Friedrichs M, Wirsdöerfer F, Fiche SB, Scneier S, Wuelling M, Vortkamp A. BMP signaling balances proliferation and differentiation of muscle satellite cell descendents. Cell Biol. 2011;12:26–43.
113. Shore EM, Xu M, LeMerer M, et al. A recurrent mutation in the BMP type 1 receptor ACVR1 causes inherited and sporadic fibrodysplasia ossificans progressiva. Nat Genet. 2006;38:525–7.
114. Hicks M, Pyle A. The path from pluripotency to skeletal muscle: developmental myogenesis guides the way. Cell Stem Cell. 2015;17(3):255–7.
115. Dyer LA, Pio X, Patterson C. Role of BMPs in endothelial cell function and dysfunction. Trends Endocrinol Metab. 2014;25(9):472–80.
116. Franco C, Gerdardt H. Blood flow boosts BMP signaling to keep vessels in shape. J Cell Biol. 2016;214(7):793.

Further Reading

Bagatain M, Khosh M, Nishoka G, Larrabbe WF Jr. Isolated nasalis reconstruction in secondary unilateral cleft lip nasal reconstruction. Laryngoscope. 1999;109:320–3.

Boddy K, Dawes GS. Fetal breathing. Br Med Bull. 1975;31(1):3–7. https://doi.org/10.1093/oxfordjournals.bmb.a071237.

Boehn A. Dental anomalies in harelip and cleft palate. Acta Odontol Scand. 1963;21(Suppl 38):1–109.

Brown RF. A reappraisal of the cleft-up nose with the report of a case. Br J Plast Surg. 1964;17:168.

Carlson B. Human embryology and developmental biology. St. Louis: CV Mosby; 1999.

Chang J, Pourquíe O. Making muscle: skeletal myogenesis in vivo and in vitro. Development. 2017;144:2104–22.

Chiego D, editor. Avery's essentials of oral histology and embryology: a clinical approach. 4th ed. St. Louis: CV Mosby; 2013.

Cohen M, Figueroa AA, Aduus H. The role of gingival mucoperiosteal flaps in the repair of alveolar clefts. Plast Reconstr Surg. 1989;83(5):812–9.

Conen PE, Erkman B, Metaxotou C. The "D" syndrome: report of four trisomic and one D/D translocation. Am J Dis Child. 1966;111(3):236–47.

Delaire J. The potential role of facial muscles in monitoring maxillary growth and morphogenesis. In: Carlson OS, McNamara Jr JA, editors. Monograph no. 38. Cranial growth series. Ann Arbor: University of Michigan Press; 1978.

Delaire J. Theoretical principles and technique of functional closure of the lip and nasal aperture. J Maxillofac Surg. 1978;6:109.

Delaire J. L'anatomie et la physiologie muscles nasolabiaux chez sujet normal pere d'une fente labiomaxillaire. Acta Orthod. 1980;8:269–85.

Delaire J, Feve R, Chateau JP, et al. Anatomie et physiologie des muscles et du fente de la lievre superieure. Rev Stomatol (Paris). 1977;78:93.

Demas P, Sotereanos GC. Closure of alveolar clefts with corticocancellous block grafts and marrow: a retrospective study. J Oral Maxillofac Surg. 1988;46(6):483–5.

Desrosiers AE, Kawamoto HK, Katchikkan HV, et al. Microform cleft lip repair with intraoral muscle interdigitation. Ann Plast Surg. 2009;62:640.

Fará M, Chlumska A, Hrivnakova J. Musculus orbiculari oris in incomplete hare-lip. Acta Chir Plast. 1965;7:125.

Fischer DM. Unilateral cleft lip repair: An anatomical subunit approximation technique. Plast Reconstr Surg 2005; 116(1): 61–71.

Fox HE. Fetal breathing movements and ultrasound. Am J Dis Child. 1976;130(2):127–9.

Frank N, Kho AT, Schalton T, Gussoni E, et al. Regulation of myogeneic progenitor proliferation in human fetal skeletal muscle by BMP4 and its antagonist gremlin. J Cell Biol. 2006;175(1):99–110.

Gifford GH, Swanson L, MacCollum OW. Congenital absence of the nose and anterior nasopharynx. Plast Reconstr Surg. 1972;50:5.

His W. Anatomie mensdilicher Embryonen. Leipzig-German y: Vogel; 1885.

His W. Die entwerklung der mensd1lichen und thierischer Physigonomen. Arch Anat Physiol (Lejpzig). 1892;27:384–434.

His W. Beobachtungen zur Geshichte der Naden und Gaumenbildwlg beim menschlischen Embryonen. Abh Gao Naturw. 1901;27:349–89.

Joos U, Friedburg H. Darstellung des Verlaufs der mirnisclen Muskulatur in der Kemspintomographie. Fortschaft Kiefer Gesichtschir. 1987;32:125.

Kim EK, Khang SK, Lee TL, Kim TG. Clinical features of the microform cleft lip and the ultrastructural characteristics of the orbicularis oris muscle. Cleft Palate Craniofac J. 2010;47(3):297–302.

Kim MC, Choi DH, Bae SG, Cho BC. Correction of minor-form and microform lip using modified muscle overlapping with a minimal skin excision. Arch Plast Surg. 2017;44(3):210–6.

Kraus BS, Jordan RE, Neptune CM. Dental abnormalities associated with cleft lip and/or palate. Cleft Palate J. 1966a;3:439.

Kraus B, Kitamura H, Latham RA. Atlas of developmental anatomy of the face. New York: Harper & Row; 1966b.

Lasseri D, Viacava P, Pollina LE. Dystrophic-like alterations characterize orbicularis oris and palatopharyngeal muscles in patients affected by cleft lip and palate. Cleft Palate Craniofac J. 2008;45(6):587–91.

Losee J, Kirschner R, editors. Comprehensive cleft care. 2nd ed. Stuttgart: Thieme; 2015.

Markus AF, Delaire J. Functional primary closure of cleft lip. Br J Oral Maxillofac Surg. 1978;31:281.

Markus AF, Delaire J, Smith WP. Facial balance in cleft lip and palate. II. Cleft lip and palate and secondary deformities. Br J Oral Maxillofac Surg. 1990;20:296.

Markus AF, Delaire J, Smith WP. Facial balance in cleft lip and palate I. Normal development and cleft palate. Br J Oral Maxillofac Surg. 1992;30:290–5.

Meyer R. Total external and internal reconstruction in arhinia. Plast Reconstr Surg. 1997;99:534–42.

Millard DR, Onizuka T, Hoaka Y, Ayoyama R, et al. Operations for microforms of cleft lip. Cleft Palate Craniofac J. 1991;28:300.

Moore KL, Persaud TV. The developing human. 6th ed. Philadelphia: WB Saunders; 1998. p. 384–9.

Nammoun JD, Siegel MI, Kimes K, et al. Premaxillary development in normal and cleft lip and palate human fetuses using three-dimensional computer reconstruction. Cleft Palate Craniofac J. 1991;28:49–53.

Nishimura H, Okatmoto N. Sequential atlas of human congenital malformations: observations of embryos, fetuses, and newborns. Baltimore: University Park Press; 1976.

Onizuka T. Operative plastic surgery. Tokyo: Takodo; 1982.

Onizuka T, Hosaka Y, Ayoyama R, Takahama H, Jinnai T, Ursi Y. Operations for microforms of cleft lip. Cleft Palate Cranifac J. 1991;28:293.

Park CG. Temporal fascia graft for the correction of the congenital scar of the lip. J Korean Soc Plast Reconstr Surg. 1986;13:67–70.

Patten BM. Olfactory complex. In: Patten BM, editor. Embryology. New York: McGraw-Hill; 1968. p. 289–90.

Sachidanandan C, Dhwan J. Skeletal muscle progenitor cells in development and regeneration. Proc Indian Natl Sci Acad. 2003;69(5):719–40.

Sanvenero-Roselli G. Developmental pathology of the face and the dysraphic syndrome—an essay of interpretation based on experimentally produced congenital defects. Plast Reconstr Surg. 1946;11(1):36–8.

Sperber G. Craniofacial embryology. London: Churchill; 1984.

Sperber G. Embryology of the head and neck. In: Potter's pathology of the fetus and want. 3rd ed. St. Louis: CV Mosby; 1999.

Stantzou A, Schirwis E, Swiss S, et al. BMP signalling regulates satellite cell- dependent post-natal muscle growth. Development 2017; 144(5): 2737–2747

Streeter GL. Developmental horizons in human embryos: description of age group XI, 13 to 20 somites and age group XII, 21 to 29 somites. Contrib Embryol Carnegie Inst. 1942;30:211.

Streeter GL. Developmental horizons in human embryos: description of age group XIII, embryos of 4 or 5 millimeters long, and age group XIV, period of identification of the lens vesicle. Contrib Embryol Carnegie Inst. 1945;31:27.

Suzuki S, Marazita ML, Murray JC, et al. Mutations in BMP4 are associated with subepithelial, microform, and overt cleft lip. Am J Hum Genet. 2009;84(3):406–11. https://doi.org/10.1016/j.ajhg.2009.02.002.

Taylor GI, Palmer JH. The vascular territories (angiosomes) of the body: experimental study and clinical applications. Br J Plast Surg. 1987;46:113.

Taylor GI, Gianoutsos MP, Morris SF. The neurovascular territories of the skin and muscles: anatomic study and clinical implications. Plast Reconstr Surg. 1994;94:1–35.

Tolarova M. Microforms of cleft lip and/or palate. Acta Chir Plast. 1969;1(1):96.

Tolarova H, Havlova Z, Ruzickova J. The distribution of characters considered to be microforms of cleft lip and/or palate in a population of normal 18–21 year-old subjects. Acta Chir Plast. 1967;9:1.

Vissiaronov VA. Correction of a deformity of the upper lip after primary plastic surgery of the bilateral cleft lip. Vestn Khir II Grek. 1988;141(8):86–8.

Vissarionov VA, Tuznaova LI, Blokhina SI. Characteristics of plastic surgery of the central part of the upper lip. Vestn Khir Im II Grek. 1990;145(7):191–2.

Wang MKH. A modified LeMesurier–Tennison technique in unilateral cleft lip repair. Plast Reconstr Surg. 1960;26:190.

Wang K-Y, Diewert VM. A morphometric analysis of craniofacial growth in cleft lip and non-cleft mouse embryos. J Craniofac Genet Dev Biol. 1992;12:141–54.

Wang H, Noulez F, Edom-Vovard F, Le Grand F, Duprez D. Bmp signaling at the tips of skeletal muscle regulates the number of fetal muscle progenitors and satellite cells during development. Dev Cell. 2010;18:643–54.

Weinberg A, Neuman A, Benmeir P, et al. A rare case of arhinia with severe airway obstruction: case report and review of the literature. Plast Reconstr Surg. 1993;91:146–9.